

**Einfluss einer fokalen Ischämie
auf die Genexpression des somatostatinergeren Systems
und die sst2-Rezeptoraktivierung im Gehirn der Ratte**

Dissertation

zur Erlangung des akademischen Grades

doctor rerum naturalium

(Dr. rer. nat.)

genehmigt durch

die Fakultät für Naturwissenschaften

der Otto-von-Guericke-Universität Magdeburg

von Magister Chun Zhou

geb. am 22. November 1969

in Jilin, V. R. China

Gutachter: Prof. Dr. Volker Höllt

Prof. Dr. Eberhard Weihe

Prof. Dr. Hans-Christian Pape

Eingereicht am: 28. April 2004

Verteidigung am: 22. November 2004

1 Introduction	1
1.1 The somatostatin neuropeptide family	1
1.2 The somatostatin receptor family	2
1.3 Agonist-dependent regulation of sst receptors	3
1.4 Distribution of somatostatin and cortistatin in the cerebral cortex	4
1.5 Distribution of sst receptors in the cerebral cortex	5
1.6 Physiological and pathophysiological significance of somatostatin and cortistatin	6
1.7 Role of neuropeptides in brain ischemia	7
1.8 Purpose of study	8
2 Materials and Methods	10
2.1 Instruments	10
2.2 Kits	10
2.3 Enzymes	10
2.4 Nucleic acids, vectors and probes	11
2.5 Animals	11
2.6 Rat permanent focal cerebral ischemia	11
2.7 Cloning of cDNAs in transcription vectors	12
2.8 Synthesis of RNA probes for in situ hybridization	13
2.9 In situ hybridization	13
2.10 Quantitative analysis of radioactive in situ hybridization	14
2.11 Combination of radioactive and non-radioactive in situ hybridization	15
2.12 Immunohistochemistry	15
3 Results	18
3.1 Spatiotemporal development of brain infarction after MCAO	18
3.2 Astroglial and microglial reaction, macrophage infiltration	19
3.3 Constitutive expression of somatostatin, cortistatin, sst1, sst2, and sst4 in the forebrain	22
3.4 Gene expression patterns of somatostatin, cortistatin, sst1, sst2, and sst4 in the cerebral cortex after focal cerebral ischemia	24
3.4.1 Opposite regulation of somatostatin and cortistatin gene expression in the non-lesioned cerebral cortex	26
3.4.2 Downregulation of cortistatin gene expression in somatostatin-negative neurons	28
3.4.3 Differential regulation of sst1, sst2, sst4, and sst5 receptor mRNA expression	31
3.4.3.1 Transient upregulation of sst2 gene expression in the perifocal and exofocal cortex	32
3.4.3.2 Selective upregulation of sst2 mRNA expression in glutamatergic neurons	34
3.4.3.3 Regulation of sst4 expression in the cerebral cortex	36

3.4.3.4 Regulation of somatostatin- and sst2-expression in the striatum	37
3.5 Constitutive localization of somatostatin, sst2, and sst4-LIR in the cerebral cortex	37
3.6 Histochemistry for somatostatin and sst2 after focal ischemia	41
3.6.1 Biphasic changes of somatostatin-LIR in the ipsilateral non-lesioned cerebral cortex	42
3.6.2 Internalization of sst2a after MCAO	42
4 Discussion	46
4.1 Analysis of the animal model of focal ischemia	46
4.2 Constitutive somatostatin, cortistatin, and somatostatin receptor expression in the cerebral cortex	47
4.2.1 Neuronal types expressing cortistatin mRNA in the cerebral cortex	48
4.2.2 Possible consequences of the distinct expression of cortistatin and somatostatin in GABAergic neurons	48
4.2.3 Glutamatergic neuron type-selective gene expression of somatostatin receptors in the cerebral cortex	49
4.3 Stage-specific changes in somatostatin, cortistatin and sst2 receptor expression	50
4.4 Implications for the somatostatinergic system in the pathophysiology of focal brain ischemia	54
4.5 Is the somatostatinergic system a promising target in ischemic cerebrovascular disease?	54
5 Summary	56
6 References	58
7 Abbreviations	68
8 Appendix	70
8.1 CURRICULUM VITAE	70
8.2 Publications and presentations	71
8.3 Acknowledgement	72
9 Zusammenfassung	73

1. Introduction

Somatostatin was first identified as a cyclic tetradecapeptide isolated from the ovine hypothalamus (Brazeau *et al.*, 1973) on the basis of its ability to inhibit the release of growth hormone from rat pituitary. It was initially termed somatotrophin-release inhibiting factor (SRIF), and later renamed somatostatin, emphasizing its role as counterpart of somatotrophin. Two bioactive forms, somatostatin-14 and its N-terminally extended form, somatostatin-28, were discovered (Pradayrol *et al.*, 1980). Apart from the original identification in the hypothalamus, high amounts of somatostatin were also detected in the central nervous system and in most peripheral organs (Hokfelt *et al.*, 1975; Patel and Reichlin, 1978; Reichlin, 1983). Both central and peripheral actions are mediated by a family of six G-protein-coupled receptors encoded by five individual genes. All of these receptors bind somatostatin-14 and somatostatin-28 with comparable affinities except for sst5, which exhibits a slightly higher affinity for somatostatin-28 than somatostatin-14 (O'Carroll *et al.*, 1992). Within the brain, somatostatin acts as a neuromodulator with widespread physiological effects on neuroendocrine functions, cell proliferation, neurotransmission, cognition and locomotor behaviour (Epelbaum, 1986). Recently, the somatostatinergic system has been extended by the discovery of cortistatin (CST), a neuropeptide displaying strong structural similarity with somatostatin, but encoded by a distinct gene (de Lecea *et al.*, 1996). It binds to all somatostatin receptors (Siehler *et al.*, 1998), and shares many pharmacological and functional properties with somatostatin (de Lecea *et al.*, 1996; Vasilake *et al.*, 1999). However, cortistatin has also effects on sleep and locomotor activity, which are distinct from somatostatin (de Lecea *et al.*, 1996; Spier and de Lecea, 2000). The name cortistatin reflects the predominant expression of this peptide in the cerebral cortex and its neuronal depressant properties.

1.1 The somatostatin neuropeptide family

Both somatostatin-14 and somatostatin-28 are products of a common gene, preprosomatostatin (Patel and O'Neil, 1988). Cortistatin is encoded by a different gene, preprocortistatin (de Lecea *et al.*, 1996). The two genes are mapped to separate chromosomes in rat, mouse and human. In the human, the gene for somatostatin is mapped to chromosome 3q28, whereas cortistatin is mapped to 1p36.

The transcriptional units of the rat somatostatin and cortistatin genes share structural similarities in that both have two exons and one intron (Montminy *et al.*, 1984; Calbet *et al.*, 1999). Analysis of the regulatory elements for the preprosomatostatin and preprocortistatin genes indicates that the regulatory elements of both genes share very few similarities. The few

features which are shared by the somatostatin and the cortistatin promoters include a CREB-like element in the similar positions and a GATA/homeo/homeo arrangement, which may be responsible for the coexpression of these genes in certain cortical interneurons (Calbet *et al.*, 1999; Puebla *et al.*, 1999).

Mammalian prosomatostatin is processed mainly at the C-terminal segment, generating the two bioactive forms, somatostatin-14 and somatostatin-28 (Patel and O'Neil, 1988). Similarly, the gene product of preprocortistatin gives rise to two cleavage products, cortistatin-14 and cortistatin-29 in the rat and cortistatin-17 and cortistatin-29 in human, which are comparable to somatostatin-14 and somatostatin-28 (Spier and de Lecea, 2000). In mouse, only a putative cortistatin-14 has been described (de Lecea *et al.*, 1997a; Spier and de Lecea, 2000).

1.2 The somatostatin receptor family

To date, five sst receptor genes have been cloned and termed sst1 through sst5 (Hoyer *et al.*, 1995; Reisine and Bell, 1995). Whereas the sst1, sst3, sst4 and sst5 genes each generate a single receptor protein, alternative splicing of the sst2 mRNA gives rise to two protein isoforms, sst2a and sst2b, which differ only in length and amino acid sequence at the carboxy-terminus (Vanetti *et al.*, 1992). All sst receptors belong to the family of G-protein-coupled receptors (GPCRs) and bind the somatostatin peptides as well as the cortistatin peptides with similar affinity (de Lecea *et al.*, 1996; Fukusumi *et al.*, 1997; Siehler *et al.*, 1998). These receptors were further classified in two types, SRIF₁ (comprising sst2, sst3 and sst5) and SRIF₂ (comprising sst1 and sst4) (Hoyer *et al.*, 1995). The classification was performed according to their affinity to octreotide and seglitide, which are synthetic peptide analogues of somatostatin. Both peptide analogues have high affinity to SRIF₁, but little or no affinity to SRIF₂ (Raynor *et al.*, 1993; Hoyer *et al.*, 1995). The five receptors range in size from 346-428 amino acid residues. They display a high degree of structural conservation across species (81-97%) and 45-61% identity between subtypes (Reisine and Bell, 1995). The nearest relatives of the sst receptors are the opioid receptors displaying 37% sequence similarity to the mouse sst1 (Reisine and Bell, 1993). All five sst receptors have been cloned in human, mouse and rat. The sst genes are devoid of introns within their protein coding region, with the exception of a cryptic intron in the mouse sst2 gene giving rise to the synthesis of the two receptor variants, sst2a and sst2b (Vanetti *et al.*, 1993). All five gene-promoters have in common that TATA- and CAAT-boxes are missing. Another remarkable feature of the sst genes is the high G/C content directly upstream of their transcriptional start sites (Kraus *et al.*, 1998; Baumeister and Meyerhof, 2000). These are tissue-specific housekeeping promoters and typical of other G protein-coupled receptors (GPCR) genes (Patel *et al.*, 1995). Transcription factor binding sites (for instance, AP1, AP2)

that are important for the regulation of sst receptor gene expression may be shared by homologous sst genes of different species, and by different sst genes of the same species (Baumeister and Meyerhof, 2000).

1.3 Agonist-dependent regulation of sst receptors

All sst receptors except for sst4 desensitize after treatment with agonist (Hipkin *et al.*, 1997; Roosterman *et al.*, 1997; Beaumont *et al.*, 1998; Hukovic *et al.*, 1998; Kreienkamp *et al.*, 1998; Liu and Schonbrunn, 2001). Depending on the cell line and sst receptor subtype, desensitization of sst receptors depends on receptor phosphorylation (Roth *et al.*, 1997a; Beaumont *et al.*, 1998; Liu and Schonbrunn, 2001). The desensitization and resensitization of GPCRs (Koenig and Edwardson, 1997a; Bloch *et al.*, 1999) is often influenced by agonist-induced receptor internalization.

The sst receptors internalize to different degrees after agonist treatment (Hukovic *et al.*, 1996; Koenig *et al.*, 1997b; Sarret *et al.*, 1999; Nouel *et al.*, 1997; Roth *et al.*, 1997b; Stroh *et al.*, 2000b). Most studies report efficient ligand-induced internalization for sst2, sst3 and sst5, and poor internalization for sst1 and sst4 (Hukovic *et al.*, 1996; Hipkin *et al.*, 1997; Nouel *et al.*, 1997; Roth *et al.*, 1997b; Kreienkamp *et al.*, 1998; Stroh *et al.*, 2000b). In some of the cases, internalization of the agonist-receptor complex is mediated by the classical clathrin-dependent endocytotic pathway (Roosterman *et al.*, 1997; Stroh *et al.*, 2000b).

Mechanisms of internalization were best studied for sst2, which was shown to internalize rapidly in several cell lines (Schwartzkop *et al.*, 1999; Hipkin *et al.*, 2000) as well as in primary neuronal cultures of cortex and hippocampus (Stroh *et al.*, 2000a). After injection of exogenous sst2 agonists into the brain, sst2a-LIR exhibits a massive redistribution from the plasma membrane into endosomal compartments (Csaba *et al.*, 2001, 2002, 2003). The observation that cerebral regions receiving a dense somatostatin innervation display low proportions of plasma membrane-associated versus intracellular sst2a receptors suggests *in vivo* internalization of sst2a by endogenous somatostatin (Dournaud *et al.*, 1998). In the case of the substance P receptor, the degree of *in vivo* internalization has been established as a selective index for the release of endogenous ligands in pathophysiological stimulation (Allen *et al.*, 1997). *In vivo* internalization of sst2 in response to endogenously released somatostatin has not been studied yet.

After internalization, sst2, sst3, sst4 and sst5 have been shown to recycle efficiently to the cell surface, suggesting that agonist-induced internalization is necessary for functional resensitization of desensitized receptors (Roth *et al.*, 1997a; Koenig *et al.*, 1998; Stroh *et al.*, 2000b; Smalley *et al.*, 2001).

In addition, it has been described previously that the *sst2a* gene was upregulated upon short- or long-term exposure to agonist (Bruno *et al.*, 1994; Hukovic *et al.*, 1996; Froidevaux *et al.*, 1999; Tannenbaum *et al.*, 2001). More recently, regulation of *sst2a* expression by somatostatin was studied in detail in brain slices, where application of somatostatin was shown to increase *sst2a* mRNA and protein levels (Boudin *et al.*, 2000). This agonist-induced stimulation of *sst2a* expression was abolished in the presence of endocytosis inhibitors and hyperosmolar sucrose, which inhibits internalization of *sst2a* receptor complexes. Furthermore, in AtT-20 cells which natively express *sst1*, *sst2*, *sst4* and *sst5*, agonist treatment significantly decreased the amount of growth hormone mRNA, which was again totally abolished in the presence of hyperosmolar sucrose (Sarret *et al.*, 1999). Taken together, these results suggest that ligand-induced endocytosis of *sst* receptors may regulate homologously the expression of the receptor gene itself as well as of other genes.

1.4 Distribution of somatostatin and cortistatin in the cerebral cortex

Somatostatin mRNA and somatostatin peptides are widely distributed in almost all brain areas of rat and human. High levels of somatostatin are found in the cerebral cortex, where the peptides are present in all cortical layers (Epelbaum, 1986; Fitzpatrick-McElligott *et al.*, 1988; Kiyama and Emson, 1990).

Coexpression analysis indicated that in the rat cerebral cortex, preprosomatostatin mRNA is co-localized with glutamate decarboxylase (GAD) mRNA, a marker for GABAergic neurons (Esclapez and Houser 1995). Consistently, the somatostatin peptides are restricted to GABAergic neurons in the cortex (Schmechel *et al.*, 1984). Since most GABAergic neurons in the cerebral cortex are interneurons, somatostatin is assumed to function as a co-transmitter in the GABAergic local cortical circuits. A subset of somatostatin neurons also contains neuropeptide Y (NPY, Hendry *et al.*, 1984) and NADPH diaphorase (Kowall and Beal 1988).

In contrast to the wide distribution of somatostatin in central and peripheral tissues, cortistatin mRNA was shown to be essentially restricted to the cerebral cortex and hippocampus (de Lecea *et al.*, 1996, 1997a, 1997b). Co-localization studies indicate that cortistatin is exclusively expressed in GABAergic neurons and that expression of cortistatin overlaps partially with somatostatin. Approximately one fourth of somatostatin-containing cells express cortistatin mRNA, and less than half of the cortistatin-expressing neurons contain somatostatin (de Lecea *et al.*, 1997a). Like other neuropeptides, cortistatin is partially co-localized with the calcium binding proteins, parvalbumin or calbindin (de Lecea *et al.*, 1997a).

GABAergic neurons in the cerebral cortex are heterogeneous, and are subdivided according to their neurochemical contents and specific innervation tendency on postsynaptic elements

(Kawaguchi and Kubota, 1997; Somogyi *et al.*, 1998; Kawaguchi and Kondo, 2002). For instance, the somata of cortical cells are innervated by GABAergic neurons containing parvalbumin. In contrast, the distal dendrites of cortical neurons are innervated by GABAergic neurons containing somatostatin (Kawaguchi and Kubota, 1997). Since somatostatin and cortistatin are present in different interneuron subpopulations, they are likely to exert distinct functions in the local cortical circuitry.

1.5 Distribution of sst receptors in the cerebral cortex

sst1 mRNA is widely distributed in the rat CNS, particularly concentrated in the hypothalamus, amygdala, cerebral cortex, and hippocampus (Perez *et al.*, 1994; Senaris *et al.*, 1994). sst1-LIR was identified presynaptically in somatostatin-containing fibres innervating the hypothalamus. Thus, the sst1 receptor may act as an autoreceptor and inhibit the release of somatostatin in the hypothalamus (Helboe *et al.*, 1998).

sst2 and sst4 mRNAs are also highly expressed in the cerebral cortex. While sst2 mRNAs display a laminar pattern in infragranular layers (Breder *et al.*, 1992; Perez *et al.*, 1994; Senaris *et al.*, 1994), sst4 mRNA is expressed both in supragranular and infragranular layers (Harrington *et al.*, 1995; Perez and Hoyer, 1995a). The distribution of sst2a-LIR in the rat cerebral cortex is in agreement with *in situ* hybridization and ligand binding studies (Dournaud *et al.*, 1996; Holloway *et al.*, 1996; Schindler *et al.*, 1997; Cole and Schindler, 2000). Ligand binding studies in sst2 knock out mice revealed that sst2 accounts for the vast majority of somatostatin-14 binding sites in the cerebral cortex (Videau *et al.*, 2003).

sst3 mRNA exhibits a widespread distribution in brain, and is homogeneously distributed throughout all cortical layers (Kaupmann *et al.*, 1993; Senaris *et al.*, 1994). sst3-LIR exhibits a similar distribution as the mRNA (Handel *et al.*, 1999). However, at the subcellular level, sst3 is localized selectively to the plasma membrane of neuronal cilia, where its function is unclear (Handel *et al.*, 1999).

sst5 mRNA is the least abundant among all sst receptors in the brain. sst5 mRNA expression is absent from most brain regions. However, some expression of sst5 mRNA has been reported in hypothalamus and pituitary (Raulf *et al.*, 1994; Thoss *et al.*, 1995, 1996). Surprisingly, sst5-LIR was described in many brain areas including basal forebrain, hippocampus and hypothalamus (Stroh *et al.*, 1999), which is contradictory to the *in situ* hybridization analysis (Bruno *et al.*, 1993; Raulf *et al.*, 1994).

Taken together, both somatostatin and cortistatin are abundantly expressed in the cortex, where they are contained in different GABAergic local circuits and appear to play a role in disorders involving neuronal hyperexcitability (see below). sst1, sst2, sst3 and sst4 are highly expressed

in cerebral cortex and hippocampus. According to ligand binding studies, sst2 appears to be the most important sst receptor in cortex. However, little is known yet about the neuronal types expressing sst2 in the cerebral cortex.

1.6 Physiological and pathophysiological significance of somatostatin and cortistatin

The main physiological actions of somatostatin involve endocrine functions, cell proliferation, animal cognition and behaviour, as well as effects on neuronal excitability and neurotransmission (Epelbaum, 1986). The antiproliferative effects of somatostatin have been applied clinically for tumor treatment (De Herder *et al.*, 2003). Early studies indicated that somatostatin has locomotor effects on animals (Plotnikoff *et al.*, 1974; Cohn and Cohn, 1975; Rezek *et al.*, 1977). Depletion of somatostatin in the brain to 50% caused an impairment in the maintenance of learned behaviour (Fitzgerald and Dokla, 1989). More recently, several studies on somatostatin knock out and sst2 knock out mice have reported impaired spatial learning and different degrees of behavioural deficits of the animals (Viollet *et al.*, 2000; Zeyda *et al.*, 2001; Dutar *et al.*, 2002; Allen *et al.*, 2003).

Electrophysiological studies revealed a depressant effect of somatostatin on the excitability of cerebrocortical pyramidal neurons through membrane hyperpolarization, which is mediated by the activation of potassium currents and/or the inhibition of Ca^{2+} currents (Moore *et al.*, 1988; Schweitzer *et al.*, 1990; Hicks *et al.*, 1998). Similar mechanisms mediate the inhibitory effects of cortistatin on neuronal activity (de Lecea *et al.*, 1996). In addition, presynaptic inhibition of excitatory neurotransmission by somatostatin was described in rat hippocampal slices and cultures (Boehm and Betz, 1997; Tallent and Siggins, 1997). Consistently, electrophysiological studies using *ex vivo* hippocampal slice of sst2 knock out mice showed an enhanced glutamatergic transmission (Dutar *et al.*, 2002).

Various disorders of the CNS like Alzheimer's, Huntington's, Parkinson's disease as well as depression are associated with altered somatostatin expression (Aronin *et al.*, 1983; Arai *et al.*, 1984; Beal *et al.*, 1988; Francis *et al.*, 1987; Gabriel *et al.*, 1993; Molchan *et al.*, 1993).

The involvement of the somatostatinergic system has been studied most detailed in epilepsy models (i.e. kindling and status epilepticus). Microdialysis studies indicate increased release of somatostatin from rat hippocampal neurons during and after kindling (Vezzani *et al.*, 1992; Marti *et al.*, 2000). Similarly, increased release of somatostatin was also detected during status epilepticus (Manfridi *et al.*, 1991; Lahtinen *et al.*, 1992; Perez *et al.*, 1995b). Both, somatostatin mRNA levels and somatostatin immunoreactivity are increased after kindling (Piwko *et al.*,

1996; Schwarzer *et al.*, 1996). After kainate-induced status epilepticus, somatostatin-positive neurons are selectively lost in the dentate gyrus, with the surviving somatostatinergic neurons showing increased somatostatin expression (Sperk *et al.*, 1992). Also the human epileptic tissues exhibit a similar pattern in the somatostatin expression in the dentate gyrus (de Lanerolle *et al.*, 1989; Robbins *et al.*, 1991). Hippocampal sst3 and sst4 mRNA levels are decreased after kainate-induced seizures, which is consistent with the decreased binding sites in the same regions (Perez *et al.*, 1995b). SRIF₁ receptor binding sites (comprising sst2, sst3, sst5) decrease significantly in the dentate gyrus after kindling (Piwko *et al.*, 1996), which was suggested to be the consequence of increased somatostatin release. In summary, kindling appears to be associated with the activation of somatostatin-containing neurons and an enhanced release of somatostatin, which is thought to limit seizure spread. Status epilepticus is associated with the loss of somatostatinergic neurons, which may contribute to the occurrence of subsequent spontaneous seizures (Vezzani and Hoyer, 1999).

The involvement of somatostatin in seizure was demonstrated by the seizure-accelerating effect of the continuous infusion of a somatostatin antibody into the rat hippocampus (Monno *et al.*, 1993). Conversely, intracerebral application of somatostatin and octreotide exhibits anticonvulsive effects (Vezzani *et al.*, 1991; Mazarati and Telegdy, 1992). Furthermore, a recent study revealed that in somatostatin knock out mice, the seizure severity was increased (Buckmaster *et al.*, 2002). Anticonvulsant properties have also been described for cortistatin (Braun *et al.*, 1998). sst2 is suggested to mediate the anticonvulsive effects in the rat hippocampus, since bilateral infusion of RC160, a sst2 selective agonist, into the dentate gyrus of rats protected against chronic seizure susceptibility resulting from kainate treatment (Perez *et al.*, 1995b; Vezzani *et al.*, 2000).

Taken together, these data suggest that the somatostatin system plays an important role in neuronal disorders involving hyperexcitability and neurodegeneration of cerebrocortical structures.

1.7 Role of neuropeptides in brain ischemia

Middle cerebral artery occlusion (MCAO) in rats, which is an animal model for human stroke, causes severe neurodegeneration in the parietal cerebral cortex. The mechanisms of neurodegeneration in experimental stroke involve energy failure, acidosis, loss of calcium homeostasis, and free radical release. Of particular relevance, however, is the excessive release of glutamate and other excitatory amino acid neurotransmitters, which leads to an overactivation of NMDA, AMPA, KA receptors and excitotoxic neuronal death (Siesjo *et al.*, 1991).

Recent work suggests that neuromodulatory peptides may be involved in the pathophysiology of cerebral ischemia. Increased protein levels of neuropeptide Y, leu-enkephalin, dynorphin and neurotensin are found in the peri-infarct region and subcortical sites following MCAO (Allen *et al.*, 1995; Cheung and Cechetto, 1995). Expression of tachykinins and tachykinin receptors is changed in distinct inhibitory and excitatory cerebrocortical circuits after MCAO (Stumm *et al.*, 2001). Intracerebroventricular injection of a neuropeptide Y-Y1 receptor agonist increased the infarct volume following transient middle cerebral artery occlusion, while injection of a Y1 antagonist reduced the infarct volume (Chen and Cheung, 2003). Another neuropeptide, PACAP, has neuroprotective properties when applied before the onset of permanent ischemia (Reglodi *et al.*, 2002). Intracerebroventricular application of somatostatin, cortistatin and the sst2 agonist octreotide reduced the extent of damage after MCAO in rats (Rauca *et al.*, 1999). The sst receptor subtypes mediating the protective effect of these peptides and the signal transduction pathways involved remained to be characterized. An earlier *in vitro* study demonstrated a neuroprotective effect of somatostatin in NMDA-induced nonapoptotic neuronal death in cortical cells, which was suggested to be mediated by a cGMP pathway (Forloni *et al.*, 1997). Based on the well established role of the somatostatin system in cerebrocortical hyperexcitability in seizures and the protective effect of exogenous somatostatin in focal cerebral ischemia, the endogenous somatostatin system is supposed to be involved in excitotoxicity following MCAO. Currently, little is known about sst receptor expression in identified inhibitory or excitatory cortical circuits. Changes in the expression of cortistatin, somatostatin, and sst receptors as well as receptor internalization have not been analyzed after focal cerebral ischemia. In addition, somatostatin knock out mice and sst receptor knock out mice await to be studied in stroke models to test the hypothesis of the involvement of endogenous somatostatin system in cerebral ischemia.

1.8 Purpose of study

Somatostatin and cortistatin are considered to have the ability to modulate glutamatergic neurotransmission in the cerebral cortex. In addition, an involvement of the somatostatinergic system is suggested in neurological disorders which are caused by excitotoxic mechanisms. Since glutamate overexcitation plays a major role in ischemic brain damage, we hypothesized that the somatostatinergic system is involved in stroke pathophysiology. Therefore, the changes in the gene expression patterns of all members of the somatostatinergic system, and the activation of sst2 was studied in the rat forebrain after experimental stroke.

In particular, the following questions were addressed in normal and ischemic rats:

- Are there changes in the gene expression of somatostatin, cortistatin, sst1, sst2, sst4 and sst5 in the forebrain during the course of permanent focal ischemia?
- How are sst2, cortistatin, and somatostatin expressed in the cerebral cortex in relation to glutamatergic excitatory and GABAergic inhibitory neurons? How are these co-expression patterns influenced by focal cerebral ischemia?
- Is there *in vivo* internalization of sst2 in ischemic pathophysiology and can it be blocked by a sst2 antagonist?

2. Materials and Methods

2.1 Instruments

Microscope AX	Zeiss (Germany)
TCS-NT Laser Scanning Confocal Microscope	
	Leica (Heidelberg, Germany)
Gene Quant RNA/DNA Calculator	
	Biochrom (England)
PTC 200 Gene Amp PCR System	
	Biozym Diagnostik (Germany)
DNA sequencer 4000	Li-cor (Germany)
Electrophoresis power supply	BIO-RAD (USA)
Gel electrophoresis system	BIO-RAD (USA)
Gene Pulse II and Pulse Controller Plus	
	BIO-RAD (USA)

2.2 Kits

RNeasy Tissue Kit	QIAGEN (Hilden, Germany)
Midi Plasmid Purification Kit	QIAGEN (Hilden, Germany)
QIAquick PCR Purification Kit	QIAGEN (Hilden, Germany)
QIAquick Gel Extraction Kit	QIAGEN (Hilden, Germany)

2.3 Enzymes

Ampli Taq DNA Polymerase	Promega (Madison, USA)
Restriction endonucleases	Biolabs (New England)
RNA Polymerase (SP6, T3, T7)	Roche Diagnostics (Mannheim)
RNase A	Roche Diagnostics (Mannheim)
RNase T1	Roche Diagnostics (Mannheim)
Superscript TM II Reverse Transcriptase	
	Gibco (Eggenstein)
Sequenase	Amersham Pharmacia Biotech (USA)

2.4 Nucleic acids, vectors and probes

Nucleic acids:

tRNA	Roche Diagnostics (Mannheim)
0.25-9.5 kb RNA-ladder	Gibco (Eggenstein)
1 kb DNA-ladder	Gibco (Eggenstein)
100 bp DNA-ladder	MBI Fermentas (Vilnius, Lithuania)

Vectors:

pGEM-T Easy Vector	Promega (Madison, USA)
pcDNA3	Invitrogen (Karlsruhe, Germany)

2.5 Animals

Male Long-Evans rats (200-300 g) were from Mollegaard (Denmark) and Charles River (Sulzfeld, Germany). The animals were maintained under controlled light and environmental conditions (12/12 hr dark/light cycle; $23 \pm 1^{\circ}\text{C}$; 55% relative humidity) and were given food and water ad libitum.

2.6 Rat permanent focal cerebral ischemia

Permanent unilateral middle cerebral artery occlusion (MCAO) was performed in male Long-Evans rats (200-300 g) as introduced by Tamura *et al.* (1981) with modifications (Culmsee *et al.*, 1999). The rats were anesthetized with 40 mg/kg pentobarbital. An incision of 2 cm was made perpendicular to the line between the external auditory canal and the lateral canthus of the left eye. The skull close to the foramen ovale was exposed by removal of the temporal muscle. A burr hole of 2 mm was made with a handhold drill under the surgical microscope in order to expose the left middle cerebral artery. After the dura was excised, the left middle cerebral artery distal to the lenticulostriate branch was occluded by microbipolar electrocoagulation using a small vessel cauterizer. The occlusion step was omitted in sham-operated animals. After occlusion or sham operation, the incisions in the left temporal muscle and skin were sutured to ensure the function of the temporal muscle after surgery. During the surgical procedures, the body temperature was maintained at $37 \pm 0.5^{\circ}\text{C}$. To prevent a decrease of body temperature, the animals were kept at an environmental temperature of 30°C up to 2 hr after MCAO.

Experimental groups: For quantitative radioactive *in situ* hybridization, brains were collected from six decapitated rats at 6 hr, 1 d, 2 d and 4 d after MCAO and four rats 6 hr, 1 d, 2 d and 4 d after sham operation. For free floating immunocytochemistry, four animals at 3 hr, 6 hr, 1 d and 2 d after MCAO and four control rats were used. For immunocytochemistry with paraffin

embedded sections, four animals at 6 hr, 1 d, 2 d and 4 d after sham operation and MCAO were included.

Intracerebroventricular administration of sst2-selective antagonist BIM-23627: Before performing MCAO, the rats were prepared for intracerebroventricular injection. The rats were anesthetized by intraperitoneal injection of 40 mg/kg pentobarbital. A burr hole (coordinates: 0.25 mm posterior, 1.6 mm lateral from bregma) was drilled through the skull. Two weeks later, the animals were anesthetized with 40 mg/kg pentobarbital. BIM-23627 (Biomeasure, USA) was dissolved in saline at a concentration of 0.5 nM. 5 µl solution were injected 30 min prior to MCAO through the prepared drilled hole to a depth of 4 mm from the skull.

2.7 Cloning of cDNAs in transcription vectors

Extraction of total RNA: Frozen brain tissue was weighted and homogenized with a ultraturrax (Janke & Kunkel Inc., Germany) at 13000 rpm in a buffer containing guanidine isothiocyanate and 1% β -mercaptoethanol. RNA extraction was performed with the RNeasy Tissue Kit (QIAGEN, Hilden) according to the instructions of the manufacture. A QIAshredder Mini column (QIAGEN), phenol/chloroform purification as well as on column DNase digestion was included.

Reverse Transcription: The reverse transcription mix consisted of 250 ng/µl total RNA, 5 nM oligo(dT)15-18, 10 mM DTT, 500 µM dNTPs, and 20 units/µl superscript II reverse transcriptase in a 20 µl reaction volume. First, the RNA and the primers were denatured at 70°C for 10 min, cooled on ice and mixed with the rest of the reagents. The reaction mixture was incubated at 25°C for 10 min, followed by 42°C for 50 min and 95°C for 5 min. For contamination controls, water was used instead of RNA.

PCR: 2% of the reverse transcription product were used as template in a reaction volume of 50 µl. The PCR reaction mix contained 200 µM dNTPs, 200 µM primers, 0.02 units/µl ampli Taq DNA polymerase, and 2.5 mM MgCl₂. Amplifying steps included: 15-30 s at 94°C, 15-30 s at 50-65°C; 30-60 s at 72°C. Optimal conditions were determined for each primer pair. PCR products were subsequently cloned into pGEM-T Easy Vector (Promega).

Transformation and culture of Escherichia coli: Competent bacteria XL1 (Promega) and recombinant plasmid were mixed in precooled cuvette. Electroporation was performed in Gene Pulse II and Pulse Controller Plus (BIO-RAD, USA). The parameters are: resistance, 400 Ohms; capacitance, 25 µf; voltage, 1 kv; time constance, 7 ms. The bacteria were first grown in 500 µl non-selective LB medium at 37°C for 0.5-1 hr, then spread on selective agar-plates and grown at 37°C overnight. A single colony was picked from the plate to inoculate a

starter culture of 2-5 ml LB medium with selective antibiotics. The culture was incubated at 37°C for 8 hr with vigorous shaking. The starter cultures were further diluted 1:1000 in selective LB medium, and grown at 37°C for 12-16 hr with vigorous shaking.

Extraction of plasmid-DNA from cultures of Escherichia coli: Plasmids from bacteria cultures (5 ml or 50 ml) were extracted with Mini- or Midi-preparation kits (QIAGEN) according to the instructions.

2.8 Synthesis of RNA probes for *in situ* hybridization

For run-off-in-vitro-transcription (Melton *et al.*, 1984), the plasmids were linearized with restriction endonucleases and purified through phenol/chloroform extraction. Synthesis of [³⁵S]-labelled probes was done in the presence of 100-150 pmol [³⁵S]-labeled UTP and/or CTP in a total reaction volume of 10 µl. The reaction mix further contained 1 µg linearized plasmid-DNA, 10 mM dithiothreitol (DTT), 0.5 mM unlabeled nucleotides (without UTP and/or CTP). For digoxigenin-labelled probes, a 1 mM nucleotide mixture containing 0.35 mM digoxigenin-11-UTP (Roche, Mannheim) was used. The transcription was performed with SP6, T7 or T3 polymerase (Roche, Mannheim). After the transcription, the probes were subjected to mild alkaline hydrolysis to reduce their size (Angerer *et al.*, 1987). The labelled probes were finally purified with Micro Bio-Spin columns P-30 (BIO-RAD).

2.9 *In situ* hybridization

Probes used for in situ hybridization: cDNA fragments of rat pre-procortistatin (de Lecea *et al.*, nucleotides 4-286) and rat NPY (Allen *et al.*, 1987, nucleotides 89-467) were amplified from rat brain RNA extracts by RT-PCR. The cDNAs of pre-prosomatostatin (Goodman *et al.*, 1982, nucleotides 32-307), GFAP (glial fibrillary acidic protein, Cowan *et al.*, 1985, nucleotides 189-1054), rat C1q (Wood *et al.*, 1988, nucleotides 33-1040), rat BNPI (brain-specific Na⁺-dependent phosphate transporter, Li and Xie, 1995, nucleotides 1465-2024), and rat GAD 67 (glutamic acid decarboxylase, Wyborski *et al.*, 1990, nucleotides 1200-2041) were used previously (Stumm *et al.*, 2001, 2002). All cDNAs were subcloned into the pGEM-T Easy vector and subjected to double-strand DNA sequencing. cDNAs of rat somatostatin receptors sst1, sst2, sst3, sst4 and sst5 cloned in the pcDNA3 vector were provided by Dr. H.J. Kreienkamp (Kreienkamp *et al.*, 1998).

Tissue preparation: Animals were killed by chloral hydrate (10 g/kg body weight, i.p.). The removed brain was frozen in isopentane at -30°C to -40°C and cut in a cryostat. Sections were mounted on adhesive slides, and stored at -70°C. Before hybridization, frozen slides were air-

dried, fixed in 4% paraformaldehyde dissolved in phosphate-buffered saline (PBS) at 4°C for 1 hr, followed by treatment with 0.4% Triton-X 100 in PBS for 10 min. Next, slides were treated for 10 min with 1.5% tri-ethanolamine/PBS, containing 0.25% acetic anhydride (Sigma). Finally, slides were washed in water and dehydrated in isopropanol.

Hybridization and washing: Radioactive probes were diluted at 50000 dpm/μl in hybridization buffer (600 mM NaCl; 10 mM TrisCl pH 7.5; 1 mM di-Na-EDTA; 0.05% (w/v) tRNA; 1x denhardt's; 50% dextran sulfate; 100 μg/ml sonicated salmon sperm DNA; 50% formamide; 20 mM DTT). To each of the dried slides, 50 μl hybridization mixture was added. Hybridization was performed overnight at 60°C in humid chambers containing 50% formamide. Posthybridization procedures consisted of a sequence of washes with decreasing salt concentration. Briefly, the slides were rinsed in 2x SSC and 1x SSC before a 30 min treatment in RNase-buffer (10 mM TrisCl; pH 8.0; 0.5 M NaCl; 1 mM EDTA; 40 μg/ml RNase A; 1 unit/ml RNase T1) at 37°C. Then the slides were transferred to 0.2x SSC and incubated at 60°C for 1 hr. Subsequently, slides were washed in H₂O and dehydrated in isopropanol.

Detection of signals: The dried slides were exposed together with [¹⁴C]-standards (American Radiolabelled Chemicals, USA). A sheet of x-ray film (β-max. Amersham) was laid over the sections and exposed for 24 to 96 hr. Autoradiography was made by coating the slides with 50% NTB-2 liquid emulsion (Kodak). Exposure times for autoradiography were 1-6 weeks. Finally, sections were stained with 0.5% cresyl violet (Fluka, NeuUlm) in 60 mM sodium acetate and 340 mM acetic acid.

2.10 Quantitative analysis of radioactive *in situ* hybridization

Quantification of mRNA levels: Quantitative analysis of mRNA levels was performed as described (Stumm *et al.*, 2001) using a Macintosh computer equipped with NIH 1.62 software. X-ray autoradiograms were placed on an illuminator screen and captured with a IMAC-CCD S30 camera (Dresden, Germany). The [¹⁴C]-based standard on the same film was captured under the same conditions as the samples. For calibration, a standard curve was generated by measuring the optical densities of the film background and the [¹⁴C] standards. The obtained values were plotted against the tissue radioactivity equivalents of the standard (given in nCi/g brain tissue cut in 20 μm thick sections). Next, a threshold level was set to exclude pixel values below background density from the measurement. Areas of interest were selected by a manual drawing procedure before the tissue radioactivity content was measured. To obtain the mean value of a region of interest in a single animal, measurements of three sections were averaged. For statistic analysis, mRNA levels of a selected brain area were compared between animals

after MCAO (n=6) and the stage-matched sham-operated animals (n=4) using a non-paired two-way Student's *t* test. When naive animals (n=3) were also included, ANOVA and Newman-Keuls multiple comparison test were used. Values of $p < 0,05$ were considered statistically significant.

Quantitative analysis of the influence of MCAO on the neuronal numbers of specific cell types:

For some of the detected mRNAs, positive cells was counted in chosen cortical areas of identical size in the MCAO group (n=6) and stage-matched sham-operated group (n=4). Data analysis between the two groups were made by non-paired Student's *t* test. In particular, for cortistatin mRNA-positive neuron analysis, a naive group (n=3) was also evaluated, and one-way Anova test followed by Newman-Keuls multiple comparison was applied for the data analysis among the three groups. Values of $p < 0,05$ were considered statistically significant.

2.11 Combination of radioactive and non-radioactive *in situ* hybridization

Digoxigenin-labeled RNA probes were added to the hybridization mixture at a final concentration of 1 µg/ml. Hybridization and the post-washing were carried out as described above. After the final wash, the hybridized slides were shortly equilibrated in buffer 1 (100 mM Tris; 150 mM NaCl; pH7.5), blocked in blocking buffer (buffer 1 + 5% normal sheep serum; 0.05% Tween 20) and incubated overnight with alkaline phosphatase-conjugated anti-digoxigenin antibody (Roche, Mannheim) diluted 1:500 with blocking buffer. Next, slides were equilibrated with buffer 1 and buffer 2 (100 mM Tris-HCl; 100 mM NaCl; 0.05% Triton) each for 15 min before detection with 0.2 mM 5-bromo-4-chloro-3-indolyl-phosphate and 0.2 mM nitroblue tetrazolium (Boehringer, Mannheim). The colour reaction was stopped by washing the slides in distilled water. The slides were then dehydrated and coated with 50% K5-emulsion (Ilford, UK). The exposure time varied between 2 and 4 weeks.

For analysis of proportional co-expression of different interneuron markers, single- and double-labeled neurons were counted in the undamaged ipsilateral cingulate and frontal cortex of animals 2 d after MCAO, and in the corresponding areas in four rats after sham operation and three naive rats. To evaluate the co-expression pattern of sst2 with VGLUT1 (vesicular glutamate transporter 1, which was originally named as BNPI) or glutamic acid decarboxylase (GAD) mRNAs, counting was made in chosen areas in laminae II/III and V/VI of the penumbra 6 hr after MCAO and the corresponding areas of the sham group.

2.12 Immunohistochemistry

Antibodies: A rabbit anti-sst2a serum (9304) was used, which is essentially identical with the previously described antibody 6291 (Schulz *et al.*, 2000). Both antisera have been characterized

on sst2 knock out mice. Antiserum 9304 was used at a dilution 1:20000 for amplified detection with free-floating sections and 1:5000 with paraffin-embedded sections (see below). Affinity purified antiserum 6002 (Schreff *et al.*, 2000) against rat sst4 was used at 2.5 µg/ml with paraffin-embedded sections (see below). A mouse monoclonal somatostatin antibody (Biomedica) was diluted 1:50 for detection without amplification. A rabbit polyclonal somatostatin antibody provided by Dr. Günther Sperk (Sperk *et al.* 1992) was used at a dilution of 1:5000 for amplified detection of free-floating sections.

Paraffin-embedded tissue: Rats were deeply anesthetized with chloral hydrate, perfused transcardially with Tyrode's solution followed by 120 ml Bouin's fixative consisting of 100 parts 0.04 M copper-II-acetate/6% picric acid, 10 parts 37% formaldehyde and 1 part acetic acid. The brains were dissected, postfixed in the same fixative overnight and washed with 70% 2-propanol. Brains were dehydrated at 40°C in 70%, 80%, 96%, and 3x 100% 2-propanol for 1 hr each, followed by 3x 1 hr in xylol. Paraffin (melting point 56°C, Vogel Histo-Comp) was applied four times at 60°C for 1 hr. The brains were cut with a rotating microtome into 7 µm-thick sections and spread on adhesive slides. The sections were then placed on a heating plate at 43°C for full extension, dried at 58°C for 6-8 hr, and stored at room temperature for further use. After deparaffinization in xylol (3x 10 min) and blocking of endogenous peroxidase with methanol + 0.125% H₂O₂ (30 min), the slides were hydrated. Then, sections were heated at 92-95°C in citrate buffer (0.01 M sodium citrate; pH 6.0) for 25 min. After incubation for 30 min in 50 mM PBS containing 5% bovine serum albumin (BSA), the sections were incubated with primary antibody dissolved in 1% BSA-PBS. On the next day, a biotinylated secondary antibody diluted 1:200 in 1% BSA-PBS was applied and incubated for 2 hr at room temperature. Next, the avidin/biotin complex (ABC) linked to peroxidase (Vector laboratories) was applied. After washing, detection was performed with diaminobenzidine (DAB) and nickel (12.5 mg DAB-tetrahydrochloride, 75 mg ammoniumnickelsulfate-hexahydrate and 14 µl 30% H₂O₂ in 100 ml PBS). The sections were finally dehydrated in alcohol and coverslipped with DPX.

Free floating sections: Rats were deeply anesthetized with chloral hydrate and transcardially perfused with Tyrode's solution followed by Zamboni's fixative (4% paraformaldehyde; 0.2% picric acid in 0.1 M phosphate buffer, pH 7.4). Brains were dissected and postfixed in the same fixative for 2 hr at room temperature. Tissue was cryoprotected by immersion in 30% sucrose for 48 hr at 4°C before being cut with a freezing microtome. Free-floating sections (30-40 µm) were washed in TPBS (10 mM phosphate buffer; 137 mM NaCl; 0.05% thimerosal; pH 7.4) before a 30 min treatment with 50% methanol. After washing with TPBS/0.3% Triton, the

sections were first pre-incubated with TPBS/3% normal goat serum (NGS) for 1 hr, and then incubated with primary antibodies diluted in TPBS/0.3% Triton/1% NGS for 48-96 hr. The primary antibody was detected by either anti-mouse or anti-rabbit secondary antibody coupled with fluorescence cyanine 3.18 for 2 hr or overnight. In some cases amplification was included, in which biotinylated anti-rabbit or anti-mouse secondary antibodies were applied, followed by sequential application of ABC complex and biotin-tyramine. Cyanine 3.18-conjugated streptavidin (Amersham) was applied for detection. The sections were dehydrated in increasing graded series of alcohol and coverslipped with DPX (Sigma).

The sections were imaged with a Leica TCS-NT laser-scanning confocal microscope (Leica Microsystem, Germany). Cyanine 3.18 was imaged with 568 nm excitation and 570-630 nm bandpass emission filters, Cyanine 5.18 was imaged with 647 nm excitation and 665 nm longpass emission filters.

Immunocytochemistry and internalization assay: The wild-type rat sst2a receptor was tagged at its amino-terminus with the T7 epitope tag sequence MASMTGGQMG using polymerase chain reaction and subcloned into a pcDNA3 expression vector (Invitrogen) containing a neomycin resistance. Human embryonic kidney (HEK) 293 cells were obtained from ATCC and grown in Dulbecco's modified Eagle's medium supplemented with 10% fetal calf serum in a humidified atmosphere containing 10% CO₂. Transfection was performed using Lipofectamine 2000 according to the instructions of the manufacturer (Invitrogen). Stable transfectants were selected in the presence of 500 g/ml G418 (Invitrogen). For immunocytochemistry, cells were grown on poly-L-lysine-treated coverslips overnight, fixed with Zamboni's fixative for 30 min and permeabilized with methanol. Then they were incubated with affinity-purified anti-T7 antibody at a concentration of 1 µg/ml in TPBS with 1% NGS overnight. Bound primary antibody was detected with biotinylated secondary antibodies followed by cyanine 3.18-conjugated streptavidin. The cells were then dehydrated, cleared in xylol, and mounted in DPX.

For internalization assays, HEK 293 cells were preincubated with 1 µg/ml of affinity-purified rabbit anti-T7 antibody for 2 hr in OPTIMEN 1 (Invitrogen) at 4°C, then treated with 1 µM somatostatin-14 (SS-14), or 1 µM BIM-23627, or both 1 µM SS-14 and 1 µM BIM-23627 in OPTIMEN at 37°C for 30 min. Subsequently, the cells were fixed and incubated with peroxidase-conjugated anti-rabbit antibody (1:1000; Amersham) for 2 hr at room temperature. After washing, the plates were developed with 250 µl of ABTS solution (Roche). After 10-30 min, 200 µl of the substrate solution from each well was transferred to a 96-well plate and analyzed at 405 nm using a microplate reader (BIO-RAD).

3. Results

3.1 Spatiotemporal development of brain infarction after MCAO

In the present study, the involvement of the somatostatinergic system in the cerebral cortex after ischemic brain damage was studied using male Long-Evans rats that were subjected to permanent middle cerebral artery occlusion (MCAO). First, the infarction of brain tissue was verified by the absence of cresyl violet (CV) staining from the lesioned area. Analysis of serial CV-stained coronal sections was performed along the rostro-caudal axis of the forebrain 6 hr, 1 d, 2 d, and 4 d after MCAO. This procedure identified the temporal and spatial process of focal degeneration of brain tissue.

Six hours after unilateral MCAO, tissue degeneration was limited to the ipsilateral parietal cortex in the forebrain (Fig. 1A), extending rostro-caudally from bregma +2.2 mm to bregma -4.8 mm. At 1 d after onset of focal ischemia, the focus was more developed in comparison to 6 hr, since it included also the ipsilateral forelimb cortex and the dorsal part of insular cortex. The ipsilateral cingulate and frontal cortex and striatum were intact (Fig. 1B). After 1 d, the focus extended from bregma +2.7 mm to bregma -4.8 mm in the longitudinal axis. The panorama of the infarct along the longitudinal axis of the brain 1 d postocclusion is shown in figure 2. From 2 d to 4 d after focal ischemia, the size of the infarct was not further increased as compared with 1 d.

Notably, beginning 1 d after sham operation, a small area of infarcted brain tissue was observed in laminae I-III at the trepanation site (not shown). Degeneration of brain tissue remote to the lesion site was not observed in sham-operated animals.

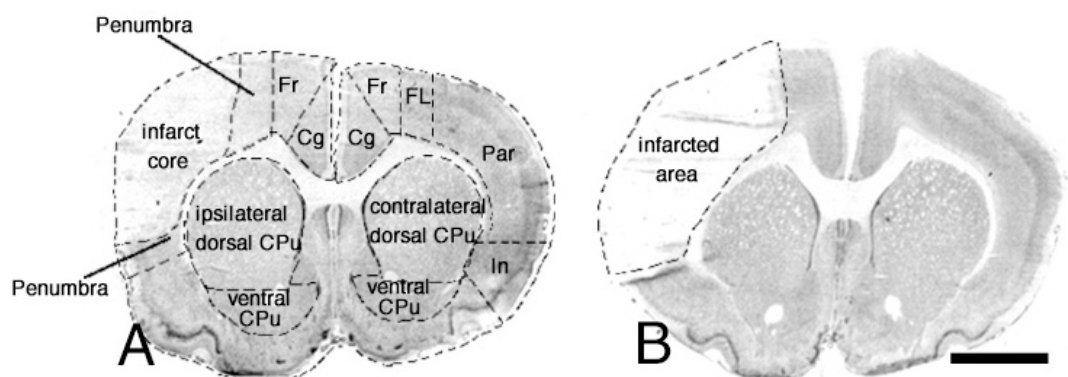


Figure 1. The development of the infarct from 6 hr to 1 d after MCAO. Shown are cresyl violet (CV)-stained coronal sections through rat forebrains at bregma +1.0 mm 6 hr (A) and 1 d (B) after MCAO. Infarcts can be determined by the absence of CV-staining. A, 6 hr after ischemia, the infarct core is relatively small as compared with 1 d (B). It includes mainly ipsilateral parietal cortex (Par). Note the cortical areas directly neighbouring the infarct (penumbra) appear less stained than the normal tissue. B, the penumbral area in A is not detectable any more at 1 d after MCAO. Delineated by dotted lines is the infarcted area, which includes the forelimb area (FL), parietal cortex and dorsal part of insular cortex (In). The cingulate (Cg) and frontal cortex (Fr) are not infarcted. CPu: caudate putamen. Scale bar: 3 mm.

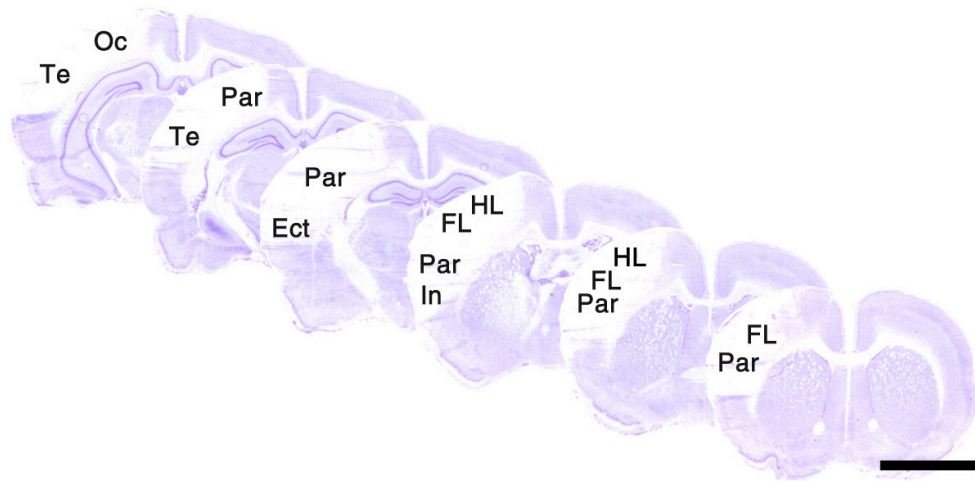


Figure 2. Demonstration of a representative infarct along the longitudinal axis of a rat brain. Depicted is a series of cresyl violet (CV)-stained sections from a rat subjected to MCAO for 1 d. Rostro-caudally, the infarct extends from bregma +2.7 to bregma -4.8. The following cerebrocortical areas are infarcted: parietal cortex (Par), forelimb area (FL), hindlimb area (HL), insular cortex (In), ectothalamic cortex (Ect), temporal area (Te) and occipital cortex (Oc). Scale bar: 5 mm.

3.2 Astroglial and microglial reaction, macrophage infiltration

To further characterize the applied model of focal brain ischemia, spatial and temporal patterns of astroglial and microglial reactions after MCAO and sham operation were characterized by gene expression analysis using the *in situ* hybridization technique. The astrogliosis was visualized by hybridizing a [35 S]-labeled probe to the mRNA of the intermediate filament glial fibrillary acidic protein (GFAP), which is synthesized specifically by astroglia and upregulated after cell activation (Fig. 3E-H,M-P) (Eng, 1985; Belluardo *et al.*, 1996; Yamashita *et al.*, 1996). Similarly, the expression of the mRNA of the complement component C1q-beta was studied, which is selectively expressed by cells of the microglia/monocyte/macrophage lineage (Schwaebler *et al.*, 1995; Haga *et al.*, 1996). Since the C1q-beta mRNA levels are strongly increased in activated macrophages and microglial cells in the CNS (Schafer *et al.*, 2000), the patterns of microglial activation and macrophage infiltration after focal ischemia are identified as strongly stained areas in the autoradiograms of the hybridized sections (Fig. 3A-D,I-L).

6 hr after focal ischemia: In the infarcted area (ipsilateral parietal cortex), both GFAP and C1q mRNA levels were strongly decreased (Fig. 3A,E, asterisks) as compared with the corresponding area in sham-operated animals (Fig. 3I,M). Together with the reduced CV-staining in this area (Fig. 1A), this indicates the early degeneration of both types of glial cells as well as neurons in the infarct. Outside the primary infarct, both GFAP and C1q expression

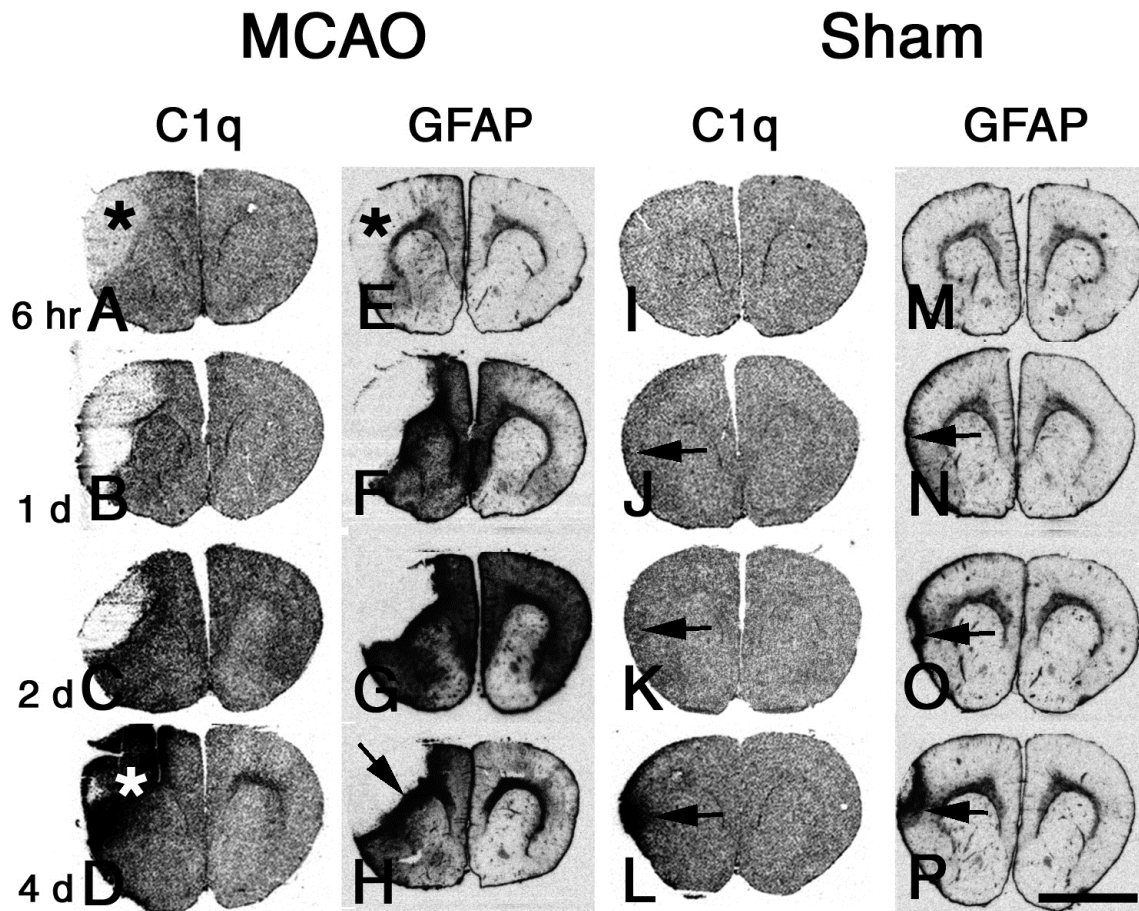


Figure 3. Spatio-temporal patterns of microglial and astroglial activation after focal cerebral ischemia. X-ray film autoradiographs of coronal sections through the forebrain at the level of bregma +1.2 mm are shown. Gene expression of C1q (A-D, I-L) and GFAP (E-H, M-P) at different time points after occlusion of the middle cerebral artery (MCAO, A-H) as well as sham operation (Sham, I-P). *6 hr after ischemia (A,E,I,M):* A slight decrease of the C1q mRNA levels and a strong decrease of GFAP mRNA levels are present in the infarcted region of cerebral cortex (A,E, asterisks). Both C1q (A) and GFAP (E) expression in the ipsilateral non-infarcted cerebral cortex and striatum is slightly increased. *1 d after ischemia (B,F,J,N):* C1q and GFAP mRNAs decrease strongly inside the infarct. Both C1q and GFAP mRNAs show a strong increase in the ipsilateral hemisphere (B,F) as compared with sham operation (J,N). GFAP expression is also increased in the contralateral areas (F). *2 d after ischemia (C,G,K,O):* Both C1q and GFAP mRNAs reach peak levels in the ipsilateral as well as contralateral hemispheres, including cerebral cortex, corpus callosum and striatum. *4 d after ischemia (D,H,L,P):* C1q mRNA levels are intensively increased inside the infarct (D, asterisk). Outside the infarct, C1q mRNA levels are almost as low as those in the sham-operated rat (L); GFAP mRNAs decrease massively in the ipsi- and contralateral hemispheres except in the perifocal area (H, arrow), where GFAP mRNA signals remain elevated, forming a rim around the infarct. I-P, comparison of the ipsilateral with the contralateral hemisphere of sham-operated rats [mRNA levels in the contralateral side are virtually equal to those in the naive brain (not shown)], GFAP and C1q mRNA expression is moderately increased in a limited cortical area directly at the trepanation site from 1 d to 4 d after sham operation (J-L, N-P, arrows). Scale bar: 5 mm.

levels were slightly increased in the ipsilateral hemisphere (Fig. 3A,E) as compared with sham-operated animals (Fig. 3I,M).

1 d after ischemia: In the infarcted area, expression of both GFAP and C1q was very low to absent (Fig. 3B,F). At this time point, CV staining exhibited virtually no viable cells in the infarct core (Fig. 2). Together, these results indicate the degeneration of the remaining cells in this area. Outside the primary lesion, both GFAP and C1q expression levels were strongly increased, reflecting activation of astroglia and microglia in the nonlesioned ipsilateral

hemisphere, including cortex, corpus callosum and striatum (Fig. 3B,F). In the contralateral side, a moderate increase in GFAP mRNA levels was detected (Fig. 3F), indicating a gradual spreading of astrocyte activation cross to the contralateral hemisphere. Activation of microglial cells was limited mostly to the ipsilateral hemisphere.

2 d after ischemia: Expression of GFAP and C1q mRNAs remained largely absent from the focus (Fig. 3C,G). Outside the infarct, almost all regions exhibited signs of microglial and astroglial activation (Fig. 3C,G). As compared with 1 d and 4 d after MCAO, GFAP and C1q expression outside the focus reached peak levels. Generally, glial reactions were stronger in the areas close to the infarct, than the regions distant to the infarct, with the contralateral striatum showing the weakest signs of glial activation (Fig. 3C,G).

4 d after ischemia: GFAP mRNA levels were decreased in nonlesioned areas as compared with 2 d. Only in the perifocal area, hybridization signals for GFAP remained elevated, forming a rim around the lesion (Fig. 3H, arrow). In contrast to GFAP, C1q mRNA expression was massively increased inside the infarct (Fig. 3D, asterisk). In the other areas, levels of C1q expression were decreased as compared with 2 d after MCAO (Fig. 3C,D).

Sham operation: In sham-operated rats, GFAP- and C1q- mRNA expression was increased in the brain area directly subjacent to the trepanation site (Fig. 3J-L,N-P arrows). Together with the absence of CV staining in the same area, this indicates that the sham operation is associated with a local degeneration of brain tissue and a minor glial activation at the trepanation site.

The analysis of the spatio-temporal patterns of brain tissue degeneration and glial activation after MCAO indicated that brain damage was induced in the MCA-related territory shortly after the onset of ischemia. Astroglial and microglial cells were activated first in the adjacent cortical area, then the glial activation spreads gradually to the contralateral hemisphere. C1q mRNA levels increased within the infarcted core 4 d postocclusion, which points to the infiltration of macrophages/microglia. The persistent increase of GFAP expression in the perifocal area reflects the formation of an astroglial scar. With consideration of the sham operation-induced small cortical infarction and local glial activation, stage-matched sham-operated control animals were included into further analysis, in order to discriminate between sham operation- and MCAO-induced effects.

3.3 Constitutive expression of somatostatin, cortistatin, sst1, sst2, and sst4 in the forebrain

The constitutive gene expression patterns of the somatostatin receptors (sst-receptors) and the endogenous sst-receptor ligands, somatostatin (SRIF) and cortistatin (CST), were analyzed in the forebrain of naive rats with the help of *in situ* hybridization histochemistry. Figure 4 shows x-ray autoradiograms of coronal sections through the septal areas hybridized with riboprobes for preprosomatostatin (A), preprocortistatin (E), sst2 (B), sst2a (F), sst1 (C), sst4 (D), and sst5 (H) mRNAs. To control the specificity of the hybridization, the respective sense-strand probes were used. In figure 4G, the result of the hybridization of the sst1-sense probe is shown, which is representative for other sense-strand probes. Similar results were obtained, when non-labelled antisense probe was added in excess to the corresponding radioactively labelled antisense probe (not shown).

Somatostatin, cortistatin: A high density of somatostatin hybridization signals could be seen scattered throughout the cerebral cortex. In the striatum, the signal density for somatostatin mRNA was lower than in the cortex (Fig. 4A). In contrast to the widespread gene expression of somatostatin, cortistatin mRNA expression was limited to the cerebral cortex. Within the cortex, cortistatin was expressed at higher levels in the deep layers and at weaker levels in the superficial layers (Fig. 4E).

sst1: Among all of the somatostatin receptors, sst1 was the most highly expressed receptor in the cerebral cortex at the mRNA level. sst1 mRNA signals were concentrated in laminae II, V and VI of the cerebral cortex and in the piriform cortex. No hybridization signal for sst1 mRNA was detected in the striatum (Fig. 4C).

sst2: The sst2 mRNA exists in two alternatively spliced isoforms (sst2a, sst2b). In the rat, sst2a mRNA contains an exon, which is not present in sst2b. Here, we used a riboprobe directed against the entire sst2-coding region, which does not discriminate between sst2a and sst2b (Fig. 4B). In addition, a riboprobe directed against the sst2a-selective exon was used (Fig. 4F). sst2 mRNA was expressed highly and homogeneously in laminae V/VI of the cerebral cortex (Fig. 4B). Other regions of the forebrain exhibiting strong sst2 receptor mRNA were the lateral and medial septum, ventral diagonal band, endopiriform nucleus, claustrum and piriform cortex. sst2 mRNA levels were close to the detection limit in the striatum (Fig. 4B). Hybridization with the sst2a-selective probe revealed an identical expression pattern as with the probe for both sst2 isoforms (Fig. 4F).

sst4: Within the cortex, sst4 gene expression was at highest level in laminae V and VIb, and to a less extent, in lamina II. Strong sst4 gene expression was also observed in the piriform cortex

and the olfactory tubercle. In the lateral septum, the diagonal band and the striatum, *sst4* gene was expressed at moderate levels (Fig. 4 D).

sst3 and *sst5*: Diffuse hybridization signals for *sst3* mRNA were seen throughout the forebrain (not shown). Expression levels of the *sst5* gene in the forebrain were at or below the detection limit (Fig. 4H).

In summary, the mRNAs of the peptides somatostatin and cortistatin are highly expressed in the cerebral cortex. Due to the abundant expression of *sst1*, *sst2*, and *sst4* in the cortex, these receptors are expected to be the prevalent *sst* receptors mediating local neuromodulatory effects of somatostatin and cortistatin. Gene expression of *sst5* was not detected in cortex. With regard to the involvement of somatostatin and its receptors in excitotoxic neuronal disorders (Vezzani *et al.*, 2000; Binaschi *et al.*, 2003), we next analyzed the effect of permanent occlusion of the MCA on gene expression of somatostatin, cortistatin, *sst1*, *sst2*, *sst4*, and *sst5* in the forebrain. The *sst3* receptor has been reported to be localized selectively in the plasma membrane of neuronal cilia (Handel *et al.*, 1999). Since neuronal functions of this receptor are unknown, further analysis of *sst3* expression was not performed.

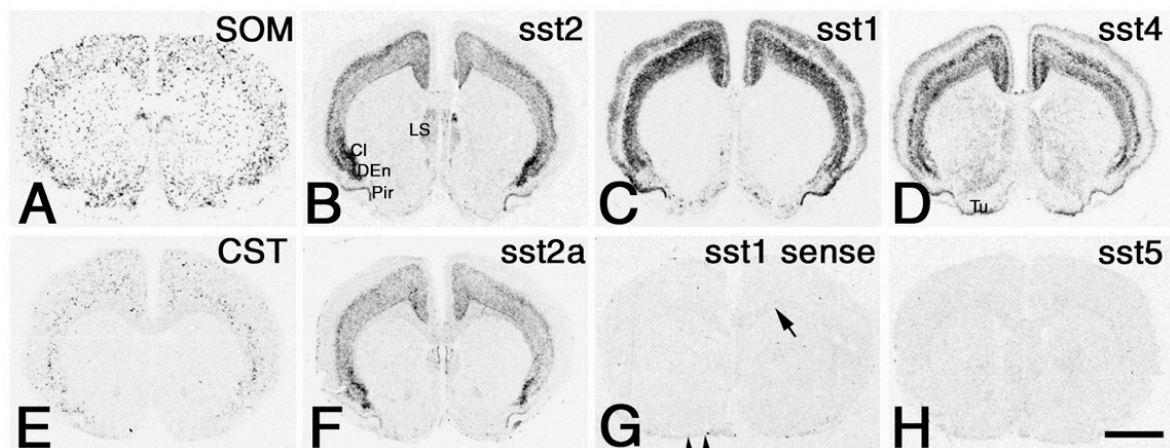


Figure 4. X-ray film autoradiographs of coronal sections after *in situ* hybridization for somatostatin (A), cortistatin (E), *sst2* (B), *sst2a* (F), *sst1* (C), *sst4* (D) and *sst5* (H) mRNAs of naive rat brains at septal level. *In situ* hybridization of *sst1* sense probe is shown as representative control (G). A, somatostatin mRNA is highly expressed by numerous scattered neurons throughout the forebrain. B, F, the distribution of *sst2* and *sst2a* mRNAs is identically abundant and homogeneous in laminae V/VI. Strong expression of both *sst2* and *sst2a* is also detected in lateral septum (LS), dorsal endopiriform cortex (DEn), claustrum (Cl) and piriform cortex (Pir). In the striatum, the *sst2/sst2a* mRNA levels are low. C, *sst1* mRNA is most prominent in laminae V/VI and piriform cortex, and less abundant in laminae II. *sst1* mRNA is absent from striatum. D, *sst4* mRNA is mainly concentrated laminae V/VIIb, and to a less extent in lamina II. Moderate *sst4* mRNA levels are also localized in piriform cortex, olfactory tubercle (Tu) and striatum. E, CST mRNA is highly and exclusively expressed in scattered neurons throughout the cerebral cortex. G, control for (C), hybridized with sense riboprobe for *sst1*. Faint, non-specific hybridization signals were present in the corpus callosum (arrow), and occasionally in the meningeal circumference of the brain (double arrowheads). H, *sst5* mRNA is not detected in the forebrain. Scale bar: 3 mm.

3.4 Gene expression patterns of somatostatin, cortistatin, sst1, sst2, and sst4 in the cerebral cortex after focal cerebral ischemia

In the infarcted area, expression levels of somatostatin, cortistatin, sst1, sst2, and sst4 were strongly reduced at 6 hr after MCAO (Fig. 5B,G,L,Q,V), as compared with the same region of sham-operated animals. Expression of those genes in the infarct was undetectable at 1 d after occlusion of the MCA and at later stages (Fig. 5C-E,H-J,M-O,R-T,W-Y). The reduction of gene expression of somatostatin, cortistatin, sst1, sst2 and sst4 in the infarct paralleled the gradual neurodegeneration in this area, which was identified in CV-stained sections of each animal.

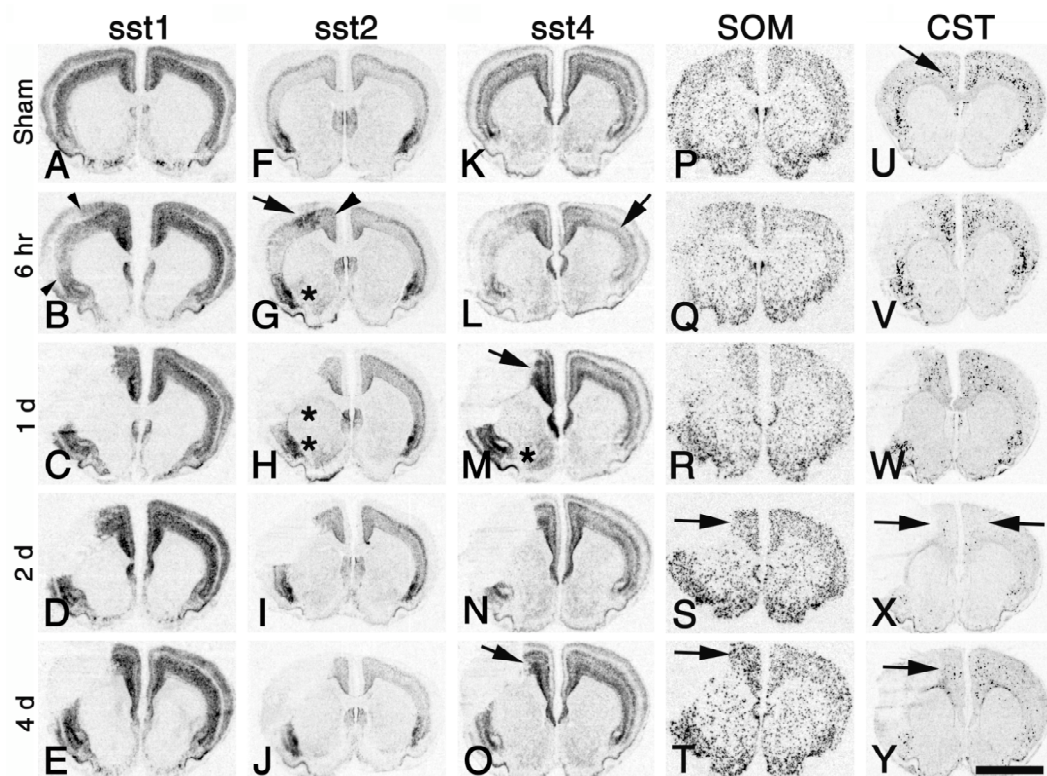


Figure 5: Patterns of changes in sst1(A-E), sst2 (F-J), sst4 (K-O), pre-prosomatostatin (SOM, P-T) and pre-procortistatin (CST, U-Y) mRNAs in the rat forebrain after middle cerebral artery occlusion (MCAO). Low-power x-ray autoradiographs of hybridized coronal sections from rats 6 hr, 1 d, 2 d and 4 d after focal ischemia, and representative sham-operated animals for each gene at the time point with the most pronounced change in expression after MCAO (A, 1 d; F, 6 hr; K, 1 d; P,U 4 d). Borders of the infarct are marked by arrowheads in B. A-E, sst1 levels are largely unaltered in non-infarcted cortical areas after MCAO (B-E) as compared with A. G, at 6 hr after MCAO, sst2 levels are increased strongly in perifocal cortical areas (arrow) and moderately in the deep layers of cingulate and frontal cortex (arrowhead). H-J, sst2 expression levels in the cortex at 1 d, 2 d, and 4 d after focal ischemia are mostly unchanged as compared with F. Striatal sst2 levels are increased in the ventral part at 6 hr (G, asterisk) and in both ventral and dorsal parts at 1d after MCAO (H, asterisks). K-O, at 1 d after MCAO, sst4 expression levels are strongly increased in non-infarcted cortical areas in the ipsilateral hemisphere (M, arrow). The depicted animal exhibits a marked upregulation of sst4 mRNA levels in the ipsilateral striatum (M, asterisk) as compared with K (changes in sst4 expression the striatum were observed only in a subpopulation of animals after 1 d). sst4 levels at 2 d after focal ischemia are unchanged (N) as compared with K. At 4 d, sst4 mRNA levels are slightly increased in ipsilateral exofocal area (O, arrow). P-T, somatostatin expression levels are moderately increased ipsilaterally in non-infarcted brain areas at 2 d and 4 d after focal ischemia (S,T, arrows) as compared with P. U-Y, CST mRNA levels are strongly reduced in the ipsi- and/or contralateral cortical hemispheres at 1 d, 2 d, and 4 d after MCAO (X,Y, arrows) as compared with U. Note that 4 d after sham operation, CST levels in the ipsilateral cortical areas (U, arrow) are slightly decreased as compared with the contralateral side. Scale bar: 5 mm.

Table1. Influence of MCAO on SRIF, sst1, sst2, and sst4 mRNA levels in cerebral cortex and caudate-putamen

		6 hr MCAO	1 d MCAO	2 d MCAO	4 dMCAO
sst1	Penumbra	60±47			
	Cg/Fr (i)	81±28	128±31	99±23	127±36
	Cg/Fr (co)	84±28	73±16	100±25	96±25
	Par (co)	61±18	102±12	105±19	101±37
sst2	Penumbra	206±42**			
	Cg/Fr (i)	137±23*	98±44	103±19	90±15
	Cg/Fr (co)	98±11	101±13	97±19	83±15
	Par (co)	101±12	112±17	117±9	84±22
	dCPu (i)	109±47	299±116*	117±83	62±55
	dCPu (co)	50±27	267±137	119±33	73±54
	vCPu (i)	363±158*	495±97**	42±11	146±104
	vCPu (co)	87±30	230±115	117±27	79±40
sst4	Penumbra	77±35			
	Cg/Fr (i)	114±17	173±49*	106±18	134±13*
	Cg/Fr (co)	89±14	105±9	99±12	115±13
	Par (co)	71±18*	87±11	104±22	123±33
	dCPu (i)	44±33	160±105	124±69	62±21
	dCPu (co)	83±61	43±32	163±160	171±63
	vCPu (i)	94±49	186±138	83±66	73±30
	vCPu (co)	84±27	53±38	154±93	116±54
SRIF	Penumbra	96±14			
	Cg/Fr (i)	109±27	98±16	171±32*	161±33*
	Cg/Fr (co)	110±27	98±22	160±18*	124±12
	Par (co)	112±30	103±28	151±43	125±58
	dCPu (i)	112±27	80±19	150±32*	142±32*
	dCPu (co)	126±47	92±33	159±38*	147±40
	vCPu (i)	104±25	77±12	128±36	127±28
	vCPu (co)	103±13	104±17	125±21	114±28

Values express mean mRNA levels \pm SD at 6 hr, 1 d, 2 d, and 4 d after middle cerebral artery occlusion (MCAO, n=6) as percentage of mean mRNA levels at 6 hr, 1 d, 2 d, and 4 d after sham operation (n=4). * $p < 0.05$; ** $p < 0.01$ versus stage-matched sham-operated groups; Student's t test. Areas of interest: Cg, cingulate cortex; Fr, frontal cortex; Par, parietal cortex; dCPu and vCPu, dorsal and ventral caudate putamen; co, contralateral side; i, ipsilateral side.

In addition to the loss of gene expression in the infarct, distinct changes in the expression patterns of somatostatin, cortistatin, sst2 and sst4 were observed in non-lesioned brain areas after MCAO. In order to quantify these changes, quantitative *in situ* hybridization analysis was performed in the forebrain. In the brain hemisphere ipsilateral to MCAO, mRNA levels were measured in the cortical penumbra, the cingulate/frontal areas of the cortex, and the dorsal and ventral striatum (see Fig.1A). Contralaterally, gene expression analysis was made in the parietal cortex (area corresponding to the infarct), the cingulate/frontal cortex, and the striatum (see Fig. 1A). Measurements of gene expression levels in the penumbra were performed only at 6 hr after MCAO, all other areas were evaluated at 6 hr, 1 d, 2 d and 4 d after MCAO. Changes in gene

expression levels were expressed as percent of the levels of the corresponding area in stage-matched sham-operated animals (Table 1).

3.4.1 Opposite regulation of somatostatin and cortistatin gene expression in the non-lesioned cerebral cortex

The overall distribution pattern of somatostatin-expressing cells observed in the forebrain of naive rats (Fig. 4A) was virtually unaltered in non-lesioned areas of the forebrain after MCAO and sham operation (Fig. 5P-T). However, there was a slight increase in somatostatin mRNA levels in the ipsilateral side 2 d and 4 d after focal ischemia (Fig. 5S,T, arrows).

Quantitative analysis of the ipsilateral cingulate/frontal cortical areas revealed, that somatostatin mRNA levels were increased by 71% and 61% ($p < 0.05$; Table 1) at 2 d and 4 d after MCAO, respectively, as compared with the corresponding area of the stage-matched sham groups. Somatostatin mRNA levels were also increased by 60% ($p < 0.05$; Table 1) at 2 d after MCAO in the contralateral cingulate/frontal cortex.

Table 2. Influence of MCAO on numbers of SRIF and CST mRNA-positive neuron in the cingulate cortex

	Control	2 d Sham	2 d MCAO
SRIF	66±1	61±4	63±3
CST	29±2	18±3**(-38%)	8±2**††(-73%)

Indicated are average numbers of SRIF and CST mRNA-positive neurons per mm² ± SD in naive animals (Control, n=3), 2 d after sham operation (2 d Sham, n=4), and 2d after middle cerebral artery occlusion (2 d MCAO, n=6). Bold values represent percent change as compared with the control group set as 100%. ** $p < 0.01$ versus control group; †† $p < 0.01$ versus sham-operated group; one-way ANOVA followed by Newman-Keuls multiple comparison.

To identify, whether the increase in somatostatin mRNA levels in the cortex after MCAO was due to an increase in somatostatin-positive cells or an increase in somatostatin mRNA levels per neuron, emulsion coating of the hybridized sections was performed (see Fig. 13A-D). Somatostatin-positive cells were counted in a 1.5 mm² square of the ipsilateral cingulate cortex of rats 2 d after MCAO and rats 2 d after sham operation. The measured density of somatostatin-expressing neurons was approximately 60 per mm² in both groups (Table 2). However, individual neurons in the ipsilateral cingulate/frontal cortex of rats 2 d and 4 d after MCAO presented stronger hybridization signals (Fig. 13C,D, reflected by the brighter appearances of scattered neurons) than those in control animals (Fig. 13A), indicating increased somatostatin mRNA levels in these cells.

In contrast to somatostatin, expression of the cortistatin gene was strongly decreased in non-lesioned cerebrocortical areas after focal ischemia. Decreased expression of the cortistatin mRNA occurred first in the penumbra at 6 hr after focal ischemia and propagated in the cortex. The decrease persisted up to 4 d (Fig. 5V-Y, arrows). Expression of cortistatin was decreased in

both hemispheres, although the ipsilateral hemisphere was more affected than the contralateral. Remarkably, cortistatin mRNA expression in the cerebral cortex was reduced also in sham-operated animals ipsilaterally (Fig. 5U, arrow). This effect was more pronounced at 6 hr in the penumbra. There was only a minor decrease in cortistatin expression in the cortex contralateral to the sham-operation (Fig. 5U).

Table 3. Influence of MCAO on cortistatin mRNA levels in cerebral cortex

	Sham				MCAO			
	6 hr	1 d	2 d	4 d	6 hr	1 d	2 d	4 d
Cg/Fr(i)	60±24	63±33	53±36*	57±21	62±14	34±10**	12±5***†	16±4***†
Cg/Fr(co)	52±26	72±23	78±41	76±27	49±20	26±12**	12±5***††	57±21
Par(i)	52±18	66±48	87±47	94±24				
Par(co)	51±19	54±18	85±35	93±37	42±16	32±14*	23±14*†	78±48
Penumbra	51±8**				40±10**			

Values express mean mRNA levels ± SD at 6 hr, 1 d, 2 d, and 4 d after sham operation (Sham, n=4) and middle cerebral artery occlusion (MCAO, n=6) as percentage of naive animals (n=3). * $p < 0.05$; ** $p < 0.01$ versus naive group; † $p < 0.05$; †† $p < 0.01$ versus stage-matched sham-operated group; one-way ANOVA followed by Newman-Keuls multiple comparison test. Areas of interest: Cg, cingulate cortex; Fr, frontal cortex; Par, parietal cortex; co, contralateral side; i, ipsilateral side.

In order to quantify changes in cortistatin gene-expression after MCAO and sham operation, cortistatin expression levels were determined in untreated animals and compared to either of the operated groups. In addition, cortistatin mRNA levels were compared between MCAO-treated and stage-matched sham-operated groups. The comparison of naive and ischemic animals revealed that cortistatin mRNA levels were decreased by 60% in the penumbra. In the ipsilateral non-lesioned cingulate/frontal areas, cortistatin expression was reduced by 66%, 88% and 84% at 1 d, 2 d, and 4 d postocclusion, respectively ($p < 0.01$ each; Table 3). In the corresponding contralateral area, cortistatin mRNA levels were decreased by 74% and 88% ($p < 0.01$ each; Table 3) at 1 d and 2 d after MCAO, respectively. In the contralateral parietal cortex, cortistatin mRNA levels were decreased by 68% and 77% ($p < 0.05$; Table 3) at 1 d and 2 d after MCAO. The comparison of naive and sham-operated animals revealed a significant decrease of cortistatin mRNA levels only ipsilaterally in forelimb area at 6 hr (-49%, $p < 0.01$) and in the cingulate/frontal cortex at 2d (-47%, $p < 0.05$; Table 3) after sham operation. The comparison of ischemic and sham-operated animals revealed statistically significant differences between the two groups at 2 d after MCAO in both hemispheres, and at 4 d in the ipsilateral cingulate/frontal cortex (Table 3).

Numbers of cortistatin-positive cells per area were determined 2 d after MCAO and sham operation in the ipsilateral cingulate/frontal cortex and compared with naive animals. Numbers

of cortistatin-positive neurons were reduced by 73% ($p < 0.01$; Table 2) in ischemic animals, and by 38% ($p < 0.01$; Table 2) in sham-operated animals, respectively.

3.4.2 Downregulation of cortistatin gene expression in somatostatin-negative neurons

Expression of cortistatin in the cerebral cortex is known to be present in somatostatin-positive and somatostatin-negative neurons (de Lecea *et al.*, 1997; this study). A large proportion of the latter population is characterized by the expression of the calcium-binding protein, parvalbumin (PV). To evaluate the impact of focal ischemia on the phenotypes of cortistatin-expressing neurons in the cerebral cortex, simultaneous *in situ* hybridization with radioactively- and DIG-labelled riboprobes was performed. Analysis of the co-expression was limited to the ipsilateral cingulate/frontal cortical areas of rats 2 d after ischemia, when the changes of cortistatin mRNA expression were most pronounced, and the corresponding areas of naive animals.

Table 4. Semiquantitative analysis of the influence of MCAO on co-expression patterns of SRIF and CST in the cingulate and frontal cortex

	SRIF	CST	co-positive	%co-positive/ SRIF-positive	%co-positive/ CST-positive
Control	188±36	74±30	40±14	17%	35%
2 d MCAO	216±5	4±2	21±4	8%	84%

Data express numbers of SRIF-expressing, CST-expressing and SRIF/CST co-positive neurons \pm SD in the cingulate and frontal cortex of naive animals (Control, n=3) and animals 2 d after middle cerebral artery occlusion (2 d MCAO, n=6), and the percentage proportion of co-positive neurons in both population.

In naive rats, cortistatin mRNA was co-expressed by 17% of the somatostatin mRNA-positive neurons and by 31% of parvalbumin mRNA-positive neurons (Fig. 6B,C, arrows; Table 4,5). After ischemia, cortistatin was expressed by 8% of somatostatin mRNA-positive neurons and only by 1% of parvalbumin mRNA-positive neurons (Fig. 6E,F, arrows; Table 4,5).

Table 5. Semiquantitative analysis of the influence of MCAO on co-expression patterns of CST and parvalbumin in the cingulate and frontal cortex

	PV	CST	co-positive	%co-positive/ PV-positive	%co-positive/ CST-positive
Control	168±17	52±15	77±15	31%	60%
2 d MCAO	250±64	15±6	3±2	1%	17%

Data express numbers of parvalbumin-expressing (PV), CST-expressing (CST) and PV/CST co-positive neurons \pm SD in the cingulate and frontal cortex of naive animals (Control, n=3) and animals 2 d after middle cerebral artery occlusion (2 d MCAO, n=6), and the percentage proportion of co-positive neurons in both population.

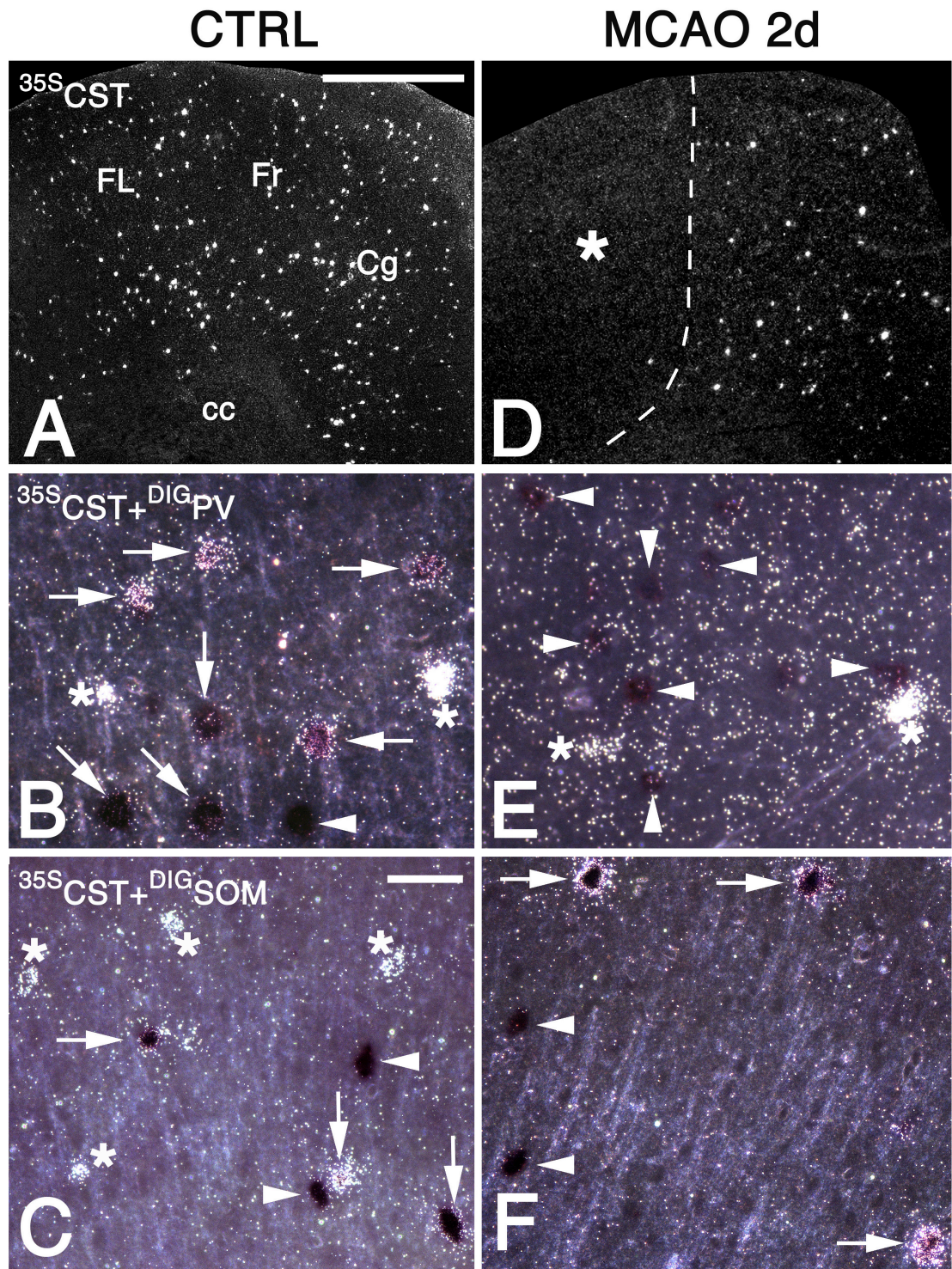


Figure 6. Phenotypes of neurons expressing cortistatin (CST) mRNA 2 d after middle cerebral artery occlusion (MCAO). *A, D*, low-power darkfield micrographs of the cingulate (Cg), frontal (Fr) and forelimb (FL) areas of a naive rat cortex (CTRL) and the corresponding regions of the ipsilateral cortex of a rat subjected to focal ischemia (MCAO 2 d) after hybridization with a [^{35}S]-labelled probe for CST mRNA (^{35}S CST). *A*, CST mRNA is expressed by numerous neurons throughout all cortical layers. *D*, the infarcted (asterisk) and non-infarcted areas are delimited by a dashed line. Note in the non-infarcted cortical areas, the number of CST-expressing cells is strongly reduced as compared with *A*, CST-expression is undetectable in the infarct (*D*). *B, C, E, F*, for phenotype identification of CST-expressing neurons, simultaneous hybridization with a [^{35}S]-labelled probe for CST mRNA (seen as *grains* in *B, C, E, F*) and digoxigenin-labelled probes for parvalbumin ($^{\text{DIG}}$ PV, *B, E*) or somatostatin ($^{\text{DIG}}$ SOM, *C, F*) mRNAs was performed ($^{\text{DIG}}$ PV and $^{\text{DIG}}$ SOM are detected by colored enzymatic reaction products in *B, C, E, F*). Shown are high-power darkfield micrographs from lamina V of the frontal cortex of an untreated rat (*B, C*) and the corresponding area of the cortex ipsilateral to 2 d MCAO (*E, F*). *B*, the co-expression analysis reveals

a PV-positive neuron (arrowhead), CST/PV-copositive neurons (arrows), and CST-positive neurons (asterisks) in the untreated cortex. *E*, after focal ischemia, CST-positive (asterisks) and PV-positive neurons (arrowheads), but no CST/PV-positive neurons are observed. *C*, detection of SOM-positive neurons (arrowheads), CST-positive neurons (asterisks), and CST/SOM-copositive neurons (arrows) in the untreated rat cortex. *F*, presence of SOM-positive (arrowheads) as well as CST/SOM-copositive neurons (arrows), and absence of CST-positive neurons 2 d after focal ischemia. cc, corpus callosum. Scale bars: *A,D*, 1.25 mm; *B,C,E,F*, 100 μ m.

Since the numbers of somatostatin and parvalbumin mRNA-positive neurons per area were unchanged after focal ischemia, these data indicated that the downregulation of cortistatin gene expression occurred preferentially in the parvalbumin-positive neuronal population of cortistatinergic neurons. Expression of the cortistatin gene in the somatostatin-expressing subpopulation was less affected by focal ischemia.

Neuropeptide Y (NPY) is selectively expressed by a subpopulation of somatostatinergic neurons in the cerebral cortex, NPY-expressing somatostatin-negative neurons are seen only rarely (Kawaguchi *et al.*, 1998). To determine, whether somatostatin/cortistatin-neurons overlap with somatostatin/NPY-neurons, co-expression of neuropeptide Y and cortistatin was analyzed as well. This revealed, that in naive rats, 36% of NPY-positive neurons contained cortistatin. Conversely, 18% of cortistatin-expressing neurons were positive for neuropeptide Y mRNA (Fig. 7).

Taken together, our *in situ* hybridization analysis of somatostatin and cortistatin mRNAs showed that the expression of both genes was largely unaffected in the non-lesioned areas at 6 hr postocclusion. However, the expression of both genes was changed 2 d and 4 d after MCAO. While somatostatin mRNA levels were moderately increased in the ipsilateral cortex, cortistatin mRNA levels were strongly

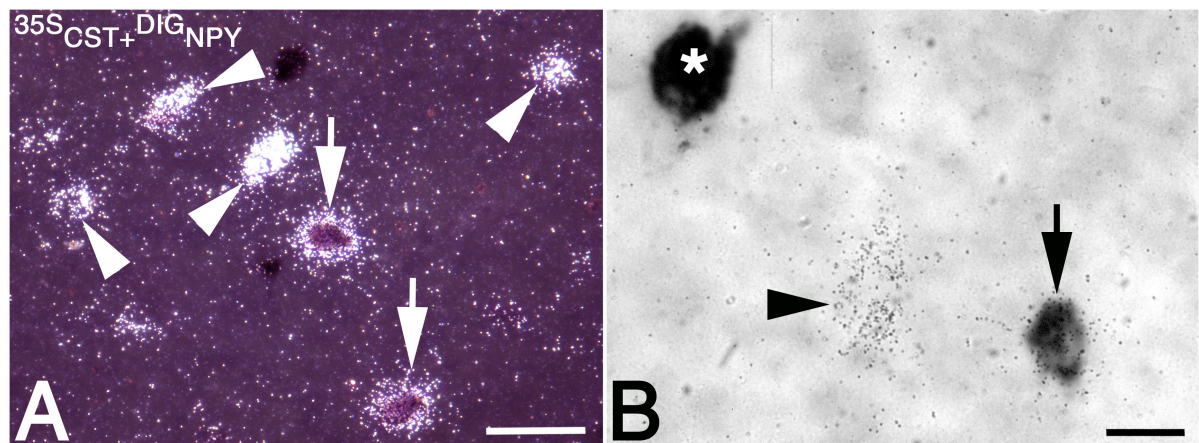


Figure 7. Co-expression of NPY and CST in neurons in cingulate cortex. Double *in situ* hybridization of the CST- and NPY-mRNA was performed by the use of a [35 S]-labelled probe for CST mRNA and a digoxigenin (DIG)-labelled probe for NPY mRNA. DIG-labelled mRNA is detected by dark-colored reaction products, and [35 S]-labelled CST mRNA is detected by grains. Lower-power darkfield (*A*) and higher-power brightfield (*B*) pictures are taken from lamina V of frontal cortex of a naive rat. NPY/CST-copositive neurons (arrows), NPY-positive neurons (asterisks) and CST-positive neurons (arrowheads) are detected. Scale bar: *A*, 50 μ m; *B*, 20 μ m.

decreased in both cortical hemispheres. Since the number of somatostatin-expressing cells per cortical area was unaltered after MCAO, somatostatin mRNA expression was most likely increased in neurons constitutively expressing this gene, and not *de novo* induced in somatostatin mRNA-negative cortical cells. Our co-expression analysis showed, that cortistatin was partially co-expressed with somatostatin in the cerebral cortex. The somatostatin/cortistatin-expressing neuronal population overlaps only partially with the NPY-containing neuronal population. After focal ischemia, cortistatin mRNA expression remained detectable in a subpopulation of somatostatin-positive neurons, but was undetectable in the vast majority of parvalbumin-expressing neurons, which are somatostatin-negative.

3.4.3 Differential regulation of *sst1*, *sst2*, *sst4*, and *sst5* receptor mRNA expression

By quantitative *in situ* hybridization, we found that no changes in the distribution patterns and the levels of *sst1* mRNA at the evaluated time points after focal ischemia (Fig. 5B-E). Expression levels of *sst5* were still at or below the detection threshold after ischemia (Fig. 8).

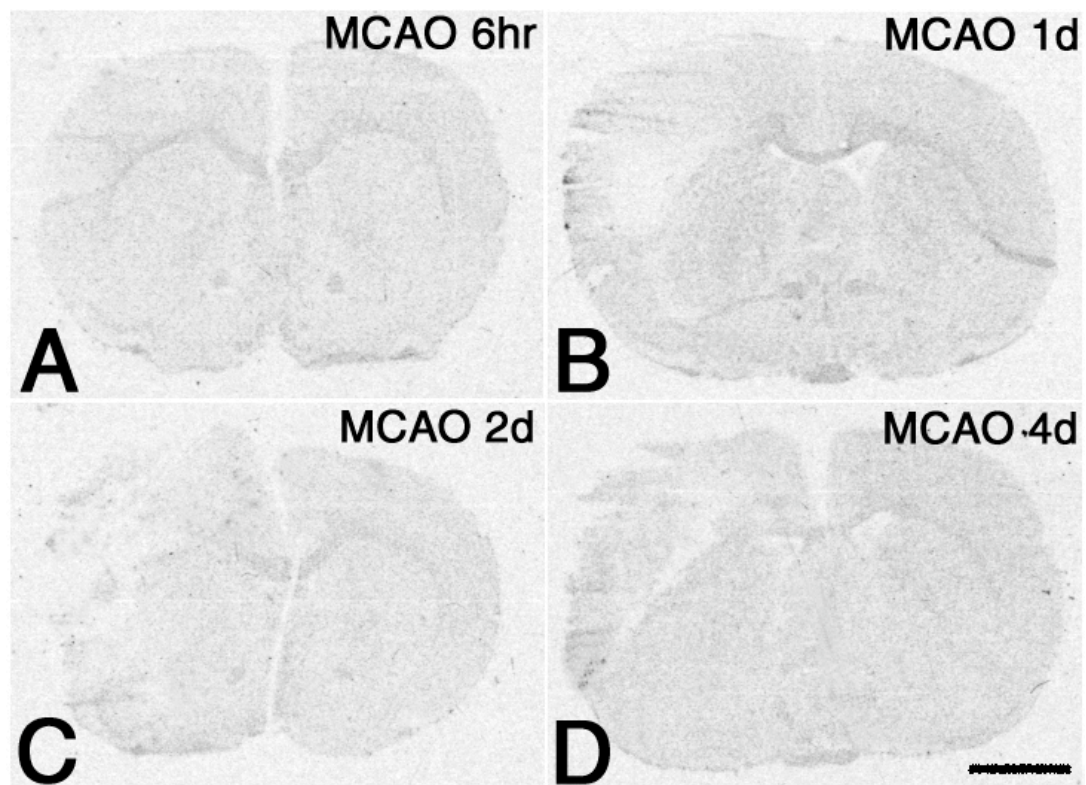


Figure 8. Absence of *sst5* mRNA in the rat forebrain after focal cerebral ischemia. Depicted are x-ray autoradiographs of coronal sections after *in situ* hybridization for *sst5* mRNA. *sst5* mRNA is not detectable in the forebrain at 6 hr (A), 1 d (B), 2 d (C) and 4 d (D) after MCAO. Scale bar: 3 mm.

In contrast, distinct changes in the expression patterns of *sst2* and *sst4* were observed subsequent to MCAO.

3.4.3.1 Transient upregulation of *sst2* gene expression in the perifocal and exofocal cortex

Detected with the probe directed to the entire *sst2*-coding region, a robust increase of *sst2* expression was observed in the perifocal cortical area 6 hr after MCAO (Fig. 5G, arrow; for identification of cortical subregions, see Fig. 1). Less pronounced changes in *sst2* expression were observed ipsilaterally in the cingulate/frontal cortical areas at the same time point (Fig. 5G, arrowhead). No changes were observed in the contralateral side. Similar changes were detected with the probe selective for *sst2a* mRNA (not shown). Patterns of *sst2* and *sst2a* expression were not altered in the cortex of sham-operated rats (Fig. 5F). Measurement of *sst2* mRNA levels revealed increases by 106% in the perifocal area ($p < 0.01$; Table 1), and by 37% ($p < 0.05$; Table 1) in the ipsilateral cingulate/frontal cortex as compared with sham-operated rats. From 1 d to 4 d after MCAO, both the distribution patterns and the mRNA levels of *sst2* and *sst2a* were unchanged in the non-lesioned cortical areas of the brain (Fig. 5H-J).

The distribution of *sst2*-expressing neurons in the cerebral cortex was analyzed in detail in emulsion-dipped sections. As demonstrated in darkfield micrographs, *sst2* mRNA-positive neurons were present only occasionally in laminae II/III and very frequently in laminae V/VI in the cortex of naive and sham-operated rats (Fig. 9A,B).

Pronounced changes in the expression pattern of *sst2* were observed 6 hr after MCAO in the perifocal area of the cortex. In laminae II/III, numerous neurons were positive for *sst2* mRNA (Fig. 9D, arrow, E, double arrows). In laminae V/VI, *sst2* expression levels were strongly increased, which was reflected by considerably higher silver grain density in individual neurons (Fig. 9E, arrow) than in those of the corresponding area of sham-operated animals (Fig. 9B, arrow). Similar changes were observed, when the *sst2a*-selective probe or the probe for all *sst2*-isoforms were used (Fig. 9C,F).

Cell counting analysis in the perifocal cortex 6 hr after MCAO revealed a 40 fold increase in the number of *sst2*-positive cells per area in laminae II/III ($p < 0.01$), and 1.9 fold in laminae V/VI as compared with the corresponding areas of sham-operated animals ($p < 0.05$; Table 6).

Together, these findings suggest, that increased *sst2* mRNA levels in the perifocal cortex were due to an upregulated expression in neurons constitutively synthesizing *sst2* mRNA, as well as induced expression of *sst2* in neurons, in which constitutive *sst2* mRNA expression levels were below the detection limit.

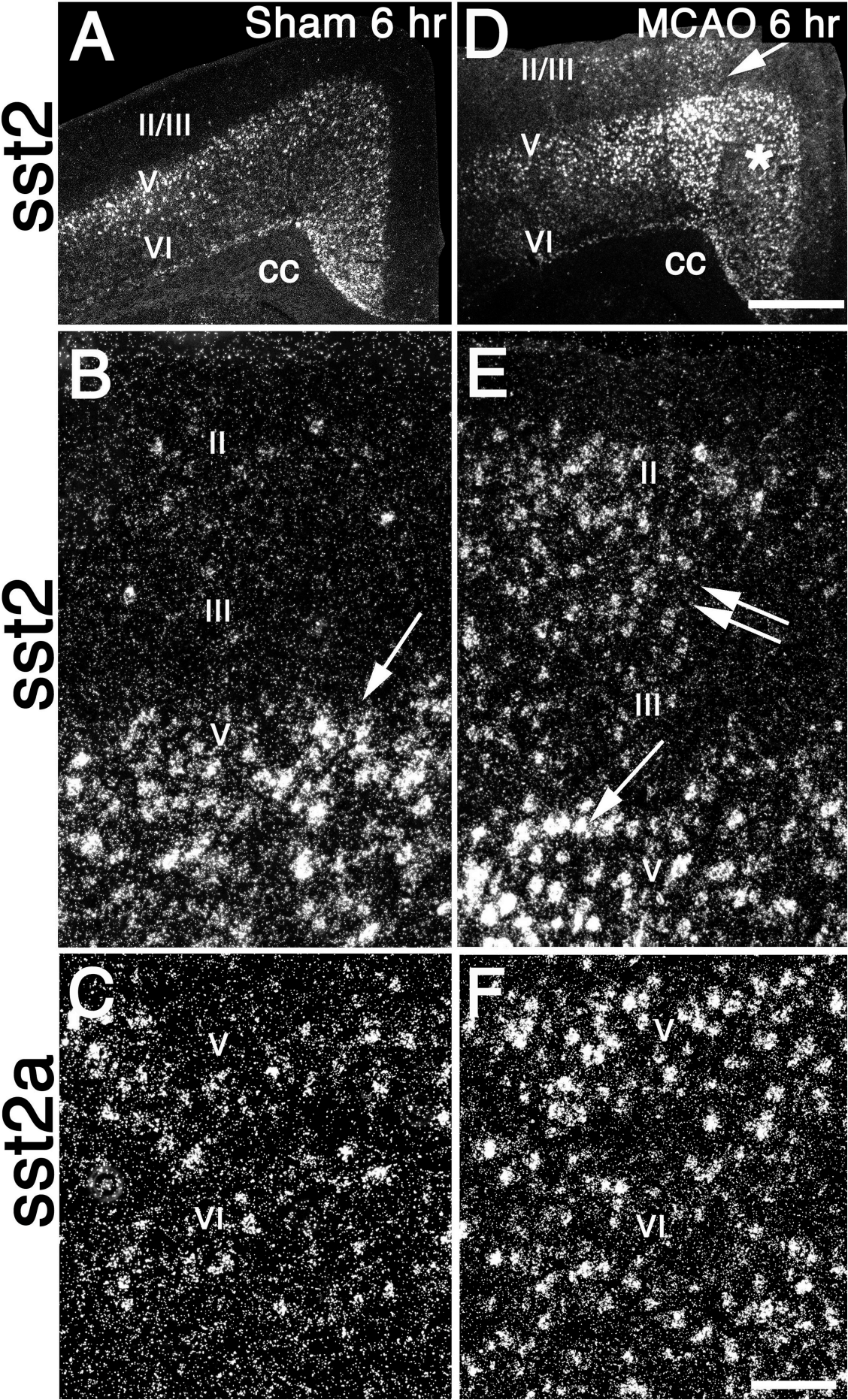


Figure 9. Upregulation of *sst2* and *sst2a* in the perifocal area 6 hr after MCAO. Radioactive *in situ* hybridization was performed with a riboprobe detecting all *sst2* isoforms (*A,B,D,E*) and a riboprobe specific for *sst2a* (*C,F*). *A, D*, Low-power darkfield micrographs of the cingulate, frontal, forelimb and parietal areas of the cerebral cortex after hybridization for *sst2* mRNA were taken from the ipsilateral side of a rat 6 hr after sham operation (*A*), and a rat 6 hr after MCAO (*D*). *A*, in sham-operated rat, *sst2* mRNA is concentrated highly in laminae V/VI. *D*, *sst2* mRNA is greatly induced in laminae II/III and strongly increased in laminae V/VI in the perifocal area (arrow) of the ischemic rat as compared with sham-operated rat (*A*). In the exofocal cingulate and frontal cortex, *sst2* mRNA levels are moderately increased in laminae V (asterisk) and unchanged in laminae II/III as compared with *A*. High-power darkfield micrographs focus on laminae II/III (*B,E*) and laminae V/VI (*C,F*) of the perifocal area of the ischemic rat and the corresponding region of the sham-operated rat. *B*, in a sham-operated rat, there are only few neurons positive for *sst2* mRNA in laminae II/III, in contrast to the massive *sst2* expression of neurons located in deep layers (laminae V, arrow). *E*, 6 hr after ischemia, remarkably more neurons are detected positive for *sst2* mRNA in laminae II/III (double arrows) and lamina V (arrow) of the perifocal area, as compared with the sham-operated rat (*B*). *C*, in the sham-operated rat, *sst2a* mRNA is expressed in many neurons in laminae V/VI. *F*, elevated *sst2a* mRNA levels per neuron as well as increase of the *sst2a*-positive neuron number are noticed in laminae V/VI of perifocal area of the 6 hr ischemic rat as compared with corresponding area in the sham-operated rat (*C*). Scale bar: *A,D*, 1 mm, *B,C,E,F*, 150 μ m.

Table 6. Influence of MCAO on numbers of *sst2* mRNA-positive neuron in the penumbral cortex

	6 hr Sham	6 hr MCAO
Layers 2/3	11 \pm 5	57 \pm 22** (+420%)
Layers 5/6	95 \pm 17	278 \pm 133* (+190%)

Indicated are average numbers of *sst2* mRNA-positive neurons per mm² \pm SD 6hr after sham operation (6 hr Sham, n=4), and 6hr after middle cerebral artery occlusion (6 hr MCAO, n=6). Evaluated were layers 2/3 and 5/6 of the penumbral cortex after MCAO and the corresponding areas in the sham group. Bold values represent percent change as compared with the sham group set as 100%. * $p < 0.05$; ** $p < 0.01$ versus sham-operated group; Student's *t* test.

3.4.3.2 Selective upregulation of *sst2* mRNA expression in glutamatergic neurons

Next, the MCAO-induced *sst2* gene upregulation in relation to GABAergic and glutamatergic neuronal phenotypes was characterized. GABAergic neurons were identified by the detection of glutamic acid decarboxylase (GAD) mRNA, which is an established marker for GABAergic interneurons. Since vesicular glutamate transporter 1 (VGLUT1) is known to be present in almost all excitatory pyramidal neurons in the cerebral cortex, VGLUT1 mRNA was detected for identifying this excitatory neuronal type (Freneau *et al.*, 2001; Varoqui *et al.*, 2002). Co-expression analysis was performed in the perifocal area of the cortex 6 hr after MCAO. Expression patterns in superficial and deep cortical layers were evaluated individually.

Laminae II/III: Cell counting of double- and single-labelled neurons revealed that 73% of *sst2*-positive neurons expressed GAD mRNA in sham-operated rats (Fig. 10A; Table 7). In contrast, 6 hr after MCAO only 13% of the *sst2*-positive neurons expressed GAD mRNA (Fig. 10B; Table 7). Because the number of GAD mRNA-expressing neurons per cortical area was unchanged 6 hr after MCAO, these data indicated that focal ischemia induced *sst2* gene expression in non-GABAergic neurons in laminae II/III. This is supported by the result that in

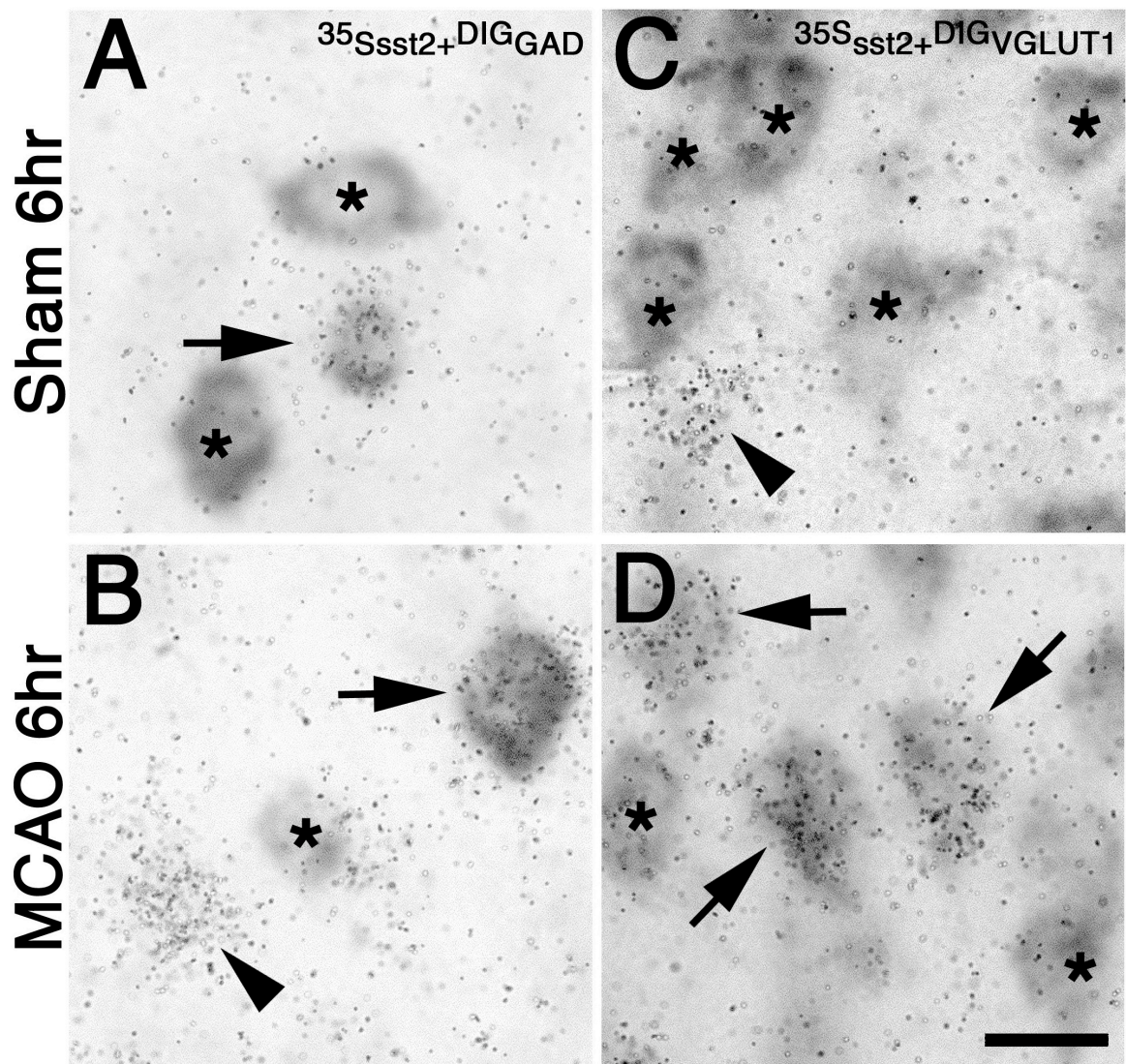


Figure 10. Phenotype identification of *sst2*-expressing neurons in the superficial layer of the perifocal cerebral cortex. Simultaneous hybridization of a [^{35}S]-labelled probe for *sst2* mRNA (seen as grains in *A-D*) with digoxigenin-labeled probes for glutamic acid decarboxylase ($^{\text{DIG}}$ GAD, *A,B*) or vesicular glutamate transporter 1 ($^{\text{DIG}}$ VGLUT1, *C,D*) mRNAs was performed ($^{\text{DIG}}$ GAD and $^{\text{DIG}}$ VGLUT1 mRNAs are detected as colored enzymatic reaction products in *A-D*). Shown are high-power brightfield micrographs taken from lamina III of the perifocal cortex of a rat 6 hr after MCAO and the corresponding region of a rat 6 hr after sham operation. *A*, in the sham-operated rat, one neuron co-expressing both *sst2*- and GAD-mRNAs (arrow), and two GAD mRNA-positive neurons (asterisks) are detected. *B*, in the cortex of the 6 hr ischemic rat, a neuron positive for *sst2* and GAD mRNA (arrow), a neuron positive for GAD mRNA (asterisk), and one positive for *sst2* mRNA (arrowhead) are identified. *C*, in the sham-operated rat, neurons positive for VGLUT1 (asterisks) or *sst2* (arrowhead) mRNA are identified, but *sst2*/VGLUT1 co-positive neurons are absent. *D*, in the ischemic rat, *sst2* and VGLUT1 mRNAs are frequently co-expressed (arrows). Note the absence of *sst2* mRNA in two neurons that are positive for VGLUT1 mRNA (asterisks). Scale bar: 20 μm .

the rats subjected to MCAO, 86% of *sst2*-expressing neurons were found to co-express VGLUT1 mRNA (Fig. 10D; Table 7), whereas only 25% of *sst2*-positive neurons co-expressed VGLUT1 in the sham-operated animals (Fig. 10C; Table 7).

Thus, *sst2* expression was induced in a substantial subpopulation of glutamatergic pyramidal neurons in laminae II/III after MCAO.

Laminae V/VI: In sham-operated rats, 95% of sst2-positive neurons expressed VGLUT1 mRNA. Only 6% of sst2-positive neurons expressed GAD (Table 7). In rats subjected to 6hr MCAO, similar proportion of sst2-positive neurons were GAD-positive (5%, Table 7) and VGLUT1-positive (96%, Table 7) as in sham-operated rats. Conversely, 59% of VGLUT1-positive neurons were sst2-positive in sham-operated rats, and 94% of these neurons were sst2-positive after ischemia. sst2 expression in GAD-positive neurons was 11% 6 hr after sham-operation and 14% after MCAO (data are not shown).

Table 7. Semiquantitative analysis of the influence of MCAO on co-expression patterns of sst2 with VGLUT1 and sst2 with GAD in the penumbral cortex

		%sst2-VGLUT1 co-positive/ sst2-positive	%sst2-GAD co-positive/ sst2-positive
Layers 2/3	6 hr Sham	25%	73%
	6 hr MCAO	86%	13%
Layers 5/6	6 hr Sham	95%	6%
	6 hr MCAO	96%	5%

Data are the proportion of glutamatergic sst2-positive neurons from all sst2-positive neurons (sst2-VGLUT1 co-positive/ sst2-positive) and the proportion of GABAergic sst2-positive neurons from all sst2-positive neurons (sst2GAD co-positive/ sst2-positive) in the penumbral cortex 6 hr after middle cerebral artery occlusion (MCAO, n=6) and in the corresponding area 6 hr after sham operation (Sham, n=4).

Taken together, the co-expression analysis indicated, that although glutamatergic neurons in laminae II/III are largely sst2-negative, more than half of these neurons contains sst2 in laminae V/VI. After MCAO, sst2 was upregulated in many glutamatergic neurons in the perifocal areas throughout laminae II-VI. In contrast, sst2 was expressed only in a small population of cerebrocortical GABAergic neurons both in sham-operated and in ischemic rats.

3.4.3.3 Regulation of sst4 expression in the cerebral cortex

6 hr after ischemia: In contrast to sst2, expression of the sst4 gene was largely unchanged in the perifocal cortex. Surprisingly, sst4 mRNA levels were decreased contralaterally in the parietal cortex (Fig. 5L, arrow), which corresponds to the infarcted area on the ipsilateral side. Quantitatively, sst4 mRNA levels were decreased by 29% ($p < 0.05$) in the contralateral parietal cortex as compared with the corresponding area 6 hr after sham operation. sst4 expression was unchanged in the cingulate/frontal areas of the cortex, both ipsilaterally and contralaterally.

1 d-4 d after ischemia: An increase in sst4 gene expression by 73% ($p < 0.05$, Table 1) was noticed in the ipsilateral cingulate/frontal cortex (Fig. 5M, arrow) as compared with the sham-operated group. Changes in sst4 expression in the cerebral cortex on the contralateral side were not observed. At later stages no changes except a slight increase in ipsilateral cingulate/frontal cortex was detected at 4 d (+34%, Table 1; Fig 5O, arrow).

3.4.3.4 Regulation of somatostatin- and sst2-expression in the striatum

In about 20% of ischemic animals, occlusion of the MCA caused an infarction in the lateral part of the striatum. In degenerated striatal tissue, mRNA expression of sst receptors, somatostatin and cortistatin was not detected. In the intact parts of the striatum, MCAO was associated with strong changes in sst2 expression and subtle changes in somatostatin expression. Changes in the gene expression levels were determined in the ventral and dorsal parts of the striatum after focal ischemia in comparison to sham-operated animals, revealing an upregulation of sst2 expression by 263% ($p < 0.05$; Table 1) in the ipsilateral ventral striatum after 6 hr (Fig. 5G, asterisk). After 1 d, the sst2 mRNA levels were increased by 199% ($p < 0.05$; Table 1) and 395% ($p < 0.01$; Table 1) in dorsal and ventral parts, ipsilaterally (Fig. 5H, asterisks). Quantification of somatostatin mRNA levels in the ipsilateral dorsal striatum revealed an increase by 50% and 42% ($p < 0.05$ each; Table 1; Fig 5S,T) at 2 d and 4 d, respectively. Contralaterally, somatostatin expression levels were increased by 59% after 2 d ($p < 0.05$; Table 1; Fig. 5S). Statistically, sst4 expression levels in the striatum were not different between sham-operated and ischemic groups. One animal out of six displayed a strong increase in sst4 mRNA levels 1 d after ischemia, which is depicted in figure 5M (asterisk). Expression of cortistatin and sst1 mRNAs was not detectable in the striatum of sham-operated or ischemic animals.

3.5 Constitutive localization of somatostatin, sst2, and sst4-LIR in the cerebral cortex

Using immunocytochemistry, the distribution of the somatostatin-, sst2- and sst4-like immunoreactivity (LIR) in the rat forebrain was determined by using specific antibodies.

Somatostatin: The somatostatin-LIR showed similar distribution pattern as somatostatin mRNA. In the forebrain, strong somatostatin-like immunoreactive (lir) neurons were found in the cerebral cortex, septum, ventral diagonal band, caudate putamen, accumbens nucleus, endopiriform nucleus, and claustrum. Detailed analysis under high magnification identified the presence of somatostatin-LIR in perikarya (Fig. 11A, arrows), dendrites, and long-expanding axons (Fig. 11A, arrowhead) in the cerebral cortex. In particular, there was a dense network of somatostatin-lir terminals in lamina I of cerebral cortex in the naive rats, as well as in the contralateral side of ischemic rats (Fig. 12C, arrow, Fig. 13E, arrow), most likely originating from somatostatin-positive cortical interneurons.

sst2, sst4: The distribution patterns of the sst2a-LIR and the sst4-LIR were also consistent with the respective mRNA expression patterns. Strong sst2a-LIR was detected in laminae V/VI of the cerebral cortex, claustrum, dorsal endopiriform nucleus, medial and lateral septum, and

ventral diagonal band. Examination under high magnification showed that sst2a-LIR was distributed diffusely and essentially in laminae V/VI. In laminae II/III, sst2a-LIR was noticed on the plasma membrane of very few multipolar neurons, presumably GABAergic neurons (not shown). The sst4-LIR could be clearly assigned to apical and basal dendrites of pyramidal-shaped neurons, with their perikarya concentrated mainly in laminae II, III and V (Fig. 14). Other regions in the forebrain exhibiting sst4-LIR were the striatum, septum, piriform cortex and olfactory tubercle.

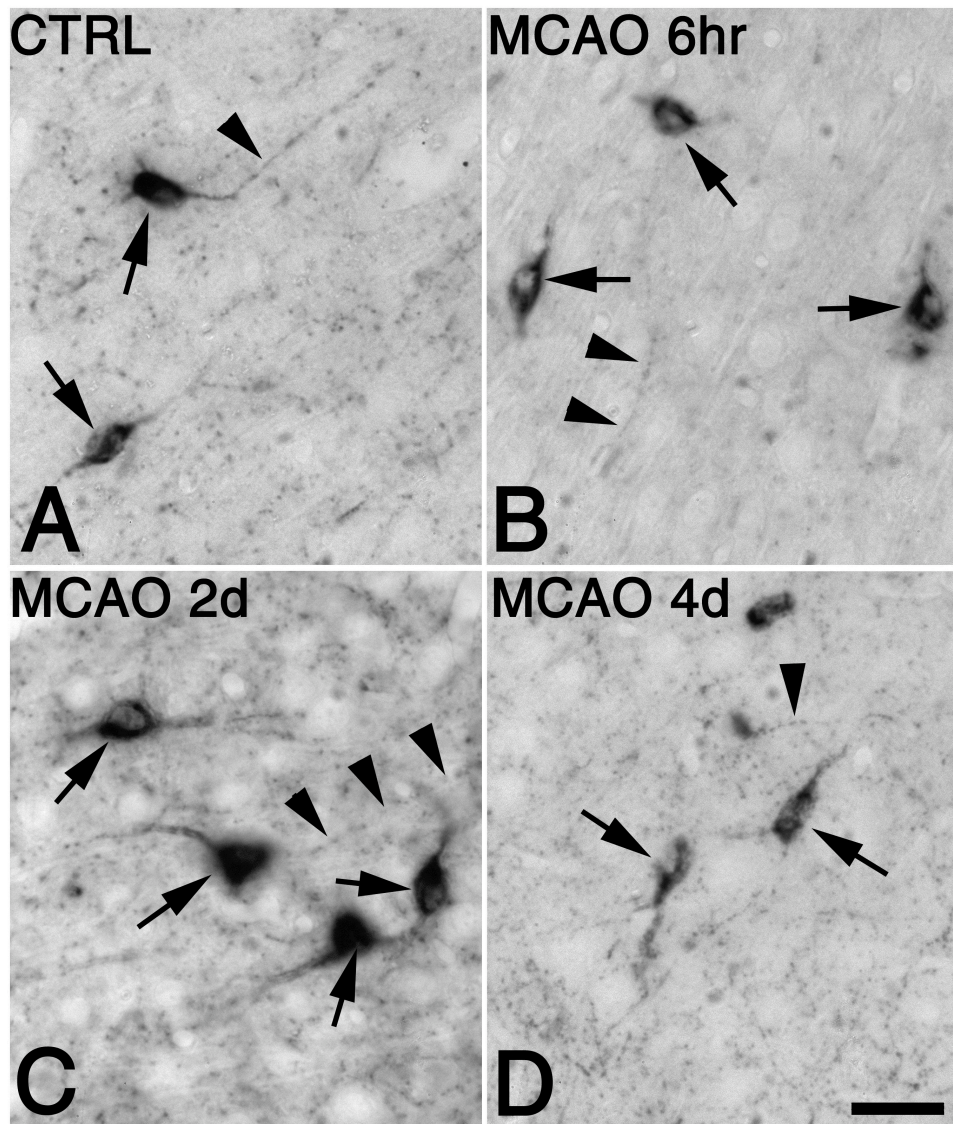


Figure 11. Details of the cellular distribution of somatostatin-like immunoreactivity (SRIF-LIR) before and after focal cerebral ischemia. Shown are high-power brightfield micrographs taken from lamina III of the cingulate cortex of a control rat (*A*), and rats 6 hr (*B*), 2 d (*C*), and 4 d (*D*) after focal ischemia. *A*, presence of strong SRIF-LIR in two neuronal cell bodies (arrows), the dendrites, as well as the axons (arrow head). Numerous terminal-like structures with varicosis are also detected. *B*, 6 hr after MCAO, SRIF-LIR staining in the cell bodies (arrows), dendrites is largely reduced as compared with control. The stained terminals are very rare (arrowhead). *C*, 2 d after MCAO, the SRIF-LIR is greatly enhanced, indicated are strongly stained cell bodies (arrows), dendrites and long-expanding axons (arrowheads). *D*, 4 d after MCAO, SRIF-LIR is greatly reduced as compared with 2 d after MCAO (*C*). Scale bar: 20 μ m.

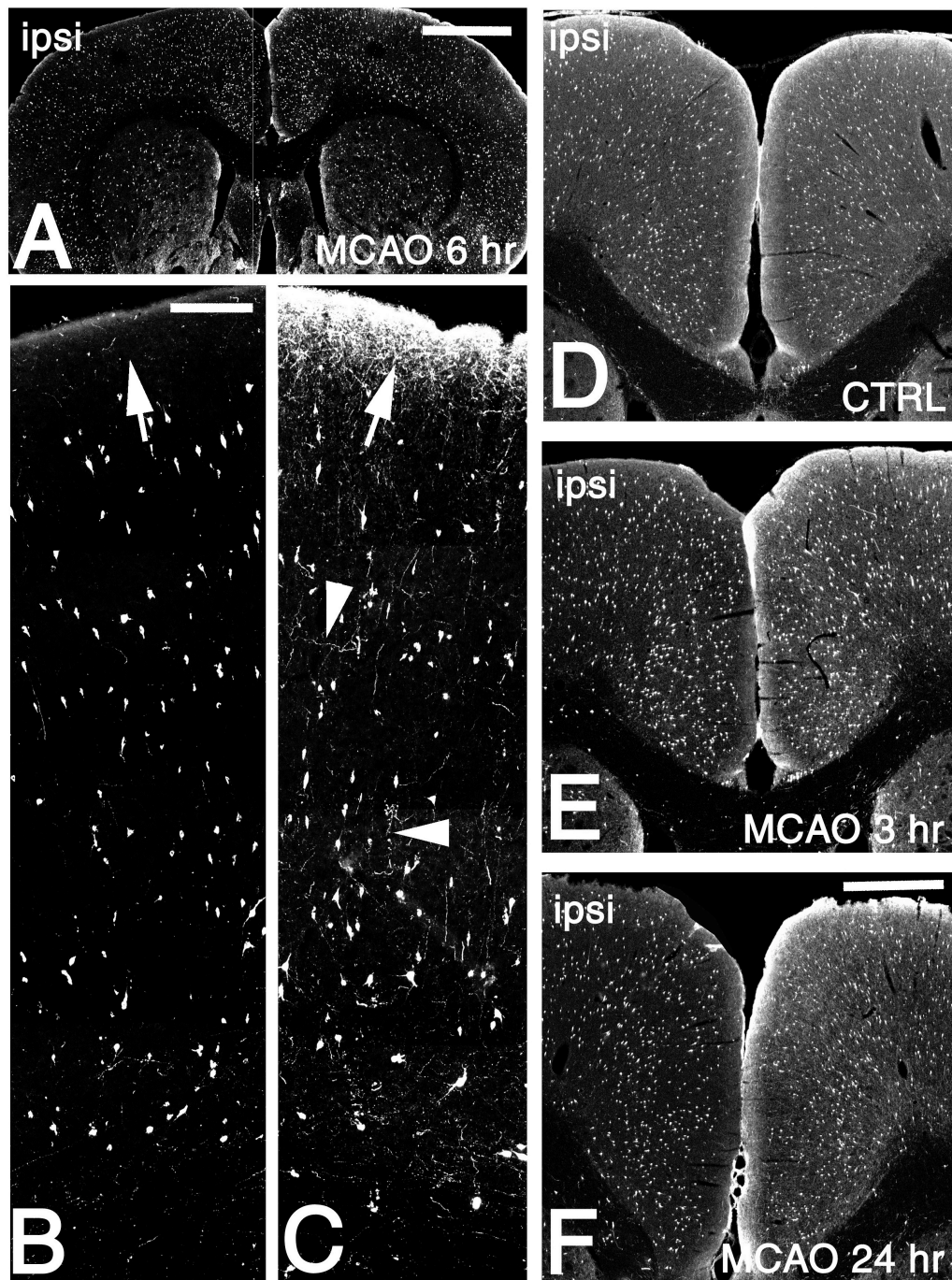


Figure 12. MCAO-induced changes of SRIF-LIR in the ipsilateral cerebral cortex. *A*, confocal image of fluorescence-immunostained coronal section through the forebrain of a rat 6 hr after MCAO. Note the markedly lower staining intensity in lamina I of the ipsilateral hemisphere as compared with contralateral side. *B*, *C*, composite images of micrographs, showing SRIF-positive cell profiles in all layers of the cerebral cortex of ipsilateral and contralateral cingulate/frontal cortex. Note the strongly stained terminal plexus in lamina I in the contralateral side (*C*, arrow), whereas the absence of staining in the corresponding ipsilateral side (*B*, arrow). Moreover, stained delicate fibers are decorated between the cell bodies throughout the cerebral cortex of the contralateral side (*C*, arrowheads), but are largely absent in the ipsilateral side. *D*, *E*, *F*, confocal images of sections from a control rat (*D*), a rat 3 hr (*E*), and a rat 24 hr after MCAO (*F*). The SRIF-LIR is identical in lamina I in both hemispheres in control rat (*D*). The decrease in SRIF staining intensity ipsilaterally can be easily noticed in the 3 hr and 24 hr ischemic rats (*E*, *F*). Scale bars: *A*, 2 mm, *B*, *C*, 300 μ m, *D*, *E*, *F*, 1 mm.

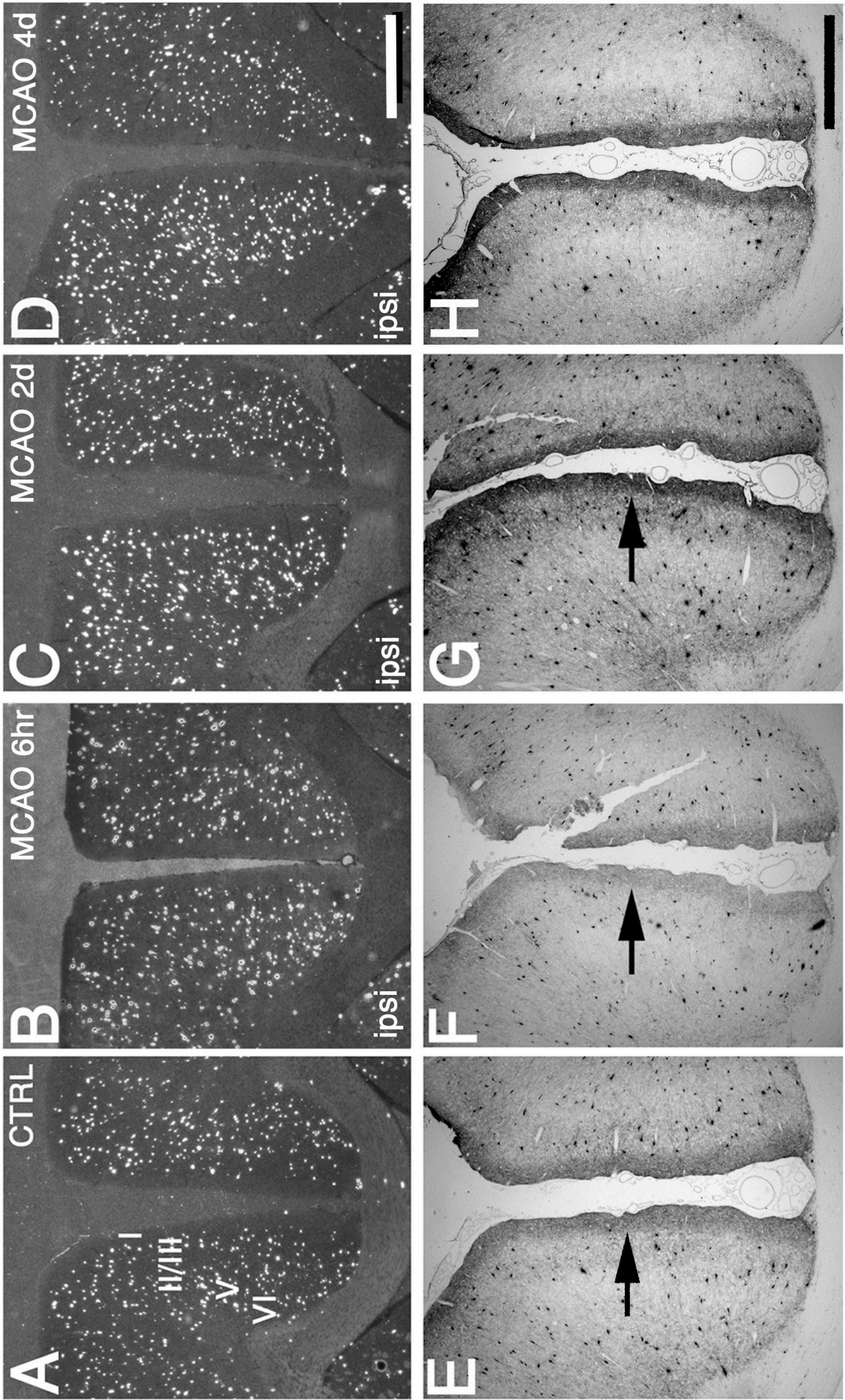


Figure 13. Demonstration of the temporal changes in the distribution patterns of SRIF mRNA and SRIF-like immunoreactivity (SRIF-LIR) in the cingulate and frontal cortex after focal cerebral ischemia. Dark-field (*A-D*) and bright-field micrographs (*E-F*) are taken from bilateral cingulate/frontal cortex of naive rats (control) and rats at 6 hr, 2 d and 4 d after middle cerebral artery occlusion (MCAO). *A*, in the untreated rat, SRIF mRNAs are expressed at high levels by numerous neurons scattered in the cingulate/frontal cortex from laminae II-VI. *B*, 6 hr after MCAO, changes of SRIF mRNA are not detected. *C,D*, 2 d and 4 d after MCAO, SRIF mRNA levels increase moderately in the ipsilateral cingulate/frontal cortex, reflected by the brighter appearances of individual neurons on the ipsilateral side. *E*, SRIF-LIR is detected frequently in the cell bodies throughout cerebral cortex. Note dense and homogeneous staining in lamina I (*E*, arrow). *F*, 6 hr after MCAO, the SRIF-LIR staining is reduced strongly in the ipsilateral cingulate/frontal cortex as compared with control rat (*E*), note strongly decreased staining in lamina I (arrow). *G*, in the 2 d ischemic rat, the SRIF-LIR staining is more intensive than in the control rat. Note the heavy staining in lamina I on the ipsilateral side (arrow). *H*, in the 4 d ischemic rat, the SRIF-LIR intensity is stronger than the in control, but weaker than in the 2 d ischemic rat (*G*). Scale bar: *A-D*, 1 mm, *E-H*, 500 μ m.

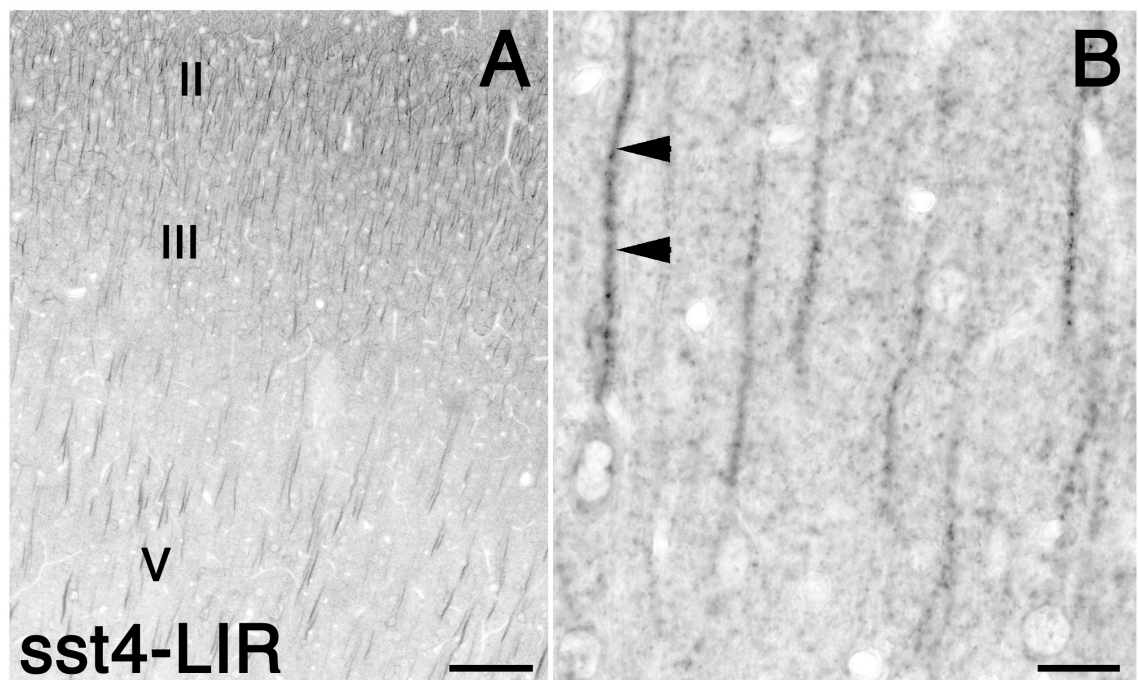


Figure 14. Constitutive distribution of sst4-like immunoreactivity (sst4-LIR) in the cerebral cortex. Low-power brightfield micrograph shows the laminar pattern of sst4-LIR in the cingulate/frontal cortex (*A*). Details of cellular distribution pattern of sst4-LIR are shown under high magnification in *B*. sst4-LIR is concentrated in cortical laminae II, III and V (*A*). At the single cell level, sst4-LIR is detectable predominantly in ascending dendrites (*B*, arrowheads). Scale bar: *A*, 100 μ m; *B*, 15 μ m.

3.6 Histochemistry for somatostatin and sst2 after focal ischemia

In the infarcted area, immunoreactivity for somatostatin, sst2a and sst4 was strongly reduced 6 hr after MCAO and totally absent at later stages, which is consistent with reduced mRNA expression and gradual neurodegeneration in this area. In addition, changes in the immunoreactivity for somatostatin and sst2a were observed in non-lesioned cortical areas after ischemia.

3.6.1 Biphasic changes of somatostatin-LIR in the ipsilateral non-lesioned cerebral cortex

After focal ischemia, a strong decrease in somatostatin-LIR was observed in the cingulate/frontal cortex, endopiriform nucleus, claustrum, and piriform cortex on the ipsilateral side. This effect was first detected at 3 hr and persisted up to 24 hr after MCAO (Fig. 12A,B,E,F). The changes were most obvious in lamina I (Fig. 12B, arrow; Fig. 13F arrow), which is particularly rich of axonal terminals. As demonstrated in figure 12B, somatostatin-LIR was also decreased in laminae II-VI. In contrast, somatostatin-LIR was not altered in the septal area and striatum. In the cerebral cortex, endopiriform nucleus and claustrum contralateral to the lesion, levels of the somatostatin-LIR exhibited only minor changes as compared with naive rats and rats 6 hr after sham operation. The described ischemia-induced changes of somatostatin were observed in all animals analyzed (3 hr, n=4; 6 hr, n=4; 24 hr, n=4).

In the cingulate/frontal cortical areas of animals 2 d and 4 d after MCAO (n=4, each), somatostatin-LIR in neuronal perikarya and processes was restored. The intensity of somatostatin-LIR at postocclusion even exceeded the levels observed in control rats (Fig. 11C,D; Fig. 13G,H).

Despite the strong decrease of somatostatin-LIR in the non-lesioned cortical areas 3 hr-24 hr after MCAO, somatostatin mRNA levels were not altered during this interval (Table 1). In contrast, increased levels of somatostatin-LIR at 2 d and 4 d after MCAO were paralleled to the slight increase in somatostatin mRNA levels (Fig. 13C,D; Table 1). Reduced somatostatin peptide content in axonal terminals is possibly due to exhaustive release and insufficient *de novo* synthesis of somatostatin during the first 24 hr after MCAO.

3.6.2 Internalization of sst2a after MCAO

To test the hypothesis that ischemia may induce enhanced release of somatostatin, we analyzed internalization of sst2a by confocal microscopy. In the cortex of controls (not shown) and in the cortex contralateral to the occluded MCA, sst2a-LIR exhibited a dense but diffuse distribution in laminae V/VI (shown for an animal 3 hr after MCAO, Fig. 15A, contralateral side, D). The ascending dendrites of pyramidal cells were also weakly stained for sst2a in laminae II/III (Fig. 15D, arrow). Due to the diffuse staining pattern, it was difficult to identify individual sst2a-positive cell bodies and dendrites (Fig. 15F,H). In the cortex ipsilateral to MCAO, a pronounced accumulation of sst2a-LIR was observed in the cytoplasm of pyramidal neurons and the dendrites as well (Fig. 15C,E,G, arrowheads and arrows), which is an indication of sst2a internalization. Strong internalization of sst2a was further seen in ipsilateral claustrum and

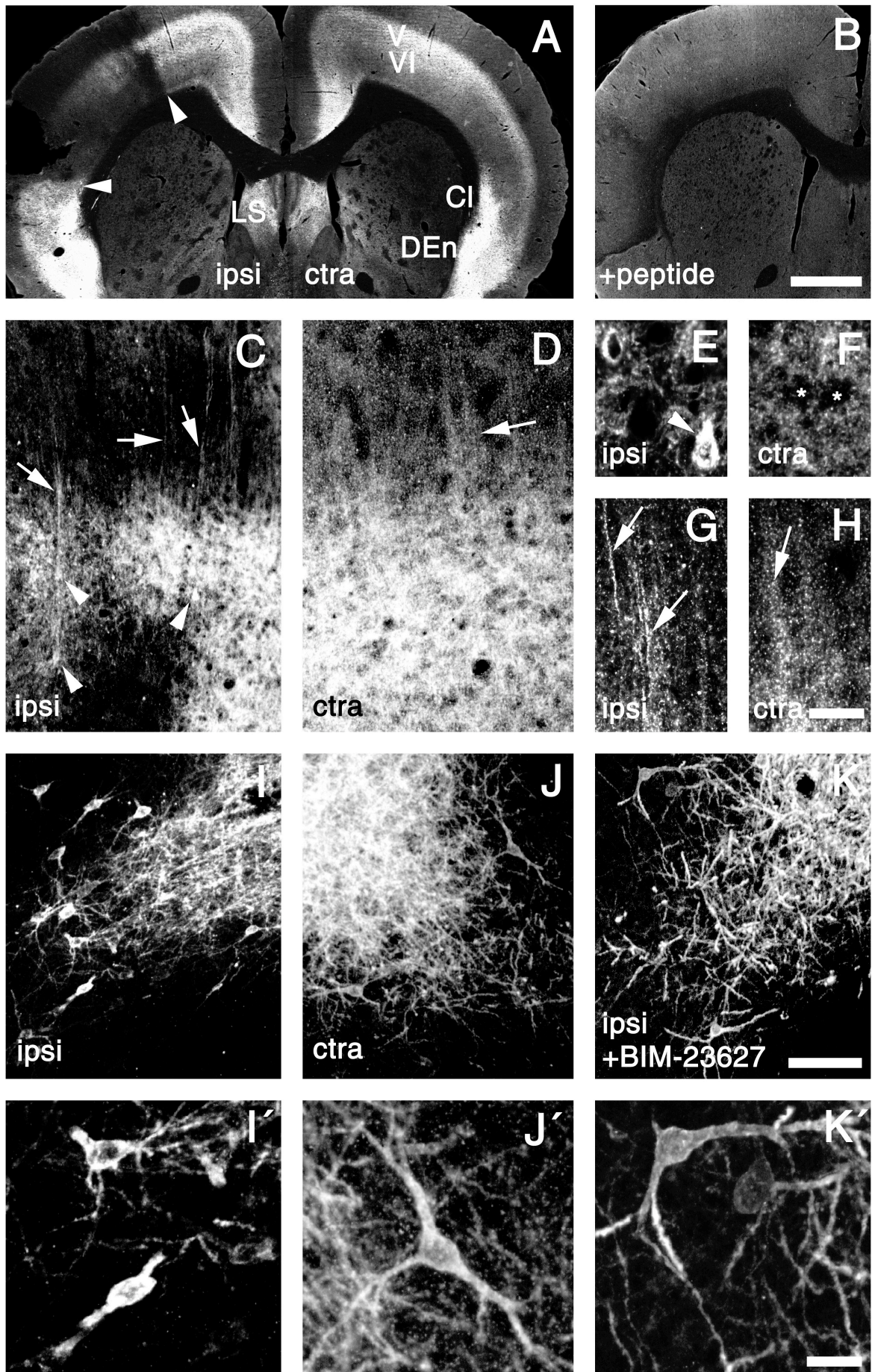


Figure 15. Ligand-induced internalization of the sst2a receptor. A-K, confocal images of sst2a-LIR in the ipsilateral (ipsi) and contralateral (ctra) brain hemispheres 3 hr after MCAO. A, in the contralateral hemisphere, strong sst2a-LIR is present throughout cortical laminae V/VI, claustrum (Cl), dorsal endopiriform nucleus (DEn) and lateral septum (LS). In the ipsilateral hemisphere, the border of the infarct is marked by arrowheads. Note the absence of sst2a-LIR from the infarct as compared with the contralateral side. C-H, details of the perifocal cortex (C,E,G) and the corresponding area on the contralateral side (D,F,H). D, sst2a-LIR is diffusely distributed over the cortical neuropil in the contralateral cortex. C, perifocally, a strong sst2a-like staining is present in pyramidal-shaped neuronal cell bodies (arrowheads) and dendrites (arrows). E,G, a neuronal cell body in lamina V (E, arrowhead) and dendrites in layer IV of the perifocal cortex (G, arrows) show strong cytoplasmic sst2a-LIR. F,H, Neuronal cell bodies (F, asterisks) and dendrites (H, arrow) in the contralateral hemisphere are diffusely decorated by sst2a-LIR. I-K, details of the ipsilateral dorsal endopiriform nucleus from a rat treated with sst2-antagonist BIM-23627 prior to MCAO (K), as well as the ipsilateral (I), and contralateral side (J) of a rat treated with saline; I'-K' are magnifications taken from areas in I-K. J,J' contralaterally, sst2a-LIR diffusely decorates the membrane and the cytoplasm of perikarya, proximal and distal dendrites of neurons. I,I', ipsilaterally, a very strong sst2a-like immunostaining is detected in the cytoplasm of perikarya and proximal dendrites. K,K', after pretreatment with BIM-23627, sst2a-LIR is present mostly at the membrane of perikarya, proximal and distal dendrites ipsilaterally. B, sst2a-like staining in the depicted ipsilateral hemisphere is completely neutralized by the peptide used for immunization. Scale bars: A,B, 1 mm, C,D,I,J,K, 80 μ m, E,F,G,H,I',J',K', 20 μ m.

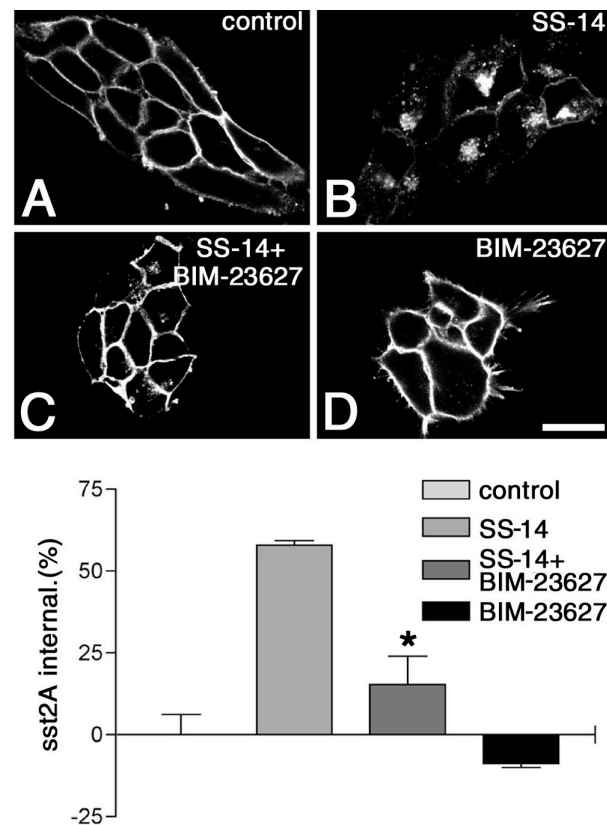


Figure 16. Blockade of somatostatin-14 (SS-14)-induced sst2a internalization by BIM-23627. Depicted are confocal images of the subcellular distribution of sst2a in HEK 293 cells either untreated (A) or exposed to 1 μ M SS-14 (B), or 1 μ M BIM-23627 alone (D), or both compounds together (C). A, sst2a is confined to the plasma membrane of untreated cultured cells. B, pretreatment with SS-14 induced an accumulation of sst2a receptors in structures within the cytoplasm, only a small part of sst2a-LIR remains on the plasma membrane. C, after pretreatment of SS-14 and BIM-23627 together, sst2a-LIR remains largely on the surface of the cells, with only a small part of the sst2a-LIR localized inside the cell bodies. D, the plasma membrane-associated distribution of sst2a is not altered by pretreatment of BIM-23627 alone. Quantitative analysis of receptor internalization by enzyme-linked immunosorbent assay (ELISA) shows that the percentage of internalized sst2a after pretreatment of SS-14, BIM-23627, and both together (control set as zero). Note the percentage of internalization of sst2a reduces greatly when SS-14 and BIM-23627 are applied together, as compared with SS-14 application alone. In cells treated with BIM-23627, internalization was even less than in the non-treated cells. Scale bar: 20 μ m.

dorsal endopiriform nucleus (compare Fig. 15I,I' and Fig. 15J,J'). This massive intracellular accumulation of sst2a-LIR was first observed at 3 hr after MCAO and lasted until 24 hr (not shown). At 2 d and 4 d after MCAO there were no clear differences in the subcellular distribution of sst2a-LIR between ischemic and control rats (not shown).

To illustrate whether the internalization of sst2a followed by focal cerebral ischemia can be blocked pharmacologically, we first checked the effect of the sst2-selective antagonist BIM-23627 on somatostatin-induced internalization in HEK293 cells stably transfected with T7 epitope-tagged sst2a. In untreated cells, sst2a was localized predominantly at the plasma membrane (Fig. 16A). Within 30 min, application of 1 μ M somatostatin-14 (SS-14) triggered internalization of sst2a receptors (Fig. 16B). BIM-23627 blocked agonist-induced internalization of sst2a when applied together with somatostatin-14 (Fig. 16C), but did not provide internalization effect of sst2a when administered alone (Fig. 16D). Quantitative analysis of receptor internalization by enzyme-linked immunosorbent assay indicated, that in cells exposed to somatostatin alone, the sst2a internalization reached 60% (control set as zero). In contrast, in cells exposed to both somatostatin-14 and BIM-23627, the internalization of sst2a was reduced to 16% ($p < 0.01$, Fig. 16 scheme). These *in vitro* data show that BIM-23627 is a suitable compound to block ligand-induced internalization of sst2a.

Next, we studied the effect of the compound *in vivo*. Either 5 μ l saline or BIM-23627 (0.5 nM) was injected intracerebroventricularly 30 min prior to occlusion of the MCA. The animals were sacrificed 3 hr after MCAO. As described above, in the rats pretreated with saline, there was a redistribution of sst2a-LIR ipsilaterally (Fig. 15 I,I'), but not contralaterally (Fig. 15, J,J'). In the rats pretreated with BIM-23627, sst2a-LIR remained on the plasma membrane of neuronal cell bodies and dendrites in the penumbra (not shown), ipsilateral claustrum, and dorsal endopiriform nucleus (Fig. 15 K,K').

Taken together, these immunohistochemical analysis provided direct evidence for ligand-induced internalization of sst2a in cortex, claustrum as well as dorsal endopiriform nucleus during the first 24 hr after focal cerebral ischemia, suggesting a massive release of endogenous ligands.

4. Discussion

Based on previous studies suggesting a role for somatostatin and cortistatin peptides in modulating glutamatergic neurotransmission, seizure, and focal ischemic brain damage in the cerebral cortex (Braun *et al.*, 1998; Rauca *et al.*, 1999; Vezzani and Hoyer, 1999), this study aimed to provide a comprehensive characterization of the expression of the somatostatinergic system in the cerebral cortex suffering from unilateral focal ischemia.

In particular, gene expression of somatostatin, cortistatin as well as the sst1, sst2, sst4 and sst5 receptors was analyzed at the end of the acute phase of ischemic damage (6 hr after onset) and in the ensuing phases (1 d-4 d after ischemia onset) in the primary infarct, the penumbra, and in permanently surviving cortical areas. To further explore cortical circuits which may be modulated by endogenous cortistatin and somatostatin peptides, neuronal types expressing these peptides and sst2 were determined. Internalization of sst2-LIR in cortical neurons was also investigated for the purpose of identifying the sites of receptor activation after focal ischemia.

The major findings include, that sst2 is constitutively expressed mainly in excitatory pyramidal cells and strongly up-regulated in this neuron population in penumbral areas during the acute phase of brain ischemia. Internalized sst2 receptors were observed in perifocal and exofocal areas from 3 hr to 24 hr after ischemia onset, which was accompanied by the reduced somatostatin-LIR. We further showed that the expression levels of the somatostatin and cortistatin genes were oppositely regulated between 2 d and 4 d after focal ischemia, pointing to different functions of these peptides in the cortex. This was corroborated by the observation, that somatostatin and cortistatin are expressed mostly in non-overlapping populations of inhibitory cortical neurons.

4.1 Analysis of the animal model of focal ischemia

Throughout this study, the permanent middle cerebral artery occlusion (MCAO) model in the inbred Long-Evans rat was used, which is an established model of focal brain ischemia (Tamura *et al.*, 1981; Ginsberg and Busto, 1989; Wolz and Kriegelstein, 1996; Culmsee *et al.*, 1999). Rat MCAO models are the most frequently used stroke models in preclinical studies because of their simplicity and reproducibility. In order to evaluate our stroke model, the

MCAO-induced cellular degeneration and glial activation profiles were characterized using histological, *in situ* hybridization and immunohistochemical methods. In this model, the unilateral occlusion of the MCA generated an expanding focus of degenerating brain parenchyma in the temporoparietal cortex. As indicated by nissl staining, cell degeneration happened during the first 24 hr after ischemia onset. Rostrally, the focus always included the forelimb area of the cortex, the parietal cortex and the dorsal insular cortex. Along the longitudinal axis, the lesion typically extended from bregma +2.7 mm to bregma -4.8 mm. In order to characterize patterns of astroglial and microglial activation, which are associated with brain damage, inflammation and repair, *in situ* hybridization for GFAP and C1q was applied, which are established markers of astrocytes and microglia/macrophages in the brain (Eng, 1985; Walker *et al.*, 1995, 1998; Haga *et al.*, 1996). Since expression of both genes is up-regulated upon cellular activation, *in situ* hybridization for both mRNAs is a sensitive tool for the detection of gliosis (Belluardo *et al.*, 1996; Yamashita *et al.*, 1996; Schafer *et al.*, 2000; Lynch *et al.*, 2004). This showed a pronounced astrocytosis and microgliosis, which was initiated at 6 hr, peaked at 2 d after MCAO and subsided afterwards. In 4 d ischemic animals, the infarct was characterized by massive infiltration of macrophages/microglia and a surrounding astroglial scar. Both, the kinetics of tissue degeneration and the spatiotemporal patterns of glial activation in our animal model are consistent with other studies on mouse and rat MCAO models (Yamashita *et al.*, 1996; Van Beek *et al.*, 2000).

4.2 Constitutive somatostatin, cortistatin, and somatostatin receptor expression in the cerebral cortex

Our *in situ* hybridization results showed that somatostatin and cortistatin mRNAs were present with high abundance and similar distribution patterns in the cerebral cortex of control rats, which is in good concordance with previous findings (Fitzpatrick-McElligott *et al.*, 1988; Kiyama and Emson, 1990; de Lecea *et al.*, 1997a). In the cortex, both peptides were found to be synthesized exclusively by GABAergic neurons (Schmechel *et al.*, 1984; Esclapez and Houser, 1995; de Lecea *et al.*, 1997a).

Previous pharmacological studies showed, that somatostatin and cortistatin peptides bind to all somatostatin receptors with high affinity (de Lecea *et al.*, 1996; Fukusumi *et al.*, 1997; Siehler *et al.*, 1998). Because of the pharmacological similarities, structural homologies and

overlapping distribution of the two peptides, the question arises whether they both exert identical functions in the cerebral cortex. To address this question, we analyzed the phenotypes of the peptide-synthesizing cells in the cingulate and frontal cortex in detail.

4.2.1 Neuronal types expressing cortistatin mRNA in the cerebral cortex. First, we performed co-expression analysis for cortistatin and somatostatin in relation to each other. In addition, their co-expression with parvalbumin and neuropeptide Y was evaluated, which are selective markers for distinct subpopulations of cerebrocortical GABAergic neurons. We found that 17% of somatostatin mRNA positive neurons expressed cortistatin. Conversely, 35% of cortistatin-expressing neurons were positive for somatostatin mRNA. Co-localization of somatostatin and parvalbumin in the same neuron was never observed. In contrast, cortistatin/parvalbumin-positive cells represented more than half of the cortistatin population, and one-third of the parvalbumin population. Previous studies showed that neuropeptide Y-positive neurons are a subpopulation of somatostatin-positive neurons, with neuropeptide Y expressed in non-somatostatinergic cells being very exceptional (Kawaguchi and Kubota, 1997). Here we showed for the first time that cortistatin/neuropeptide Y-positive neurons accounted for 18% of cortistatin neurons and approximately 36% of the neuropeptide Y-positive population. Based on these data and those of de Lecea *et al.* (de Lecea *et al.*, 1997a), it can be concluded that cortistatin and somatostatin are expressed by distinct although partially overlapping subsets of GABAergic neurons. We suggest that cortistatin-expressing GABAergic neurons in the cortex comprise two major populations: (1) somatostatin-positive neurons (35% of all cortistatin-neurons, half of which are also positive for neuropeptide Y), and (2) parvalbumin-positive neurons. (>50% of all cortistatin-neurons).

4.2.2 Possible consequences of the distinct expression of cortistatin and somatostatin in GABAergic neurons. It is well established that GABAergic neurons in the cortex are heterogeneous, and can be subdivided into distinct classes by their neurochemical properties (Kawaguchi and Kubota, 1997; Kawaguchi and Kondo, 2002). Each subtype has a different firing pattern and a characteristic innervation tendency of postsynaptic elements. The segregation of axons of inhibitory neurons is thought to permit different patterns of postsynaptic inhibition (Kawaguchi and Kubota, 1997; Somogyi *et al.*, 1998). The parvalbumin-positive GABAergic neurons, which are known as fast-spiking neurons, have their post-synaptic targets mainly surrounding the soma or axon initial segment. In contrast, somatostatin neurons are either regular-spiking or burst-spiking and form synapse with

dendritic spines and shafts of small or medium-sized dendrites (De Lima and Morrison, 1989; Kawaguchi and Kubota, 1997). Interneurons targeting the perisomatic area tend to inhibit the output of other neurons by interfering with the generation of action potentials. Interneurons with their terminals on the distal dendrites are most likely responsible for controlling the afferent input, thus decrease the flow of information into other neurons (Miles *et al.*, 1996; Somogyi *et al.*, 1998). Hence, cortistatin contained in parvalbumin-positive neurons is likely to modulate the perisomatic region of postsynaptic cells, while cortistatin in somatostatin-positive neurons may predominantly target the dendritic spine-bearing areas of neurons. Thus, functional differences between somatostatin and cortistatin in cortex are very likely.

4.2.3 Glutamatergic neuron type-selective gene expression of somatostatin receptors in the cerebral cortex. Most GABAergic neurons in the cerebral cortex are thought to exclusively target neurons within the cortex in an interneuron-like manner. To identify the postsynaptic targets of the cortistatin- and somatostatin-expressing GABAergic cells, we studied the mRNA expression of *sst1*, *sst2* and *sst4* in the cortex. Our results revealed that *sst1* mRNAs distributed predominantly in laminae II, V and VI of the cerebral cortex, *sst2* mRNAs were concentrated in infragranular layers, and *sst4* mRNAs were mainly detected in laminae II, V and VIb. The partially overlapping distribution of *sst1*, *sst2*, and *sst4* mRNAs in discrete cortical layers were observed in agreement with previous studies (Breder *et al.*, 1992; Kaupmann *et al.*, 1993; Perez *et al.*, 1994; Senaris *et al.*, 1994; Hervieu and Emson, 1998). Since *sst2* and (to a much less extent) *sst4* are the preponderant binding sites for cortistatin and somatostatin in cortex (Videau C *et al.*, 2003), we analyzed neuronal type-selective expression and subcellular localization of *sst2* and *sst4* in detail. Our phenotype-analysis by double *in situ* hybridization revealed that *sst2* was preferentially expressed by excitatory neurons in the cortex. *sst4*-LIR neurons clearly were of the glutamatergic pyramidal cell type; the presence of *sst4*-LIR in multipolar non-pyramidal cells was very rare. In addition, we identified postsynaptic localization of *sst2* as well as *sst4* in cortical neurons in agreement with previous works (Schindler *et al.*, 1997; Schreff *et al.*, 2000; Schulz *et al.*, 2000). Taken together, our findings indicate that under physiological conditions, *sst2*- and *sst4*-mediated effects of somatostatin and cortistatin are mainly directed towards excitatory neurons in the cortex. This assumption is supported by the concept that excitatory

neurons are the predominant targets of GABAergic neurons in the cortex (Cobb *et al.*, 1997; Somogyi *et al.*, 1998) and by the *in vitro* observation that somatostatin induced hyperpolarization of pyramidal cells in the rat anterior cingulate cortex via sst2 (Hicks *et al.*, 1998).

4.3 Stage-specific changes in somatostatin, cortistatin, and sst2 receptor expression

Given that somatostatin may selectively inhibit glutamatergic transmission in the cortex (Boehm and Betz, 1997; Tallent and Siggin, 1997), the endogenous somatostatin system might be of particular relevance in neurological disorders involving excitotoxic neuronal death. In stroke models, excessive glutamate release from neurons in the penumbral cortical area is a major cause for the enlargement of the primary infarct during the first hours after ischemia (Choi and Rothman, 1990; Siesjo *et al.*, 1992, 1995). Therefore, we next addressed, whether the somatostatin system may be involved in the pathophysiology of cerebral ischemia.

Activation of many GPCRs *in vitro* and *in vivo* can be detected by showing redistribution of the receptors from the membrane to intracellular compartments (Allen *et al.*, 1997). Here, we analyzed the effect of focal ischemia on sst2a internalization in perifocal and exofocal areas of the cortex at various time points after MCAO. This was accompanied by the immunohistochemical analysis of the somatostatin-content in the brain.

From 3 hr to 24 hr after MCAO, sst2a was found to internalize in the perifocal and ipsilateral exofocal cortical areas, but not in the contralateral hemisphere. Regions exhibiting sst2a internalization showed a strong decrease in somatostatin-LIR in axon terminals whereas somatostatin-LIR was largely unaltered in the contralateral hemisphere. To illustrate whether sst2a receptor internalization was driven by endogenous ligands, we attempted to block internalization by a sst2a-selective compound. Quantitative internalization studies *in vitro* indicated that the synthetic sst2-selective antagonist BIM-23627 was capable of blocking somatostatin-14-induced internalization of sst2a. Application of BIM-23627 into the cerebroventricle immediately before MCAO prevented internalization of sst2a-LIR in the ipsilateral ischemic hemisphere. In animals receiving BIM-23627 but no MCAO, sst2-LIR was even slightly enriched at the neuronal plasma membrane as compared with animals not treated

with the compound. Taken together, these data strongly suggest that sst2a receptors are indeed activated by endogenous ligands in the ipsilateral hemisphere after focal ischemia.

Previous studies showed that application of octreotide, a synthetic sst2-agonist, into the brain evoked massive local sst2-internalization (Csaba *et al.*, 2001, 2002, 2003). Constitutive activation and internalization of sst2 in brain was suggested, based on the observation that sst2-LIR is present in intracellular neuronal compartments in regions with abundant somatostatinergic innervation, whereas sst2-LIR is more often associated with the plasma membrane in regions exhibiting sparse somatostatin-LIR (Dournaud *et al.*, 1998). Reduced binding sites of SRIF₁-type receptors (sst2,3,5) in the molecular layer of the dentate gyrus of kindled rats were interpreted as sign for sst-receptor (mainly sst2) internalization driven by enhanced release of somatostatin (Piwko *et al.*, 1996). However, none of these studies proved activation and internalization of sst receptors by endogenous ligands under neuropathological status. Thus, our study is the first to provide direct evidence for *in vivo* internalization of sst2a in stroke pathophysiology.

Internalization of sst2a after focal ischemia was always paralleled by strongly reduced levels of somatostatin-LIR in axon terminals. This decrease could be the consequence of impaired synthesis or increased release of the peptide. Somatostatin synthesis appeared to be undisturbed at the transcriptional level, since *in situ* hybridization histochemistry indicated no changes in somatostatin mRNA levels in non-infarcted areas during the first 24 hr after MCAO. Due to energy failure, cerebral protein synthesis is known to be impaired in the penumbra during the first 2 hr after brain ischemia which may partially account for the observed reduction in somatostatin peptide levels (Hossmann, 1994; Christensen *et al.*, 1996). In the ipsilateral exofocal area, however, suppression of protein synthesis was not reported, but strongly reduced somatostatin-levels were observed. Thus, release of somatostatin from axonal terminals is a possible explanation for this finding. This assumption is further supported by the spatial and temporal overlap between sst2a-internalization and decreased somatostatin peptide levels.

Studies of cortical, striatal and hippocampal neuronal primary cultures indicated that excitatory amino acids (EAA) increase somatostatin release mainly via NMDA-receptor and Ca²⁺-dependent mechanisms (Tapia-Arancibia and Astier, 1989; Williams *et al.*, 1991; Fontana *et*

al., 1996). More recently, Hathway and co-workers demonstrated by *in vivo* microdialysis that application of the ionotropic glutamate receptor agonists AMPA and NMDA increases somatostatin release in the striatum (Hathway *et al.*, 1999). Furthermore, enhanced release of somatostatin from rat hippocampal neurons during and after kindling was described by several authors (Vezzani *et al.*, 1992; Marti *et al.*, 2000), providing strong evidence for EAA-driven somatostatin release in neuropathology. Since it is well established that glutamatergic transmission is increased after focal ischemia in perifocal and exofocal areas of the ipsilateral brain hemisphere (Choi and Rothman, 1990; Siesjö *et al.*, 1995), depletion of somatostatin-LIR from axon terminals during the acute phase of focal ischemia is likely to be triggered by glutamate.

In contrast to the unchanged gene expression of somatostatin in the peri- and exofocal areas at early stages, a slight upregulation of the somatostatin gene was detected in non-lesioned cortical areas from 2 d to 4 d after MCAO. In addition, we detected a massive downregulation of cortistatin gene expression in the same areas from 1 d to 4 d postischemia. Previously, Calbet and co-workers demonstrated that expression of the two genes was differentially regulated in hippocampal interneurons after i.c.v. application of kainate acid (Calbet *et al.*, 1999) and described the lack of any similarities in putative regulatory response elements of the two genes. Under physiological conditions, cortistatin is expressed in somatostatin-positive and parvalbumin-positive GABAergic neurons, which constitute segregated local circuits in cortex (Kawaguchi and Kubota, 1997). To address, whether cortistatin-expression is differentially affected in these two inhibitory circuits after focal ischemia, we performed double *in situ* hybridization for cortistatin mRNA in relation to somatostatin- and parvalbumin-mRNA. This showed that the cortistatin mRNA levels were decreased in both populations. Although cortistatin was still detectable after ischemia in some somatostatin-expressing neurons, cortistatin-expression in parvalbumin-positive neurons was largely undetectable. Thus, after focal ischemia, cortistatin-expression is almost absent in the parvalbumin-positive GABAergic cortical circuits. In the somatostatin-positive GABAergic local circuit, cortistatin-expression is unchanged or decreased, while somatostatin-expression is slightly increased both at mRNA and protein levels.

Several lines of evidences indicated recently that somatostatin-induced endocytosis of sst receptors has transcriptional effects. In particular, ligand-induced receptor (mainly sst2) internalization was supposed to be critical for the inhibition of growth hormone expression by somatostatin in AtT-20 cells (Sarret *et al.*, 1999). More recently, Boudin *et al.* have demonstrated that somatostatin-induced endocytosis of sst-receptors is responsible for transient transcriptional activation events of the sst2a gene in brain slices (Boudin *et al.*, 2000). Moreover, homologous regulation of the expression of a G-protein-coupled receptor by its own agonist has been described previously for the high affinity neurotensin receptor, which is dependent on the receptor internalization (Souaze *et al.*, 1997).

To address *in vivo*, whether internalization of sst2a after focal ischemia correlates with altered sst2 gene expression, we analyzed the gene expression of sst2 in our MCAO model. We showed that sst2 mRNA was upregulated throughout the cortical penumbra at 6 hr after MCAO. Increased sst2 gene expression was also detected in the deep cortical layers in the exofocal cingulate and frontal cortex at same time. Thus, enhanced gene expression of sst2a indeed paralleled areas exhibiting sst2a-internalization. To provide direct evidence whether internalization of sst2a is required for activation of sst2a gene expression, expression of lacZ mRNA will be studied in mice with a sst2 knock out/lacZ knock in before and after MCAO. Given, that internalization of sst2a after focal ischemia is required for enhanced transcription of sst2 gene, upregulation of the lacZ mRNA is not expected to occur.

Using double *in situ* hybridization, we determined whether the upregulation of sst2 occurred in GABAergic and glutamatergic neuronal types. We found that sst2 expression was preferentially upregulated in the glutamatergic neuronal population, but mostly unchanged in GABAergic neurons. Since glutamatergic neurons in laminae II/III and VI mainly form synapses with other neurons in the same or other cortical layers, the selective upregulation of sst2 in these neurons may affect neuronal excitability predominantly in intracortical glutamatergic circuits. With regard to the inhibitory effect of sst2-activation in the cortical neurons (Hicks *et al.*, 1998), this may represent a mechanism of autoprotection from ischemia-induced cerebrocortical hyperexcitability.

4.4 Implications for the somatostatinergic system in the pathophysiology of focal brain ischemia

Following MCAO, the ischemic focus is completely devoid of blood supply, while the surrounding tissues (penumbra) are less ischemic due to collateral blood supply from undamaged blood vessels. The penumbra zone is compromised to damages caused by both the reduction in blood supply and the exposure to chemical mediators such as nitric oxide and free radicals released from cells in the ischemic focus. In this series of events, neuronal depolarization, the release of excitatory amino acids from presynaptic endings and activation of postsynaptic glutamate receptors play a crucial role (Choi and Rothman 1990; Siesjo *et al.*, 1992, 1995). Neurons exposed to the glutamatergic hyperactivation suffer from perturbed intracellular signal transduction pathways, which finally lead to neuronal necrosis and apoptosis. In animal models, it was suggested that excitotoxicity has the tendency to propagate from the infarct-adjacent areas to more distant regions (Ruppin *et al.*, 1999). Somatostatin is known to inhibit glutamatergic transmission in cortex and to inhibit neuronal excitability mainly through sst2 receptors (Boehm and Betz, 1997; Tallent and Siggins, 1997; Hicks *et al.*, 1998). Hence, activation of sst2 gene expression and increased somatostatinergic transmission in the penumbral area during the excitotoxic phase of focal brain ischemia provide evidence for the involvement of this system in the pathophysiology of stroke.

4.5 Is the somatostatinergic system a promising target in ischemic cerebrovascular disease?

Upregulation of sst2 gene expression in the penumbra zone, increased somatostatin release as well as internalization of sst2a in the perifocal cortical area point to enhanced somatostatinergic transmission, which may contribute to enhanced inhibition in the cortex surrounding the primary infarct. This in turn may limit the spread of hyperexcitation. Hence, neuroprotective effects of the endogenous somatostatin system are possible. However, pharmacological evidence supporting this idea is sparse. Until now only Rauca *et al.* have demonstrated that exogenous application of somatostatin-14, octreotide and cortistatin-14 five minutes after MCAO can reduce infarct size (Rauca *et al.*, 1999). In addition, neuroprotective effect of somatostatin in neuronal culture has been reported (Forloni *et al.*, 1997). To test the hypothesis

that somatostatinergic transmission via sst2 plays a role in reducing focal ischemic brain damage, future studies will examine ischemic brain damage in mice lacking the sst2 receptor.

5. Summary

Somatostatin and its structurally related neuropeptide cortistatin exert their physiological actions via a family of six G-protein-coupled receptors (sst1, sst2a, sst2b, sst3, sst4, sst5). Activation of somatostatin receptors has predominantly inhibitory effects on neurotransmission in the central nervous system. Somatostatinergic transmission in the central nervous system is affected in several neurological disorders including Alzheimer's disease, Huntington's disease and epilepsy. Somatostatin, cortistatin and sst receptors are abundantly expressed in the cerebral cortex, where this system is thought to inhibit glutamatergic transmission.

In the present study, the distribution of somatostatin, cortistatin, sst1, sst2 and sst4 receptors was analyzed in the cerebral cortex at the mRNA and protein levels under both physiological conditions and after permanent unilateral occlusion of the middle cerebral artery (MCAO). Using double-labelling strategies, neurochemical phenotypes of neurons expressing somatostatin, cortistatin and sst2 receptors were identified. Spatial and temporal patterns of sst2a internalization after MCAO were analyzed to identify the sites of sst2a activation.

Our results revealed that somatostatin and cortistatin mRNAs are constitutively expressed in the cortex, where they exhibit a partially overlapping distribution. In particular, cortistatin is co-expressed in 17% of somatostatinergic neurons and 31% of parvalbumin-positive neurons, which comprise distinct subsets of GABAergic local circuit neurons in the cortex. At the mRNA level, sst1, sst2 and sst4 are abundantly expressed in the cerebral cortex, each of which has a characteristic laminar distribution. Analysis of the phenotype of sst2- and sst4-expressing neurons showed that the vast majority of these neurons are glutamatergic pyramidal cells. Furthermore, immunohistochemistry identified the somato-dendritic localization of both receptors, indicating postsynaptic functions. Therefore, cortistatin and somatostatin may predominantly regulate the excitability of pyramidal cells via postsynaptic sst receptors.

For the first time we demonstrated changes in the expression of cortistatin, somatostatin, sst1, sst2, and sst4 after MCAO. From 3 hr to 24 hr, a decrease in somatostatin-LIR and internalization of sst2a in the peri- and exofocal areas were observed, indicating activation of sst2a after ischemic brain damage. In addition, a robust increase in sst2 mRNA levels was shown in the cortical penumbra at 6 hr after MCAO. sst2 mRNA was upregulated selectively in glutamatergic neurons. From 2 d to 4 d after focal ischemia, opposite gene regulation of somatostatin and cortistatin was seen in non-lesioned areas of the cortex. In particular, levels of somatostatin mRNA were slightly increased, while cortistatin mRNA levels were massively decreased. Co-expression analysis after MCAO showed that cortistatin mRNA levels were

below the detection limit in the vast majority of parvalbumin-positive GABAergic neurons, while cortistatin expression was still detectable in numerous somatostatin-positive neurons. Taken together, our data provide evidence for the presence of somatostatin and cortistatin in distinct but overlapping GABAergic circuits of the cerebral cortex. Somatostatin and cortistatin are suggested to have different effects on other neurons due to their different selectivity on postsynaptic elements. We further provide evidence for the activation of somatostatinergic transmission in peri- and exofocal areas of the cerebral cortex during early stages of focal ischemic brain damage. Since somatostatin is known to inhibit glutamatergic neurotransmission in cortex, these data suggest that the endogenous somatostatin system may counteract hyperexcitability after stroke. Since sst2 and sst4 are expressed selectively in glutamatergic neurons of the cerebral cortex, they are interesting targets to interfere with hyperexcitability after brain ischemia. Possible neuroprotective effects of sst2 receptors will be further investigated using mice lacking of sst2. Moreover, the development of highly selective somatostatin receptor ligands will permit functional analysis of individual receptors in stroke pathophysiology.

6. References

- Allen BJ, Rogers SD, Ghilardi JR, Menning PM, Kuskowski MA, Basbaum AI, Simone DA, Mantyh PW (1997) Noxious cutaneous thermal stimuli induce a graded release of endogenous substance P in the spinal cord: imaging peptide action in vivo. *J Neurosci* 17:5921-5927.
- Allen GV, Cheung RT, Cechetto DF (1995) Neurochemical changes following occlusion of the middle cerebral artery in rats. *Neuroscience* 68:1037-1050.
- Allen J, Novotny J, Martin J, Heinrich G (1987) Molecular structure of mammalian neuropeptide Y: analysis by molecular cloning and computer-aided comparison with crystal structure of avian homologue. *Proc Natl Acad Sci U S A* 84:2532-2536.
- Allen JP, Hathway GJ, Clarke NJ, Jowett MI, Topps S, Kendrick KM, Humphrey PP, Wilkinson LS, Emson PC (2003) Somatostatin receptor 2 knockout/lacZ knockin mice show impaired motor coordination and reveal sites of somatostatin action within the striatum. *Eur J Neurosci* 17:1881-1895.
- Angerer LM, Cox KH, Angerer RC (1987) Demonstration of tissue-specific gene expression by in situ hybridization. *Methods Enzymol* 152:649-661.
- Arai H, Moroji T, Kosaka K (1984) Somatostatin and vasoactive intestinal polypeptide in postmortem brains from patients with Alzheimer-type dementia. *Neurosci Lett* 52:73-78.
- Aronin N, Cooper PE, Lorenz LJ, Bird ED, Sagar SM, Leeman SE, Martin JB (1983) Somatostatin is increased in the basal ganglia in Huntington disease. *Ann Neurol* 13:519-526.
- Baumeister H, Meyerhof W (2000) Gene regulation of somatostatin receptors in rats. *J Physiol Paris* 94:167-177.
- Beal MF, Mazurek MF, Ellison DW, Swartz KJ, McGarvey U, Bird ED, Martin JB (1988) Somatostatin and neuropeptide Y concentrations in pathologically graded cases of Huntington's disease. *Ann Neurol* 23:562-569.
- Beaumont V, Hepworth MB, Luty JS, Kelly E, Henderson G (1998) Somatostatin receptor desensitization in NG108-15 cells. A consequence of receptor sequestration. *J Biol Chem* 273:33174-33183.
- Belluardo N, Mudo G, Jiang XH, Condorelli DF (1996) Induction of astroglial gene expression by experimental seizures in the rat: spatio-temporal patterns of the early stages. *Glia* 16:174-186.
- Binaschi A, Bregola G, Simonato M (2003) On the role of somatostatin in seizure control: clues from the hippocampus. *Rev Neurosci* 14:285-301.
- Bloch B, Dumartin B, Bernard V (1999) In vivo regulation of intraneuronal trafficking of G protein-coupled receptors for neurotransmitters. *Trends Pharmacol Sci* 20:315-319.
- Boehm S, Betz H (1997) Somatostatin inhibits excitatory transmission at rat hippocampal synapses via presynaptic receptors. *J Neurosci* 17:4066-4075.
- Boudin H, Sarret P, Mazella J, Schonbrunn A, Beaudet A (2000) Somatostatin-induced regulation of SST(2A) receptor expression and cell surface availability in central neurons: role of receptor internalization. *J Neurosci* 20:5932-5939.
- Braun H, Schulz S, Becker A, Schroder H, Holtt V (1998) Protective effects of cortistatin (CST-14) against kainate-induced neurotoxicity in rat brain. *Brain Res* 803:54-60.
- Brazeau P, Vale W, Burgus R, Ling N, Butcher M, Rivier J, Guillemin R (1973) Hypothalamic polypeptide that inhibits the secretion of immunoreactive pituitary growth hormone. *Science* 179:77-79.
- Breder CD, Yamada Y, Yasuda K, Seino S, Saper CB, Bell GI (1992) Differential expression of somatostatin receptor subtypes in brain. *J Neurosci* 12:3920-3934.

- Bruno JF, Xu Y, Berelowitz M (1994) Somatostatin regulates somatostatin receptor subtype mRNA expression in GH3 cells. *Biochem Biophys Res Commun* 202:1738-1743.
- Bruno JF, Xu Y, Song J, Berelowitz M (1993) Tissue distribution of somatostatin receptor subtype messenger ribonucleic acid in the rat. *Endocrinology* 133:2561-2567.
- Buckmaster PS, Otero-Corchon V, Rubinstein M, Low MJ (2002) Heightened seizure severity in somatostatin knockout mice. *Epilepsy Res* 48:43-56.
- Calbet M, Guadano-Ferraz A, Spier AD, Maj M, Sutcliffe JG, Przewlocki R, de Lecea L (1999) Cortistatin and somatostatin mRNAs are differentially regulated in response to kainate. *Brain Res Mol Brain Res* 72:55-64.
- Chen SH, Cheung RT (2003) Intracerebroventricular injection of a neuropeptide Y-Y1 receptor agonist increases while BIBP3226, a Y1 antagonist, reduces the infarct volume following transient middle cerebral artery occlusion in rats. *Neuroscience* 116:119-126.
- Cheung RT, Cechetto DF (1995) Neuropeptide changes following excitotoxic lesion of the insular cortex in rats. *J Comp Neurol* 362:535-550.
- Choi DW, Rothman SM (1990) The role of glutamate neurotoxicity in hypoxic-ischemic neuronal death. *Annu Rev Neurosci* 13:171-182.
- Christensen T, Bruhn T, Frank L, Diemer NH (1996) Differential effect of NMDA and AMPA receptor blockade on protein synthesis in the rat infarct borderzone. *Acta Neurol Scand* 93:160-167.
- Cobb SR, Halasy K, Vida I, Nyiri G, Tamas G, Buhl EH, Somogyi P (1997) Synaptic effects of identified interneurons innervating both interneurons and pyramidal cells in the rat hippocampus. *Neuroscience* 79: 629-648. Erratum in: *Neuroscience* 80:971.
- Cohn ML, Cohn M (1975) 'Barrel rotation' induced by somatostatin in the non-lesioned rat. *Brain Res* 96:138-141.
- Cole SL, Schindler M (2000) Characterisation of somatostatin sst2 receptor splice variants. *J Physiol Paris* 94:217-237.
- Cowan NJ, Lewis SA, Balcerek JM, Krek V, Shelanski M (1985) Structural implications of a cDNA clone encoding mouse glial fibrillary acidic protein. *Ann N Y Acad Sci* 455:575-582.
- Csaba Z, Bernard V, Helboe L, Bluett-Pajot MT, Bloch B, Epelbaum J, Dournaud P (2001) In vivo internalization of the somatostatin sst2A receptor in rat brain: evidence for translocation of cell-surface receptors into the endosomal recycling pathway. *Mol Cell Neurosci* 17:646-661.
- Csaba Z, Simon A, Helboe L, Epelbaum J, Dournaud P (2002) Neurochemical characterization of receptor-expressing cell populations by in vivo agonist-induced internalization: insights from the somatostatin sst2A receptor. *J Comp Neurol* 454:192-199.
- Csaba Z, Simon A, Helboe L, Epelbaum J, Dournaud P (2003) Targeting sst2A receptor-expressing cells in the rat hypothalamus through in vivo agonist stimulation: neuroanatomical evidence for a major role of this subtype in mediating somatostatin functions. *Endocrinology* 144:1564-1573.
- Culmsee C, Stumm RK, Schafer MK, Weihe E, Kriegstein J (1999) Clenbuterol induces growth factor mRNA, activates astrocytes, and protects rat brain tissue against ischemic damage. *Eur J Pharmacol* 379:33-45.
- De Herder WW, Hofland LJ, Van Der Lely AJ, Lamberts SW (2003) Somatostatin receptors in gastroentero-pancreatic neuroendocrine tumours. *Endocr Relat Cancer* 10:451-458.
- de Lanerolle NC, Kim JH, Robbins RJ, Spencer DD (1989) Hippocampal interneuron loss and plasticity in human temporal lobe epilepsy. *Brain Res* 495:387-395.
- de Lecea L, Criado JR, Prospero-Garcia O, Gautvik KM, Schweitzer P, Danielson PE, Dunlop CL, Siggins GR, Henriksen SJ, Sutcliffe JG (1996) A cortical neuropeptide with neuronal depressant and sleep-modulating properties. *Nature* 381:242-245.

- de Lecea L, del Rio JA, Criado JR, Alcantara S, Morales M, Danielson PE, Henriksen SJ, Soriano E, Sutcliffe JG (1997a) Cortistatin is expressed in a distinct subset of cortical interneurons. *J Neurosci* 17:5868-5880.
- de Lecea L, Ruiz-Lozano P, Danielson PE, Peelle-Kirley J, Foye PE, Frankel WN, Sutcliffe JG (1997b) Cloning, mRNA expression, and chromosomal mapping of mouse and human preprocortistatin. *Genomics* 42:499-506.
- de Lima AD, Morrison JH (1989) Ultrastructural analysis of somatostatin-immunoreactive neurons and synapses in the temporal and occipital cortex of the macaque monkey. *J Comp Neurol*. May 8;283:212-227.
- Dournaud P, Boudin H, Schonbrunn A, Tannenbaum GS, Beaudet A (1998) Interrelationships between somatostatin sst2A receptors and somatostatin-containing axons in rat brain: evidence for regulation of cell surface receptors by endogenous somatostatin. *J Neurosci* 18:1056-1071.
- Dournaud P, Gu YZ, Schonbrunn A, Mazella J, Tannenbaum GS, Beaudet A (1996) Localization of the somatostatin receptor SST2A in rat brain using a specific anti-peptide antibody. *J Neurosci* 16:4468-4478.
- Dutar P, Vaillend C, Viollet C, Billard JM, Potier B, Carlo AS, Ungerer A, Epelbaum J (2002) Spatial learning and synaptic hippocampal plasticity in type 2 somatostatin receptor knock-out mice. *Neuroscience* 112:455-466.
- Eng LF (1985) Glial fibrillary acidic protein (GFAP): the major protein of glial intermediate filaments in differentiated astrocytes. *J Neuroimmunol* 8:203-214.
- Epelbaum J (1986) Somatostatin in the central nervous system: physiology and pathological modifications. *Prog Neurobiol* 27:63-100.
- Esclapez M, Houser CR (1995) Somatostatin neurons are a subpopulation of GABA neurons in the rat dentate gyrus: evidence from colocalization of pre-prosomatostatin and glutamate decarboxylase messenger RNAs. *Neuroscience* 64:339-355.
- Fitzgerald LW, Dokla CP (1989) Morris water task impairment and hypoactivity following cysteamine-induced reductions of somatostatin-like immunoreactivity. *Brain Res* 505:246-250.
- Fitzpatrick-McElligott S, Card JP, Lewis ME, Baldino F Jr (1988) Neuronal localization of prosomatostatin mRNA in the rat brain with in situ hybridization histochemistry. *J Comp Neurol* 273:558-572.
- Fontana G, De Bernardi R, Ferro F, Gemignani A, Raiteri M (1996) Characterization of the glutamate receptors mediating release of somatostatin from cultured hippocampal neurons. *J Neurochem* 66:161-168.
- Forloni G, Lucca E, Angeretti N, Chiesa R, Vezzani A (1997) Neuroprotective effect of somatostatin on nonapoptotic NMDA-induced neuronal death: role of cyclic GMP. *J Neurochem* 68:319-327.
- Francis PT, Bowen DM, Lowe SL, Neary D, Mann DM, Snowden JS (1987) Somatostatin content and release measured in cerebral biopsies from demented patients. *J Neurol Sci* 78:1-16.
- Freneau RT Jr, Troyer MD, Pahner I, Nygaard GO, Tran CH, Reimer RJ, Bellocchio EE, Fortin D, Storm-Mathisen J, Edwards RH (2001) The expression of vesicular glutamate transporters defines two classes of excitatory synapse. *Neuron* 31:247-260.
- Froidevaux S, Hintermann E, Torok M, Macke HR, Beglinger C, Eberle AN (1999) Differential regulation of somatostatin receptor type 2 (sst 2) expression in AR4-2J tumor cells implanted into mice during octreotide treatment. *Cancer Res* 59:3652-3657.
- Fukusumi S, Kitada C, Takekawa S, Kizawa H, Sakamoto J, Miyamoto M, Hinuma S, Kitano K, Fujino M (1997) Identification and characterization of a novel human cortistatin-like peptide. *Biochem Biophys Res Commun* 232:157-163.
- Gabriel SM, Bierer LM, Haroutunian V, Purohit DP, Perl DP, Davis KL (1993) Widespread deficits in somatostatin but not neuropeptide Y concentrations in Alzheimer's disease cerebral cortex. *Neurosci Lett* 155:116-120.

- Ginsberg MD, Busto R (1989) Rodent models of cerebral ischemia. *Stroke* 20:1627-1642.
- Goodman RH, Jacobs JW, Dee PC, Habener JF (1982) Somatostatin-28 encoded in a cloned cDNA obtained from a rat medullary thyroid carcinoma. *J Biol Chem* 257:1156-1159.
- Haga S, Aizawa T, Ishii T, Ikeda K (1996) Complement gene expression in mouse microglia and astrocytes in culture: comparisons with mouse peritoneal macrophages. *Neurosci Lett* 216:191-194.
- Handel M, Schulz S, Stanarius A, Schreff M, Erdtmann-Vourliotis M, Schmidt H, Wolf G, Holtt V (1999) Selective targeting of somatostatin receptor 3 to neuronal cilia. *Neuroscience* 89:909-926.
- Harrington KA, Schindler M, Humphrey PP, Emson PC (1995) Expression of messenger RNA for somatostatin receptor subtype 4 in adult rat brain. *Neurosci Lett* 188:17-20.
- Hathway GJ, Humphrey PP, Kendrick KM (1999) Evidence that somatostatin sst2 receptors mediate striatal dopamine release. *Br J Pharmacol* 128:1346-1352.
- Helboe L, Stidsen CE, Moller M (1998) Immunohistochemical and cytochemical localization of the somatostatin receptor subtype sst1 in the somatostatinergic parvocellular neuronal system of the rat hypothalamus. *J Neurosci* 18:4938-4945.
- Hendry SH, Jones EG, Emson PC (1984) Morphology, distribution, and synaptic relations of somatostatin- and neuropeptide Y-immunoreactive neurons in rat and monkey neocortex. *J Neurosci* 4:2497-2517.
- Hervieu G, Emson PC (1998) The localization of somatostatin receptor 1 (sst1) immunoreactivity in the rat brain using an N-terminal specific antibody. *Neuroscience* 85:1263-1284.
- Hicks GA, Feniuk W, Humphrey PP (1998) Outward current produced by somatostatin (SRIF) in rat anterior cingulate pyramidal cells in vitro. *Br J Pharmacol* 124:252-258.
- Hipkin RW, Friedman J, Clark RB, Eppler CM, Schonbrunn A (1997) Agonist-induced desensitization, internalization, and phosphorylation of the sst2A somatostatin receptor. *J Biol Chem* 272:13869-13876.
- Hipkin RW, Wang Y, Schonbrunn A (2000) Protein kinase C activation stimulates the phosphorylation and internalization of the sst2A somatostatin receptor. *J Biol Chem* 275:5591-5599.
- Hokfelt T, Efendic S, Hellerstrom C, Johansson O, Luft R, Arimura A (1975) Cellular localization of somatostatin in endocrine-like cells and neurons of the rat with special references to the A1-cells of the pancreatic islets and to the hypothalamus. *Acta Endocrinol Suppl (Copenh)* 200:5-41.
- Holloway S, Feniuk W, Kidd EJ, Humphrey PP (1996) A quantitative autoradiographical study on the distribution of somatostatin sst2 receptors in the rat central nervous system using [125I]-BIM-23027. *Neuropharmacology* 35:1109-1120.
- Hossmann KA (1994) Glutamate-mediated injury in focal cerebral ischemia: the excitotoxin hypothesis revised. *Brain Pathol* 4:23-36.
- Hoyer D, Bell GI, Berelowitz M, Epelbaum J, Feniuk W, Humphrey PP, O'Carroll AM, Patel YC, Schonbrunn A, Taylor JE, et al (1995) Classification and nomenclature of somatostatin receptors. *Trends Pharmacol Sci* 16:86-88.
- Hukovic N, Panetta R, Kumar U, Patel YC (1996) Agonist-dependent regulation of cloned human somatostatin receptor types 1-5 (hSSTR1-5): subtype selective internalization or upregulation. *Endocrinology* 137:4046-4049.
- Hukovic N, Panetta R, Kumar U, Rocheville M, Patel YC (1998) The cytoplasmic tail of the human somatostatin receptor type 5 is crucial for interaction with adenylyl cyclase and in mediating desensitization and internalization. *J Biol Chem* 273:21416-21422.

- Kaupmann K, Bruns C, Hoyer D, Seuwen K, Lubbert H (1993) Distribution and second messenger coupling of four somatostatin receptor subtypes expressed in brain. *FEBS Lett* 331:53-59.
- Kawaguchi Y, Kubota Y (1997) GABAergic cell subtypes and their synaptic connections in rat frontal cortex. *Cereb Cortex* 7:476-486.
- Kawaguchi Y, Kondo S (2002) Parvalbumin, somatostatin and cholecystokinin as chemical markers for specific GABAergic interneuron types in the rat frontal cortex. *J Neurocytol* 31:277-287.
- Kiyama H, Emson PC (1990) Distribution of somatostatin mRNA in the rat nervous system as visualized by a novel non-radioactive in situ hybridization histochemistry procedure. *Neuroscience* 38:223-244.
- Koenig JA, Edwardson JM (1997a) Endocytosis and recycling of G protein-coupled receptors. *Trends Pharmacol Sci* 18:276-287.
- Koenig JA, Edwardson JM, Humphrey PP (1997b) Somatostatin receptors in Neuro2A neuroblastoma cells: ligand internalization. *Br J Pharmacol* 120:52-59.
- Koenig JA, Kaur R, Dodgeon I, Edwardson JM, Humphrey PP (1998) Fates of endocytosed somatostatin sst2 receptors and associated agonists. *Biochem J* 336:291-298.
- Kowall NW, Beal MF (1988) Cortical somatostatin, neuropeptide Y, and NADPH diaphorase neurons: normal anatomy and alterations in Alzheimer's disease. *Ann Neurol* 23:105-114.
- Kraus J, Woltje M, Schonwetter N, Holtt V (1998) Alternative promoter usage and tissue specific expression of the mouse somatostatin receptor 2 gene. *FEBS Lett* 428:165-170.
- Kreienkamp HJ, Roth A, Richter D (1998) Rat somatostatin receptor subtype 4 can be made sensitive to agonist-induced internalization by mutation of a single threonine (residue 331). *DNA Cell Biol* 17:869-878.
- Lahtinen H, Brankack J, Koivisto E, Riekkinen PJ (1992) Somatostatin release in rat neocortex during gamma-hydroxybutyrate-provoked seizures: microdialysis combined with EEG recording. *Brain Res Bull* 29:837-841.
- Li H, Xie Z (1995) Molecular cloning of two rat Na⁺/Pi cotransporters: evidence for differential tissue expression of transcripts. *Cell Mol Biol Res*;41:451-460.
- Liu Q, Schonbrunn A (2001) Agonist-induced phosphorylation of somatostatin receptor subtype 1 (sst1). Relationship to desensitization and internalization. *J Biol Chem* 276:3709-3717.
- Lynch NJ, Willis CL, Nolan CC, Roscher S, Fowler MJ, Weihe E, Ray DE, Schwaeble WJ (2004) Microglial activation and increased synthesis of complement component C1q precedes blood-brain barrier dysfunction in rats. *Mol Immunol* 40:709-716.
- Manfridi A, Forloni GL, Vezzani A, Fodritto F, De Simoni MG (1991) Functional and histological consequences of quinolinic and kainic acid-induced seizures on hippocampal somatostatin neurons. *Neuroscience* 41:127-135.
- Marin P, Delumeau JC, Tence M, Cordier J, Glowinski J, Premont J (1991) Somatostatin potentiates the alpha 1-adrenergic activation of phospholipase C in striatal astrocytes through a mechanism involving arachidonic acid and glutamate. *Proc Natl Acad Sci U S A* 88:9016-9020.
- Marti M, Bregola G, Morari M, Gemignani A, Simonato M (2000) Somatostatin release in the hippocampus in the kindling model of epilepsy: a microdialysis study. *J Neurochem* 74:2497-2503
- Mazarati AM, Telegdy G (1992) Effects of somatostatin and anti-somatostatin serum on picrotoxin-kindled seizures. *Neuropharmacology* 31:793-797.

- Melton DA, Krieg PA, Rebagliati MR, Maniatis T, Zinn K, Green MR (1984) Efficient in vitro synthesis of biologically active RNA and RNA hybridization probes from plasmids containing a bacteriophage SP6 promoter. *Nucleic Acids Res* 12:7035-7056.
- Miles R, Toth K, Gulyas AI, Hajos N, Freund TF (1996) Differences between somatic and dendritic inhibition in the hippocampus. *Neuron* 16:815-823.
- Molchan SE, Hill JL, Martinez RA, Lawlor BA, Mellow AM, Rubinow DR, Bissette G, Nemeroff CB, Sunderland T (1993) CSF somatostatin in Alzheimer's disease and major depression: relationship to hypothalamic-pituitary-adrenal axis and clinical measures. *Psychoneuroendocrinology* 18:509-519.
- Monno A, Rizzi M, Samanin R, Vezzani A (1993) Anti-somatostatin antibody enhances the rate of hippocampal kindling in rats. *Brain Res* 602:148-152.
- Montminy MR, Goodman RH, Horovitch SJ, Habener JF (1984) Primary structure of the gene encoding rat preprosomatostatin. *Proc Natl Acad Sci U S A* 81:3337-3340.
- Moore SD, Madamba SG, Joels M, Siggins GR (1988) Somatostatin augments the M-current in hippocampal neurons. *Science* 239:278-280.
- Nouel D, Gaudriault G, Houle M, Reisine T, Vincent JP, Mazella J, Beaudet A (1997) Differential internalization of somatostatin in COS-7 cells transfected with SST1 and SST2 receptor subtypes: a confocal microscopic study using novel fluorescent somatostatin derivatives. *Endocrinology* 138:296-306.
- O'Carroll AM, Lolait SJ, Konig M, Mahan LC (1992) Molecular cloning and expression of a pituitary somatostatin receptor with preferential affinity for somatostatin-28. *Mol Pharmacol* 42:939-946.
- Patel YC, Greenwood MT, Panetta R, Demchyshyn L, Niznik H, Srikant CB (1995) The somatostatin receptor family. *Life Sci* 57:1249-1265.
- Patel YC, O'Neil W (1988) Peptides derived from cleavage of prosomatostatin at carboxyl- and amino-terminal segments. Characterization of tissue and secreted forms in the rat. *J Biol Chem* 263:745-751.
- Patel YC, Reichlin S (1978) Somatostatin in hypothalamus, extrahypothalamic brain, and peripheral tissues of the rat. *Endocrinology* 102:523-530.
- Perez J, Hoyer D (1995a) Co-expression of somatostatin SSTR-3 and SSTR-4 receptor messenger RNAs in the rat brain. *Neuroscience* 64:241-253.
- Perez J, Rigo M, Kaupmann K, Bruns C, Yasuda K, Bell GI, Lubbert H, Hoyer D (1994) Localization of somatostatin (SRIF) SSTR-1, SSTR-2 and SSTR-3 receptor mRNA in rat brain by in situ hybridization. *Naunyn Schmiedebergs Arch Pharmacol* 349:145-160.
- Perez J, Vezzani A, Civenni G, Tutka P, Rizzi M, Schupbach E, Hoyer D (1995b) Functional effects of D-Phe-c[Cys-Tyr-D-Trp-Lys-Val-Cys]-Trp-NH₂ and differential changes in somatostatin receptor messenger RNAs, binding sites and somatostatin release in kainic acid-treated rats. *Neuroscience* 65:1087-1097.
- Piwko C, Thoss VS, Samanin R, Hoyer D, Vezzani A (1996) Status of somatostatin receptor messenger RNAs and binding sites in rat brain during kindling epileptogenesis. *Neuroscience* 75:857-868.
- Plotnikoff NP, Kastin AJ, Schally AV (1974) Growth hormone release inhibiting hormone: neuropharmacological studies. *Pharmacol Biochem Behav* 2:693-696.
- Pradayrol L, Jornvall H, Mutt V, Ribet A (1980) N-terminally extended somatostatin: the primary structure of somatostatin-28. *FEBS Lett* 109:55-58.
- Puebla L, Mouchantaf R, Sasi R, Khare S, Bennett HP, James S, Patel YC (1999) Processing of rat preprocortistatin in mouse AtT-20 cells. *J Neurochem* 73:1273-1277.

- Rauca C, Schafer K, Holtt V (1999) Effects of somatostatin, octreotide and cortistatin on ischaemic neuronal damage following permanent middle cerebral artery occlusion in the rat. *Naunyn Schmiedebergs Arch Pharmacol* 360:633-638.
- Raulf F, Perez J, Hoyer D, Bruns C (1994) Differential expression of five somatostatin receptor subtypes, SST1-5, in the CNS and peripheral tissue. *Digestion* 55 Suppl 3:46-53.
- Raynor K, Murphy WA, Coy DH, Taylor JE, Moreau JP, Yasuda K, Bell GI, Reisine T (1993) Cloned somatostatin receptors: identification of subtype-selective peptides and demonstration of high affinity binding of linear peptides. *Mol Pharmacol* 43:838-844.
- Reglodi D, Tamas A, Somogyvari-Vigh A, Szanto Z, Kertes E, Lenard L, Arimura A, Lengvari I (2002) Effects of pretreatment with PACAP on the infarct size and functional outcome in rat permanent focal cerebral ischemia. *Peptides* 23:2227-2234.
- Reichlin S Somatostatin (1983) *N Engl J Med* 309:1495-1501.
- Reisine T, Bell GI (1993) Molecular biology of opioid receptors. *Trends Neurosci* 16:506-510.
- Reisine T, Bell GI (1995) Molecular biology of somatostatin receptors. *Endocr Rev* 16:427-442.
- Rezek M, Havlicek V, Hughes KR, Friesen H (1977) Behavioural and motor excitation and inhibition induced by the administration of small and large doses of somatostatin into the amygdala. *Neuropharmacology* 16:157-162.
- Robbins RJ, Brines ML, Kim JH, Adrian T, de Lanerolle N, Welsh S, Spencer DD (1991) A selective loss of somatostatin in the hippocampus of patients with temporal lobe epilepsy. *Ann Neurol* 29:325-332.
- Roosterman D, Roth A, Kreienkamp HJ, Richter D, Meyerhof W (1997) Distinct agonist-mediated endocytosis of cloned rat somatostatin receptor subtypes expressed in insulinoma cells. *J Neuroendocrinol* 9:741-751.
- Roth A, Kreienkamp HJ, Meyerhof W, Richter D (1997a) Phosphorylation of four amino acid residues in the carboxyl terminus of the rat somatostatin receptor subtype 3 is crucial for its desensitization and internalization. *J Biol Chem* 272:23769-23774.
- Roth A, Kreienkamp HJ, Nehring RB, Roosterman D, Meyerhof W, Richter D (1997b) Endocytosis of the rat somatostatin receptors: subtype discrimination, ligand specificity, and delineation of carboxy-terminal positive and negative sequence motifs. *DNA Cell Biol* 16:111-119.
- Ruppin E, Ofer E, Reggia JA, Revett K, Goodall S (1999) Pathogenic mechanisms in ischemic damage: a computational study. *Comput Biol Med* 29:39-59.
- Sarret P, Nouel D, Dal Farra C, Vincent JP, Beaudet A, Mazella J (1999) Receptor-mediated internalization is critical for the inhibition of the expression of growth hormone by somatostatin in the pituitary cell line AtT-20. *J Biol Chem* 274:19294-19300.
- Schafer MK, Schwaeble WJ, Post C, Salvati P, Calabresi M, Sim RB, Petry F, Loos M, Weihe E (2000) Complement C1q is dramatically up-regulated in brain microglia in response to transient global cerebral ischemia. *J Immunol* 164:5446-5452.
- Schindler M, Sellers LA, Humphrey PP, Emson PC (1997) Immunohistochemical localization of the somatostatin SST2(A) receptor in the rat brain and spinal cord. *Neuroscience* 76:225-240.
- Schmechel DE, Vickrey BG, Fitzpatrick D, Elde RP (1984) GABAergic neurons of mammalian cerebral cortex: widespread subclass defined by somatostatin content. *Neurosci Lett* 47:227-232.
- Schreff M, Schulz S, Handel M, Keilhoff G, Braun H, Pereira G, Klutzny M, Schmidt H, Wolf G, Holtt V (2000) Distribution, targeting, and internalization of the sst4 somatostatin receptor in rat brain. *J Neurosci* 20:3785-3797.

- Schulz S, Handel M, Schreff M, Schmidt H, Holtt V (2000) Localization of five somatostatin receptors in the rat central nervous system using subtype-specific antibodies. *J Physiol Paris* 94:259-264.
- Schwaeble W, Schafer MK, Petry F, Fink T, Knebel D, Weihe E, Loos M (1995) Follicular dendritic cells, interdigitating cells, and cells of the monocyte-macrophage lineage are the C1q-producing sources in the spleen. Identification of specific cell types by in situ hybridization and immunohistochemical analysis. *J Immunol* 155:4971-4978.
- Schwartzkop CP, Kreienkamp HJ, Richter D (1999) Agonist-independent internalization and activity of a C-terminally truncated somatostatin receptor subtype 2 (delta349). *Neurochem* 72:1275-1282.
- Schwarzer C, Sperk G, Samanin R, Rizzi M, Gariboldi M, Vezzani A (1996) Neuropeptides-immunoreactivity and their mRNA expression in kindling: functional implications for limbic epileptogenesis. *Brain Res Brain Res Rev* 22:27-50.
- Schweitzer P, Madamba S, Siggins GR (1990) Arachidonic acid metabolites as mediators of somatostatin-induced increase of neuronal M-current. *Nature* 346:464-467.
- Senaris RM, Humphrey PP, Emson PC (1994) Distribution of somatostatin receptors 1, 2 and 3 mRNA in rat brain and pituitary. *Eur J Neurosci* 6:1883-1896.
- Siehler S, Seuwen K, Hoyer D (1998) [125I]Tyr10-cortistatin14 labels all five somatostatin receptors. *Naunyn Schmiedeberg Arch Pharmacol* 357:483-489.
- Siesjo BK (1992) Pathophysiology and treatment of focal cerebral ischemia. Part II: Mechanisms of damage and treatment. *J Neurosurg* 77:337-354.
- Siesjo BK, Memezawa H, Smith ML (1991) Neurocytotoxicity: pharmacological implications. *Fundam Clin Pharmacol* 5:755-767.
- Siesjo BK, Zhao Q, Pahlmark K, Siesjo P, Katsura K, Folbergrova J (1995) Glutamate, calcium, and free radicals as mediators of ischemic brain damage. *Ann Thorac Surg* 59:1316-1320.
- Smalley KS, Koenig JA, Feniuk W, Humphrey PP (2001) Ligand internalization and recycling by human recombinant somatostatin type 4 (h sst(4)) receptors expressed in CHO-K1 cells. *Br J Pharmacol* 132:1102-1110.
- Somogyi P, Tamas G, Lujan R, Buhl EH (1998) Salient features of synaptic organisation in the cerebral cortex. *Brain Res Brain Res Rev* 26:113-135.
- Souaze F, Rostene W, Forgez P (1997) Neurotensin agonist induces differential regulation of neurotensin receptor mRNA. Identification of distinct transcriptional and post-transcriptional mechanisms. *J Biol Chem* 272:10087-10094.
- Sperk G, Marksteiner J, Gruber B, Bellmann R, Mahata M, Ortler M (1992) Functional changes in neuropeptide Y- and somatostatin-containing neurons induced by limbic seizures in the rat. *Neuroscience* 50:831-846.
- Spier AD, de Lecea L (2000) Cortistatin: a member of the somatostatin neuropeptide family with distinct physiological functions. *Brain Res Brain Res Rev* 33:228-241.
- Stroh T, Jackson AC, Dal Farra C, Schonbrunn A, Vincent JP, Beaudet A (2000a) Receptor-mediated internalization of somatostatin in rat cortical and hippocampal neurons. *Synapse* 38:177-186.
- Stroh T, Jackson AC, Sarret P, Dal Farra C, Vincent JP, Kreienkamp HJ, Mazella J, Beaudet A (2000b) Intracellular dynamics of sst5 receptors in transfected COS-7 cells: maintenance of cell surface receptors during ligand-induced endocytosis. *Endocrinology* 141:354-365.
- Stroh T, Kreienkamp HJ, Beaudet A (1999) Immunohistochemical distribution of the somatostatin receptor subtype 5 in the adult rat brain: predominant expression in the basal forebrain. *J Comp Neurol* 412:69-82.

- Stumm R, Culmsee C, Schafer MK, Kriegstein J, Weihe E (2001) Adaptive plasticity in tachykinin and tachykinin receptor expression after focal cerebral ischemia is differentially linked to gabaergic and glutamatergic cerebrocortical circuits and cerebrovenular endothelium. *J Neurosci* 21:798-811.
- Stumm RK, Rummel J, Junker V, Culmsee C, Pfeiffer M, Kriegstein J, Holtt V, Schulz S (2002) A dual role for the SDF-1/CXCR4 chemokine receptor system in adult brain: isoform-selective regulation of SDF-1 expression modulates CXCR4-dependent neuronal plasticity and cerebral leukocyte recruitment after focal ischemia. *J Neurosci*. Jul 15;22(14):5865-5878.
- Tallent MK, Siggins GR (1997) Somatostatin depresses excitatory but not inhibitory neurotransmission in rat CA1 hippocampus. *J Neurophysiol* 78:3008-3018.
- Tamura A, Graham DI, McCulloch J, Teasdale GM (1981) Focal cerebral ischaemia in the rat: 1. Description of technique and early neuropathological consequences following middle cerebral artery occlusion. *J Cereb Blood Flow Metab* 1:53-60.
- Tannenbaum GS, Turner J, Guo F, Videau C, Epelbaum J, Beaudet A (2001) Homologous upregulation of sst2 somatostatin receptor expression in the rat arcuate nucleus in vivo. *Neuroendocrinology* 74:33-42.
- Tapia-Arancibia L, Astier H (1989) Actions of excitatory amino acids on somatostatin release from cortical neurons in primary cultures. *J Neurochem* 53:1134-1141.
- Thoss VS, Perez J, Duc D, Hoyer D (1995) Embryonic and postnatal mRNA distribution of five somatostatin receptor subtypes in the rat brain. *Neuropharmacology* 34:1673-1688.
- Thoss VS, Perez J, Probst A, Hoyer D (1996) Expression of five somatostatin receptor mRNAs in the human brain and pituitary. *Naunyn Schmiedebergs Arch Pharmacol* 354:411-419.
- Van Beek J, Chan P, Bernaudin M, Petit E, MacKenzie ET, Fontaine M (2000) Glial responses, clusterin, and complement in permanent focal cerebral ischemia in the mouse. *Glia* 31:39-50.
- Vanetti M, Kouba M, Wang X, Vogt G, Holtt V (1992) Cloning and expression of a novel mouse somatostatin receptor (SSTR2B). *FEBS Lett* 311:290-294.
- Vanetti M, Vogt G, Holtt V (1993) The two isoforms of the mouse somatostatin receptor (mSSTR2A and mSSTR2B) differ in coupling efficiency to adenylate cyclase and in agonist-induced receptor desensitization. *FEBS Lett* 331:260-266.
- Varoqui H, Schafer MK, Zhu H, Weihe E, Erickson JD (2002) Identification of the differentiation-associated Na⁺/PI transporter as a novel vesicular glutamate transporter expressed in a distinct set of glutamatergic synapses. *J Neurosci* 22:142-155.
- Vasilaki A, Lanneau C, Dournaud P, De Lecea L, Gardette R, Epelbaum J (1999) Cortistatin affects glutamate sensitivity in mouse hypothalamic neurons through activation of sst2 somatostatin receptor subtype. *Neuroscience* 88:359-364.
- Vezzani A, Hoyer D (1999) Brain somatostatin: a candidate inhibitory role in seizures and epileptogenesis. *Eur J Neurosci* 11:3767-3776.
- Vezzani A, Monno A, Rizzi M, Galli A, Barrios M, Samanin R (1992) Somatostatin release is enhanced in the hippocampus of partially and fully kindled rats. *Neuroscience* 51:41-46.
- Vezzani A, Rizzi M, Conti M, Samanin R (2000) Modulatory role of neuropeptides in seizures induced in rats by stimulation of glutamate receptors. *J Nutr* 130:1046S-1048S.
- Vezzani A, Serafini R, Stasi MA, Vigano G, Rizzi M, Samanin R (1991) A peptidase-resistant cyclic octapeptide analogue of somatostatin (SMS 201-995) modulates seizures induced by quinolinic and kainic acids differently in the rat hippocampus. *Neuropharmacology* 30:345-352.
- Videau C, Hochgeschwender U, Kreienkamp HJ, Brennan MB, Viollet C, Richter D, Epelbaum J (2003) Characterisation of [125I]-Tyr0DTrp8-somatostatin binding in sst1- to sst4- and SRIF-gene-invalidated mouse brain. *Naunyn Schmiedebergs Arch Pharmacol* 367:562-571.

Viollet C, Vaillend C, Videau C, Bluet-Pajot MT, Ungerer A, L'Heritier A, Kopp C, Potier B, Billard J, Schaeffer J, Smith RG, Rohrer SP, Wilkinson H, Zheng H, Epelbaum J (2000) Involvement of sst2 somatostatin receptor in locomotor, exploratory activity and emotional reactivity in mice. *Eur J Neurosci* 12:3761-3770.

Walker DG (1998) Expression and regulation of complement C1q by human THP-1-derived macrophages. *Mol Chem Neuropathol* 34:197-218.

Walker DG, Kim SU, McGeer PL (1995) Complement and cytokine gene expression in cultured microglial derived from postmortem human brains. *J Neurosci Res* 40:478-493.

Williams JS, Berbekar I, Weiss S (1991) N-methyl-D-aspartate evokes the release of somatostatin from striatal interneurons in primary culture. *Neuroscience* 43:437-444.

Wolz P, Krieglstein J (1996) Neuroprotective effects of alpha-lipoic acid and its enantiomers demonstrated in rodent models of focal cerebral ischemia. *Neuropharmacology* 35:369-375.

Wood L, Pulaski S, Vogeli G (1988) cDNA clones coding for the complete murine B chain of complement C1q: nucleotide and derived amino acid sequences. *Immunol Lett* 17:115-119.

Wyborski RJ, Bond RW, Gottlieb DI (1990) Characterization of a cDNA coding for rat glutamic acid decarboxylase. *Brain Res Mol Brain Res* 8:193-198.

Yamashita K, Vogel P, Fritze K, Back T, Hossmann KA, Wiessner C (1996) Monitoring the temporal and spatial activation pattern of astrocytes in focal cerebral ischemia using in situ hybridization to GFAP mRNA: comparison with sgp-2 and hsp70 mRNA and the effect of glutamate receptor antagonists. *Brain Res* 735:285-297.

Zeyda T, Diehl N, Paylor R, Brennan MB, Hochgeschwender U (2001) Impairment in motor learning of somatostatin null mutant mice. *Brain Res* 906:107-114.

7. Abbreviations

ABC	avidin/biotin complex
AMPA	α -amino-3-hydroxy-5-methylisoxazole-4-propionic acid
BNPI	brain-specific Na^+ -dependent phosphate transporter
BSA	bovine serum albumin
C1q	complement C1q
cDNA	complementary deoxyribonucleic acid
cm	centimeter
CNS	central nervous system
CST	cortistatin
CTP	cytidine triphosphate
CV	cresyl violet
DAB	diaminobenzidine
DIG	digoxigenin
DNA	deoxyribonucleic acid
dNTP	2'-deoxyribonucleoside triphosphate
DTT	dithiothreitol
EAA	excitatory amino acid
EDTA	ethylene diaminetetraacetic acid
et al.	and colleagues
G	gram
G418	geneticin
GABA	γ -aminobutyric acid
GAD	glutamic acid decarboxydase
G Protein	guanine nucleotide-binding protein
GFAP	glial fibrillary acidic protein
GPCR	G protein-coupled receptor
HEK 293	human embryonic kidney 293
i.c.v.	intracerebroventrically
i.p.	intraperitoneally
ISH	<i>in situ</i> hybridization
KA	kainic acid
Kb	kilobase

L	liter
M	molar
MCAO	middle cerebral artery occlusion
mg	milligram
ml	milliliter
mM	millimolar
mRNA	messenger ribonucleic acid
ms	millisecond
NADPH	reductive nicotinamide adenine dinucleotide phosphate
nCi/g	nanocuries/gram
NGS	normal goat serum
nM	nanomolar
NMDA	N-methyl-D-aspartate glutamate receptors
NPY	neuropeptide Y
PBS	phosphate-buffered saline
PCR	Polymerase Chain Reaction
pmol	picomol
PV	parvalbumin
RT-PCR	reverse transcriptional PCR
SRIF	somatostatin
SS-14	somatostatin-14
sst1-5	somatostatin receptors 1-5
sst2a-lir	sst2a-like immunoreactive
sst2a-LIR	sst2a-like immunoreactivity
Tris	tris(hydroxymethyl)aminomethane
tRNA	transfer RNA
μ M	micromolar
UTP	uridine triphosphate
V	volt
VGLUT1	vesicular glutamate transporter 1
w/v	weight/volume
XL-1	stem of Escherichia coli

8. Appendix

8.1 CURRICULUM VITAE

Name: Zhou, Chun

Birthday: 22. 11. 1969

Nationality: Chinese

Education:

<u>Mar. 2001 – now</u>	Ph. D student Department of Pharmacology and Toxicology, Otto-von-Guericke University Magdeburg Supported by Volkswagen Stiftung
<u>Sep. 1996 – July 1999</u>	Master student Department of Physiology, Dalian Medical University, Dalian, China
<u>Sep. 1987 – July 1993</u>	Bachelor of Medicine Norman Bethune's University of Medical Sciences, Changchun, China

Occupation:

<u>Mar. 2001 –now</u>	Ph. D Department of Pharmacology and Toxicology, Otto-von-Guericke University Magdeburg
<u>Oct. 1999 –Oct. 2000</u>	Visiting scholar Institute of Pharmacology and Toxicology, University Innsbruck, Austria Theme of study: The relationship between ectopic somatostatin expression and neurodegeneration of hippocampal pyramidal neurons after kainic acid-induced seizures
<u>July 1998 – Feb. 2001</u>	Lecturer Department of Physiology, Dalian Medical University, Dalian, China
<u>July 1993 – June 1998</u>	Teaching assistant Department of Physiology, Dalian Medical University, Dalian, China

Magdeburg, 28.04.2004

.....
Chun Zhou

8.2 Publications

- Ralf K. Stumm, *Chun Zhou*, Toshiaki Ara, Francoise Lazarini, Monique Dubois-Dalcq, Takashi Nagasawa, Volker Höllt, and Stefan Schulz (2003) CXCR4 Regulates Interneuron Migration in the Developing Neocortex. *J. Neuroscience* 23: 5123-5130
- Ralf K. Stumm, *Chun Zhou*, Stefan Schulz and Volker Höllt (2003) Neuronal Types Expressing μ - and κ -Opioid Receptor mRNA in the Rat Hippocampal Formation. *J. Comp. Neurology* 469: 107-118

Presentations

Oral:

Chun Zhou A Potential Role of sst2 in Focal Cerebral Ischemia. 22nd Blankenese Conference Hamburg 2002, Germany.

Poster:

- *Chun Zhou*, Ralf K. Stumm, Karina Schäfer, Christine Rauca, Stefan Schulz and Volker Höllt A Role of Somatostatin in Focal Cerebral Ischemia Neuroprotection and Neuro-repair 3rd International Symposium Magdeburg 2003, Germany.
- Ralf K. Stumm, *Chun Zhou*, Francoise Lazarini, Monique Dubois-Dalcq, Toshiaki Ara, Takashi Nagasawa, Vera Junker, Carsten Culmsee, Josef Kriglstein, Volker Höllt and Stefan Schulz The SDF-1 Chemokine Receptor CXCR4 Directs Cellular Migration in the Embryonic and Lesioned Adult Brain Neuroprotection and Neurorepair 3rd International Symposium Magdeburg 2003, Germany.
- *Chun Zhou*, Ralf K. Stumm, Stefan Schulz and Volker Höllt A Potential Role of sst2 in Focal Cerebral Ischemia 22nd Blankenese Conference Hamburg 2002, Germany.
- *Chun Zhou*, Ralf K. Stumm, Heinz Rüttrich, Maria Wagner and Volker Höllt Long-Term Potentiation Alters Gene-Expression of Opioids But Not of μ -Opioid-Receptors in the Dentate Gyrus 43rd Spring Meeting Deutsch Gesellschaft für experimentelle und klinische Pharmakologie und Toxiologie 2002, Mainz, Germany.
- Ralf Stumm, *Chun Zhou*, Stefan Schulz, Heinz Rüttrich, Martin Schäfer, Maria Wagner and Volker Höllt Temporal Dynamics of Cellular Opioid And Opioid Receptor Gene-Expression During Hippocampal Long-Term Potentiation (LTP) INRC Meeting 2001, Helsinki, Finland.

8.3 Acknowledgement

This thesis is based on the experimental studies carried out during my staying in the Institute of Pharmacology and Toxicology, University Magdeburg. I treasure this exciting period of my life very much and I would like to express my gratitude to many people involved in this work.

I wish to express my sincere gratitude to my supervisor, Professor Volker Höllt, for his scientific guidance, for his optimistic and humorous attitude, for his enthusiastic and sustained support on the project.

Dr. Ralf Stumm is my practical supervisor, who guided me with his excellent scientific knowledge and intuition, fruitful ideas and strong responsibility throughout my study. I would like to say many thanks to him for his patience, his inspiring discussions, strict criticisms, and especially for his great effort paid on the revision of my thesis.

Dr. Stefan Schulz provided me with many constructive ideas and very patient, invaluable supervision on my work. I am very grateful for his considerable support not only on my academic work, but also on my daily life.

The laboratory technicians, Karina Schäfer, Anke Reichenauer and Dana Mayer get thanks for their excellent technical work and enjoyable conversations.

All the colleagues in the institute gave me friendly help and support, which makes my study a pleasant and unforgettable experience.

Finally, I dedicate this work to my parents, who are although ten thousand miles away, but always support me emotionally all through my study.

9. Zusammenfassung

Somatostatin und das strukturell verwandte Neuropeptid Cortistatin vermitteln ihre physiologischen Wirkungen über eine Familie von sechs G-Protein gekoppelten Rezeptoren (sst1, sst2a, sst3, sst4, sst5). In den meisten Strukturen des Zentralnervensystems hat die Aktivierung dieser Rezeptoren eine Inhibition der Neurotransmission zur Folge. Die somatostatinerge Neurotransmission selbst ist in mehreren neurologischen Störungen des Zentralnervensystems wie der Alzheimerschen Erkrankung, der Huntingtonschen Erkrankung und in Epilepsien betroffen. Im Zentralnervensystem werden Somatostatin, Cortistatin und die sst-Rezeptoren im zerebralen Kortex am stärksten exprimiert. Hier scheinen sst-Rezeptoren insbesondere die glutamaterge Signalübertragung zu beeinflussen.

In der vorliegenden Arbeit wurde die Verteilung des Somatostatins, des Cortistatins und der sst-Rezeptoren sst1, sst2 und sst4 im zerebralen Kortex auf mRNA- und Proteinebene unter physiologischen Bedingungen und nach einer fokalen Hirnischämie (induziert durch den permanenten unilateralen Verschluss der *Arteria cerebri media*, MCAO) untersucht. Mit Hilfe von Doppelmarkierungsstrategien wurden die neurochemischen Phänotypen von Neuronen identifiziert, die Somatostatin, Cortistatin und den sst2-Rezeptor exprimieren. Nach der MCAO wurden die räumlichen und zeitlichen Muster der sst2a-Rezeptorinternalisierung untersucht, um Strukturen zu identifizieren, in denen der sst2a-Rezeptor nach einer Hirnischämie aktiviert wird.

Unsere Ergebnisse zeigen, dass die Somatostatin- und Cortistatin-mRNAs konstitutiv im zerebralen Kortex exprimiert werden, wo sie eine partiell überlappende Verteilung aufweisen. Im Einzelnen ist Cortistatin in 17% der somatostatinergen Neurone und 31% der parvalbuminhaltigen Neurone koexprimiert, welche unterschiedliche Klassen der GABAergen kortikalen Interneurone bilden. Auf mRNA-Ebene werden sst1, sst2 und sst4 abundant im zerebralen Kortex gebildet, wo ihre Verteilung jeweils eine charakteristische Schichtung aufweist. Die Typisierung der sst2- und sst4-exprimierenden Neurone zeigte, dass die überwiegende Mehrheit dieser Zellen glutamaterge Pyramidenneurone sind. Zudem konnten wir immunhistochemisch die vorwiegend somatodendritische Lokalisation der sst2- und sst4-Rezeptoren zeigen, was auf postsynaptische Funktionen hinweist. Zusammengenommen unterstützen diese Ergebnisse, dass Cortistatin und Somatostatin im zerebralen Kortex über postsynaptische Rezeptoren Einfluss auf glutamaterge Pyramidenzellen nehmen.

Erstmals zeigen wir Veränderungen in der Expression der Cortistatin-, Somatostatin-, sst1-, sst2- und sst4-Gene nach der fokalen Hirnischämie. Im Zeitraum von 3h bis 24h nach der MCAO war die Somatostatinimmunreaktivität in peri- und exofokalen Regionen des Infarkts

reduziert. Zeitlich und räumlich überlappend war der sst2a-Rezeptor in Neuronen verstärkt internalisiert, was eine sst2a-Rezeptoraktivierung anzeigt. Zudem konnten wir eine deutliche Erhöhung der sst2-mRNA-Spiegel in glutamatergen Neuronen der kortikalen Penumbrazone 6h nach der MCAO zeigen. Im Zeitraum von 2d bis 4d nach der fokalen Ischämie waren die Somatostatin- und Cortistatin-mRNAs in nicht geschädigten kortikalen Arealen gegenläufig reguliert. Während die Somatostatin-mRNA-Spiegel leicht erhöht waren, waren die Cortistatin-Expressionsspiegel drastisch reduziert. Koexpressionsanalysen nach der MCAO zeigten, dass die Cortistatin-mRNA-Spiegel in parvalbuminhaltigen Neuronen unter die Detektionsgrenze absanken, wohingegen Cortistatin in zahlreichen somatostatinhaltigen Neuronen detektierbar blieb.

Zusammengenommen zeigen unsere Ergebnisse Somatostatin und Cortistatin sowohl in getrennten als auch in überlappenden GABAergen Verbindungen des zerebralen Kortex. Wegen der unterschiedlichen Konnektivität von somatostatin- bzw. cortistatinhaltigen Interneuronen dürften die beiden Neuropeptide unterschiedliche Funktionen innerhalb des kortikalen Netzwerks ausüben. Weiterhin weisen wir die Aktivierung der somatostatinerger Transmission in peri- und exofokalen Arealen des Kortex während der Frühphase einer Hirnischämie nach. Da Somatostatin die glutamaterge Übertragung im Kortex inhibiert, weisen unsere Ergebnisse darauf hin, dass das Somatostatinsystem nach einem Schlaganfall Übererregungsprozessen entgegen wirken könnte. Da sst2 und sst4 selektiv in glutamatergen Neuronen des Kortex exprimiert werden, stellen diese Rezeptoren interessante Zielstrukturen dar, um die Übererregung im zerebralen Kortex nach einem Schlaganfall zu beeinflussen. Mögliche neuroprotektive Effekte des sst2-Rezeptors werden von uns gegenwärtig in sst2-defizienten Mäusen geprüft. Zudem wird die Entwicklung selektiver Somatostatinrezeptorliganden die Analyse individueller sst-Rezeptorfunktionen in der Schlaganfallpathobiologie erlauben.